Electronic Supplementary Material (ESI) for New Journal of Chemistry.

Supporting Information

Synthesis, structures and antimicrobial activity of copper derivatives of N-substituted imidazolidine-2-thiones : unusual bio-activity against *Staphylococcus epidermidis* and *Enterococcus faecalis*†

Tarlok S. Lobana[a,*], Jaspreet K. Aulakh[a], Heena Sood[b], Daljit S. Arora[b], Isabel Garcia-Santos[c], Manpreet Kaur[d], Courtney E. Duff[d] and Jerry P. Jasinski[d]

[a]*Department of Chemistry, Guru Nanak Dev University, Amritsar-143 005, India*

[b]*Department of Microbiology, Guru Nanak Dev University, Amritsar-143 005, India*

[c]*Departamento de Quimica Inorganica, Facultad de Farmacia, Universidad de Santiago, 15782-Santiago, Spain*

[d]*Department of Chemistry, Keene State College, Keene NH 03435–2001 USA*

* Corresponding author: *E-mail address:* tarlokslobana@yahoo.co.in; Fax: +91-183-2258820

1S. ESI-mass data.

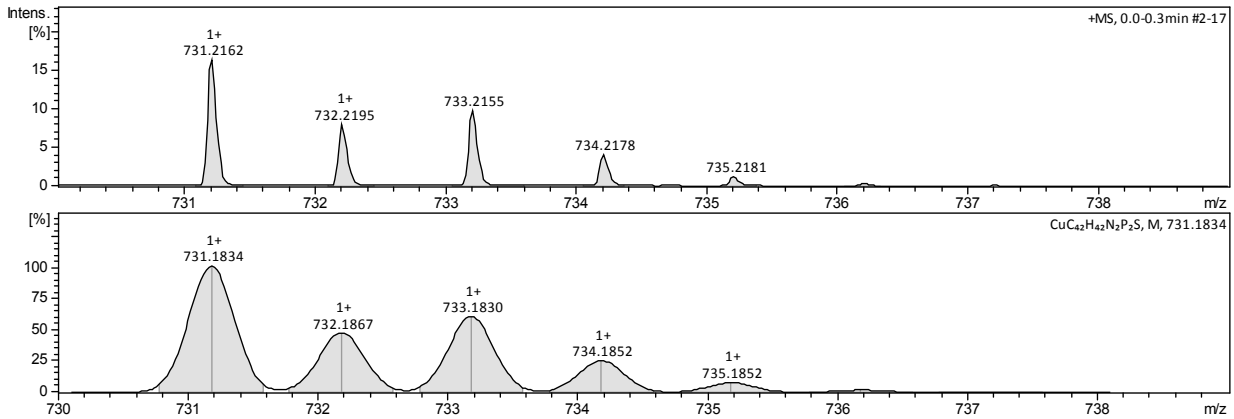

Fig. S1. ESI-mass spectrum due to $[Cu(L\text{-}NPr^n)(PPh_3)_2]^+$, species **A** ($CuC_{42}H_{42}N_2P_2S$; m/z = calcd, 731.18, obsd 731.21) with isotopic pattern (complex **1**).

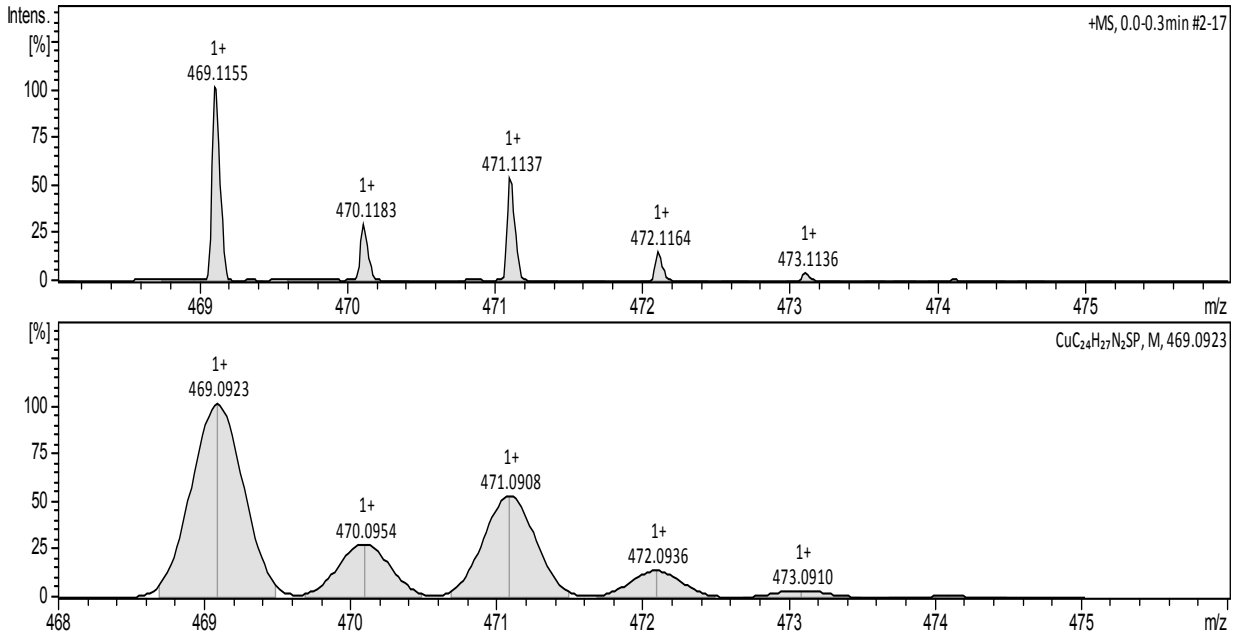

Fig. S2. ESI-mass spectrum due to $[Cu(L\text{-}NPr^n)(PPh_3)]^+$, species **B** ($CuC_{24}H_{27}N_2PS$; m/z = calcd, 469.09, obsd 469.11) with isotopic pattern (complex **1**).

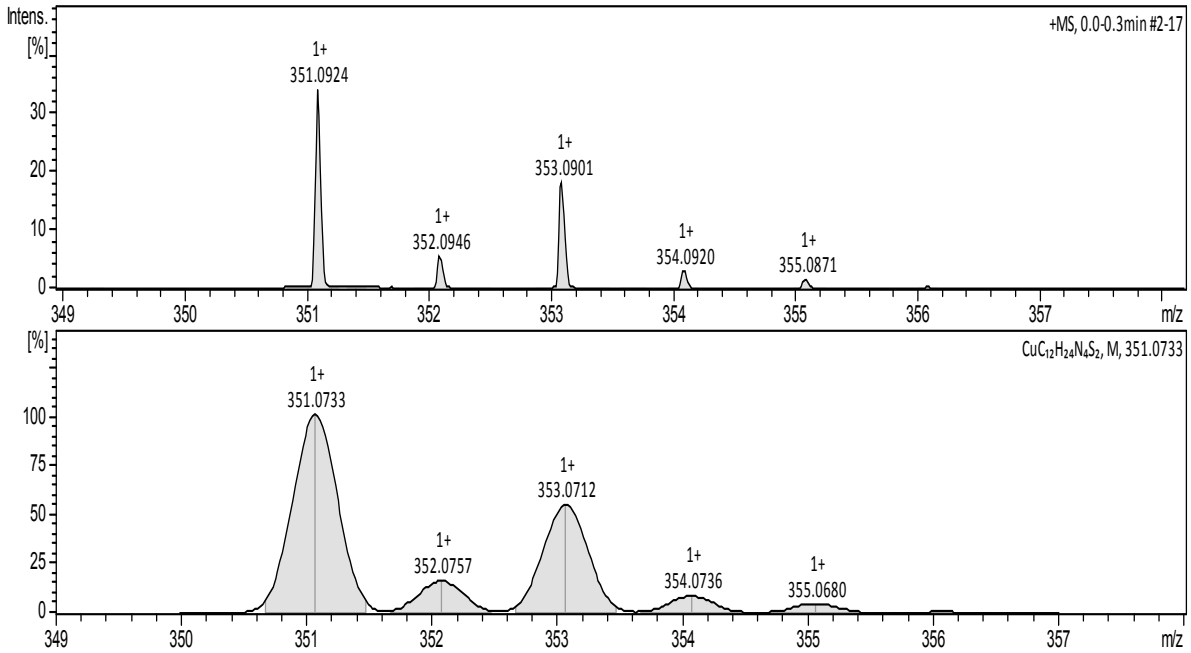

Fig. S3. ESI-mass spectrum due to $[Cu(L\text{-}NPr^n)_2]^+$, species **C** ($CuC_{12}H_{24}N_4S_2$; m/z = calcd, 351.07, obsd 351.09) with isotopic pattern (complex **1**).

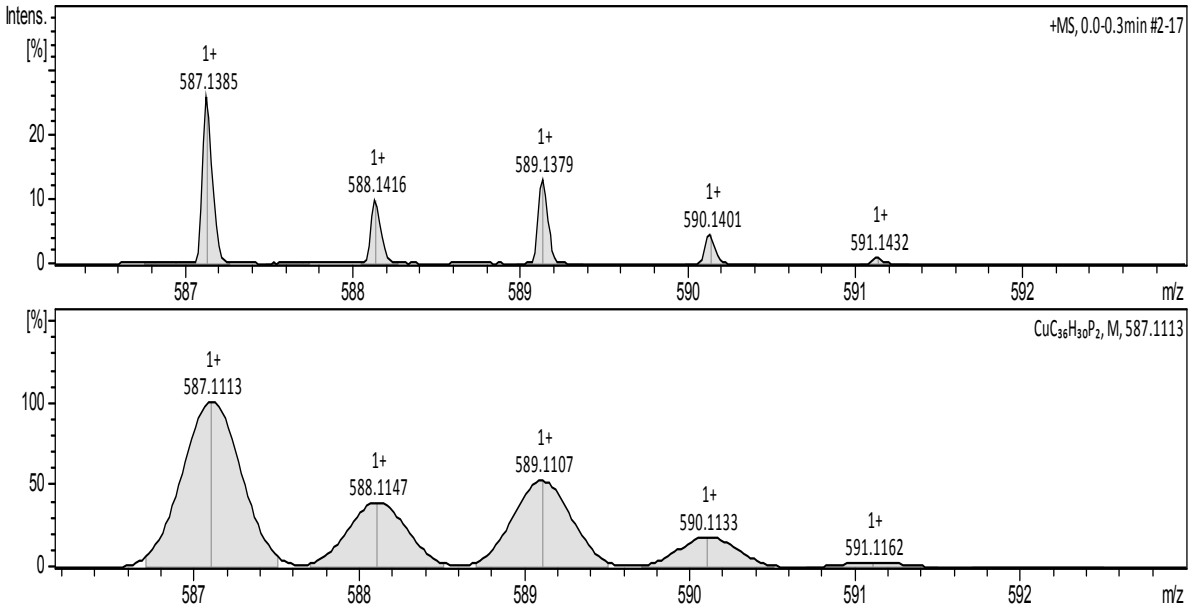

Fig. S4. ESI-mass spectrum due to $[Cu(PPh_3)_2]^+$, species **D** ($CuC_{36}H_{30}P_2$; m/z = calcd, 587.11, obsd 587.13) with isotopic pattern (complex **1**).

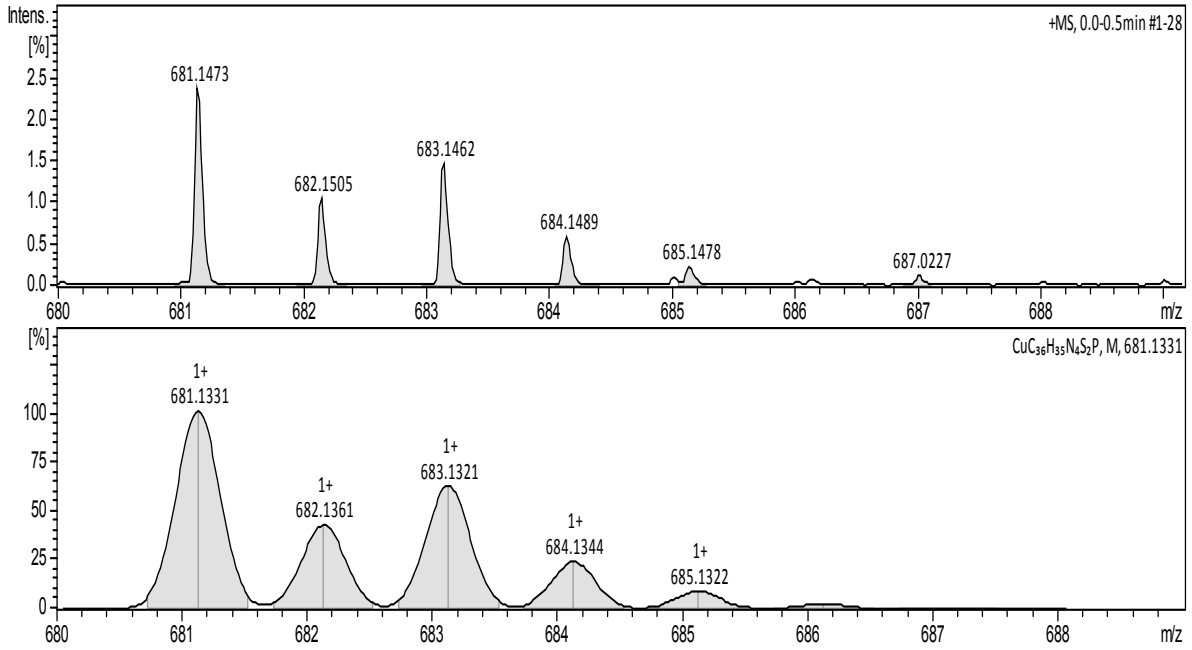

Fig. S5. ESI-mass spectrum due to $[Cu(L\text{-}NPh)_2(PPh_3)]^+$, species **E**; m/z = calcd, 681.13, obsd 681.14) with isotopic pattern (complex **5**).

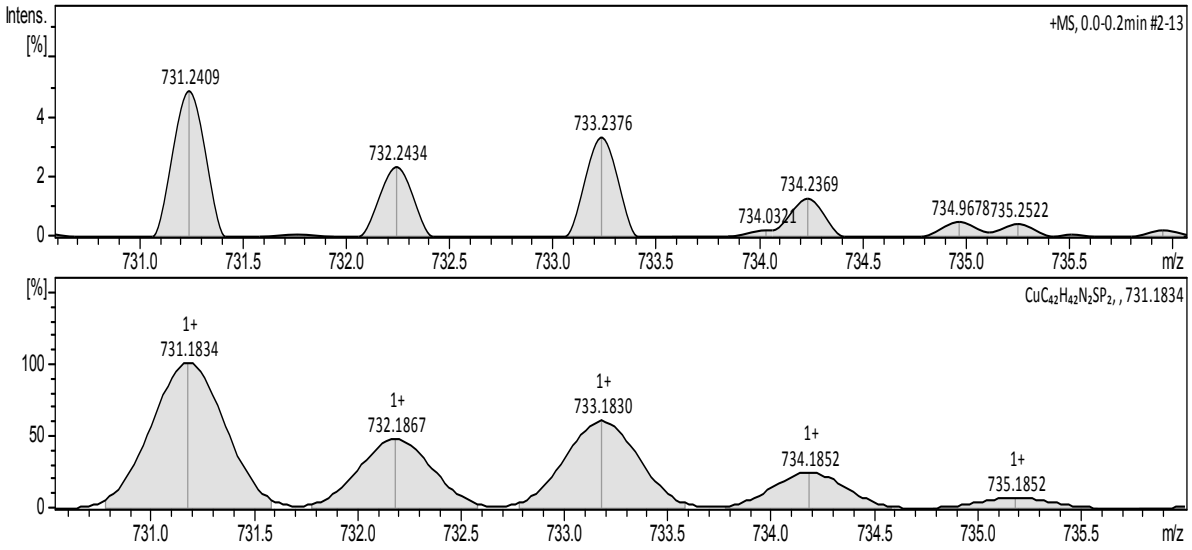

Fig. S6. ESI-mass spectrum due to $[Cu(L\text{-}NPr^n)(PPh_3)_2]^+$, species **A** ($CuC_{42}H_{42}N_2SP_2$; m/z = calcd, 731.18, obsd 731.24) with isotopic pattern (complex **2**).

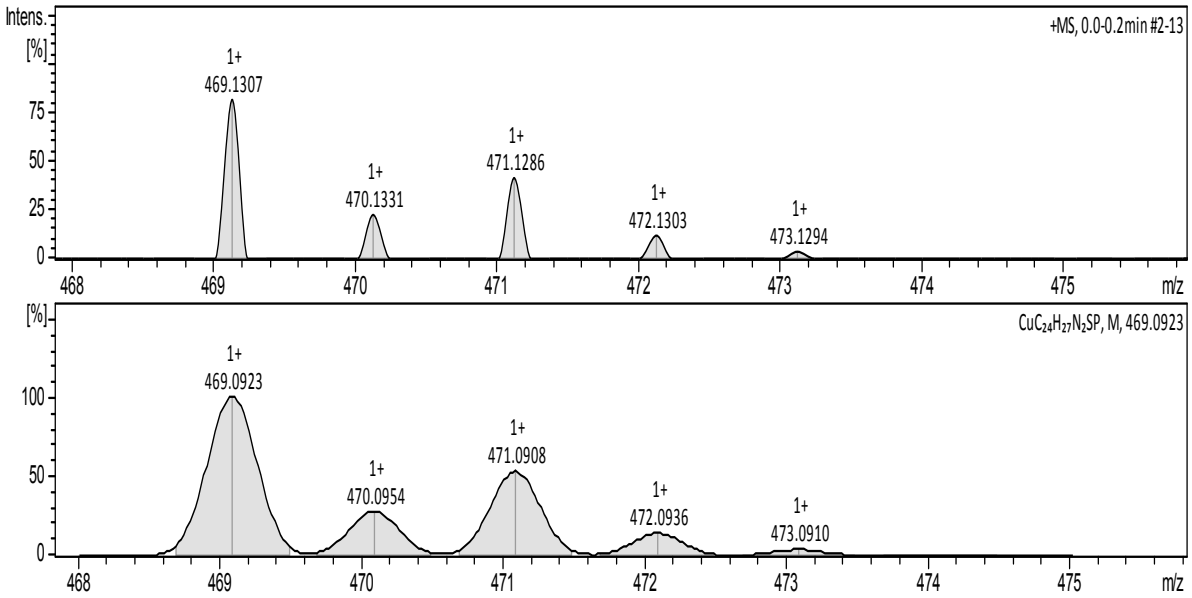

Fig. S7. ESI-mass spectrum due to $[Cu(L\text{-}NPr^n)(PPh_3)]^+$, species **B** ($CuC_{24}H_{27}N_2SP$; m/z = calcd, 469.09, obsd 469.13) with isotopic pattern (complex **2**).

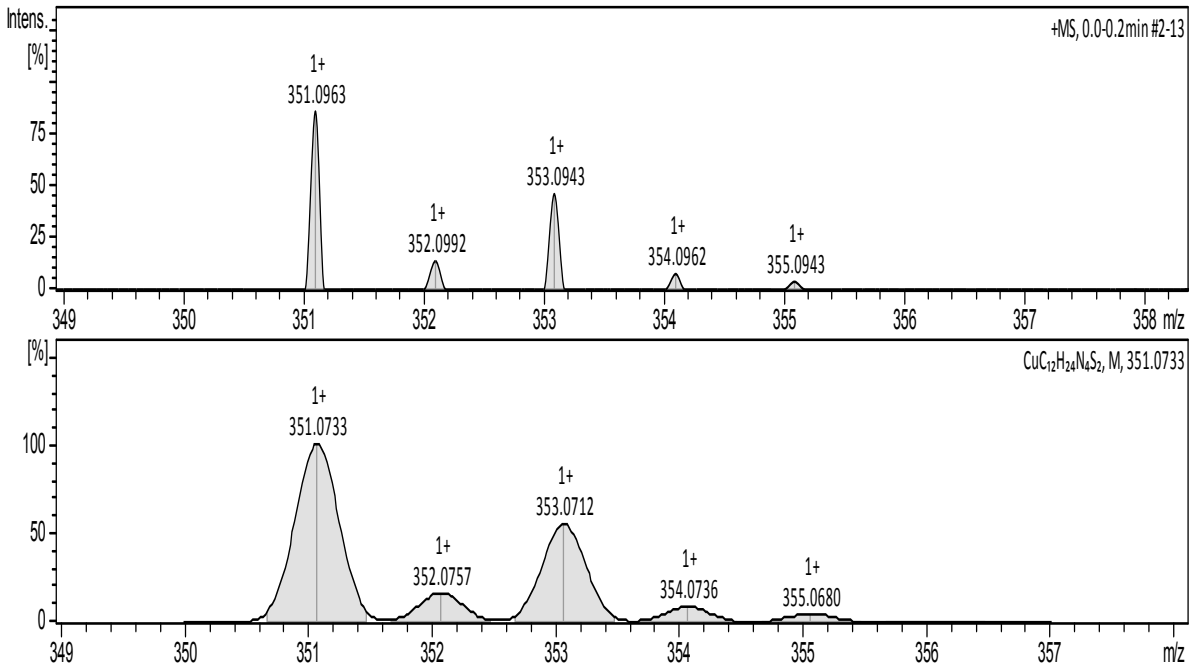

Fig. S8. ESI-mass spectrum due to $[Cu(L\text{-}NPr^n)_2]^+$, species **C** ($CuC_{12}H_{24}N_4S_2$; m/z = calcd, 351.07, obsd 351.09) with isotopic pattern (complex **2**).

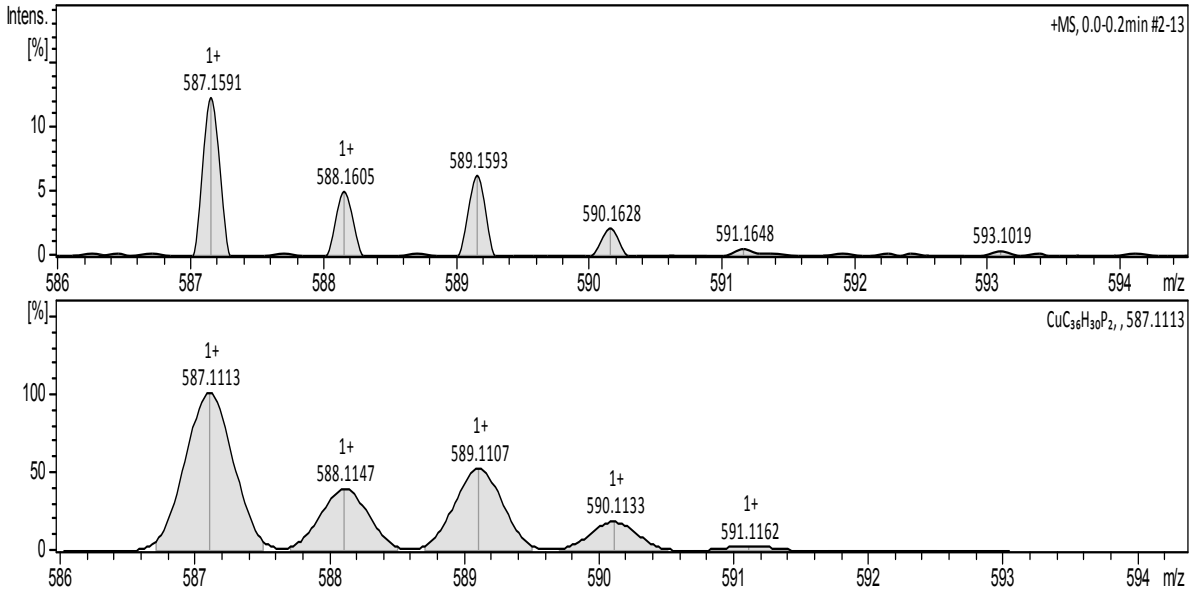

Fig. S9. ESI-mass spectrum due to $[Cu(PPh_3)_2]^+$, species **D** ($CuC_{36}H_{30}P_2$; m/z = calcd, 587.11, obsd 587.15) with isotopic pattern (complex **2**).

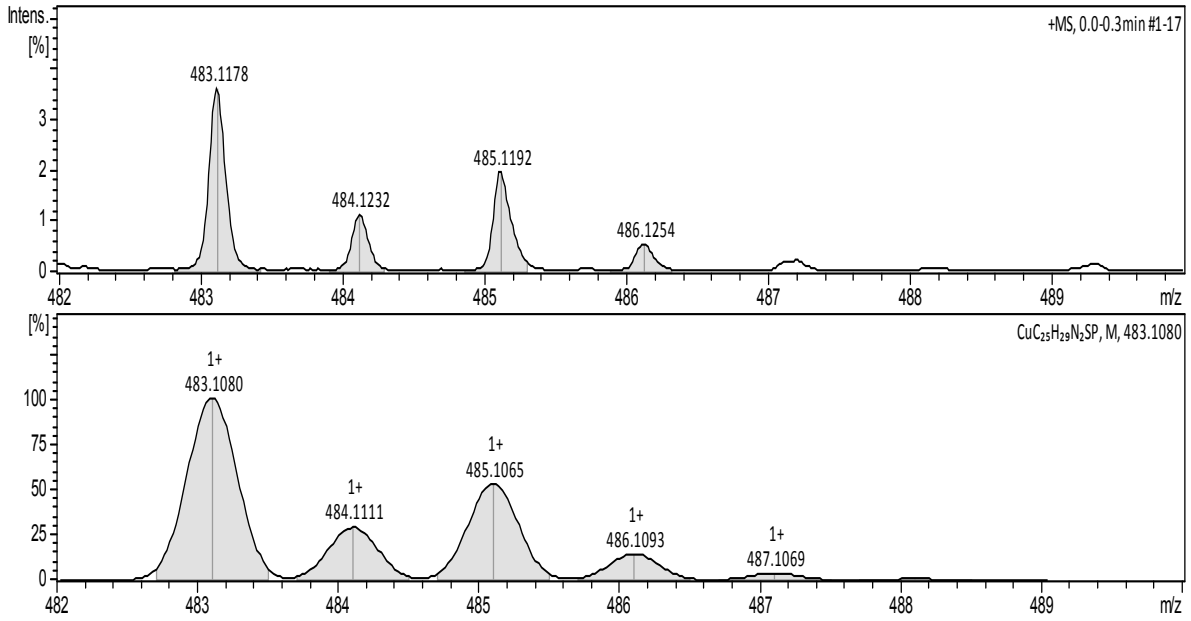

Fig. S10. ESI-mass spectrum due to $[Cu(L\text{-}NBu^n)(PPh_3)]^+$, species **B** ($CuC_{25}H_{29}N_2SP$; m/z = calcd, 483.10, obsd 483.11) with isotopic pattern (complex **3**).

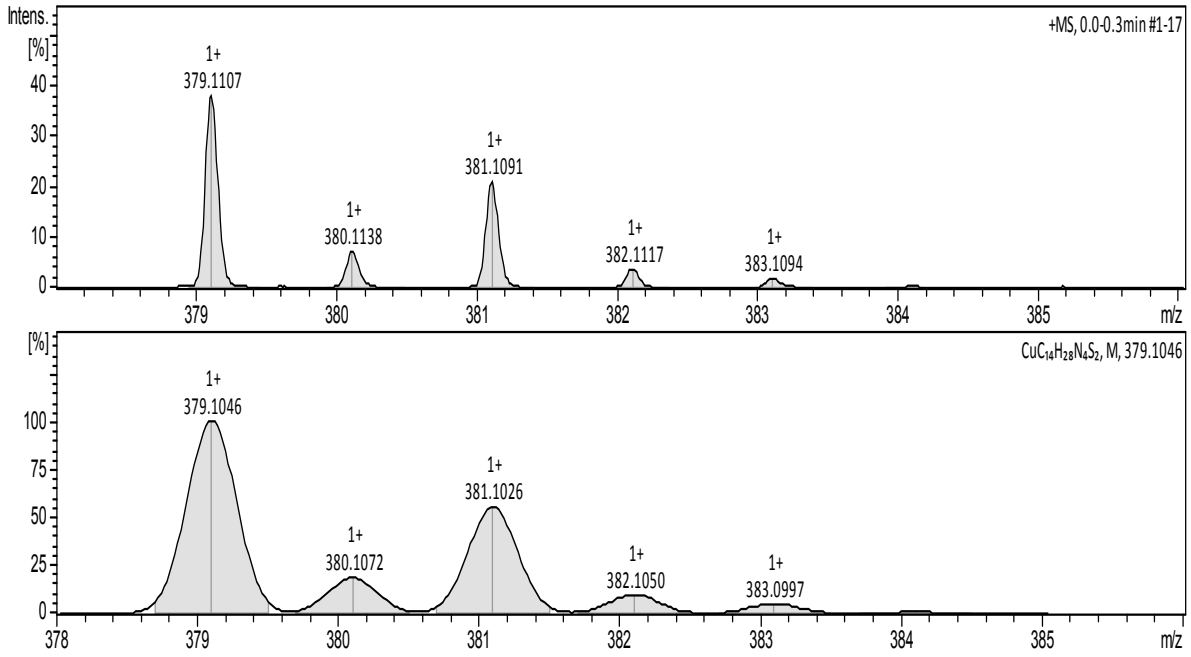

Fig. S11. ESI-mass spectrum due to $[Cu(L\text{-}NBu^n)_2]^+$, species **C** ($CuC_{14}H_{28}N_4S_2$; m/z = calcd, 379.10, obsd 379.11) with isotopic pattern (complex **3**).

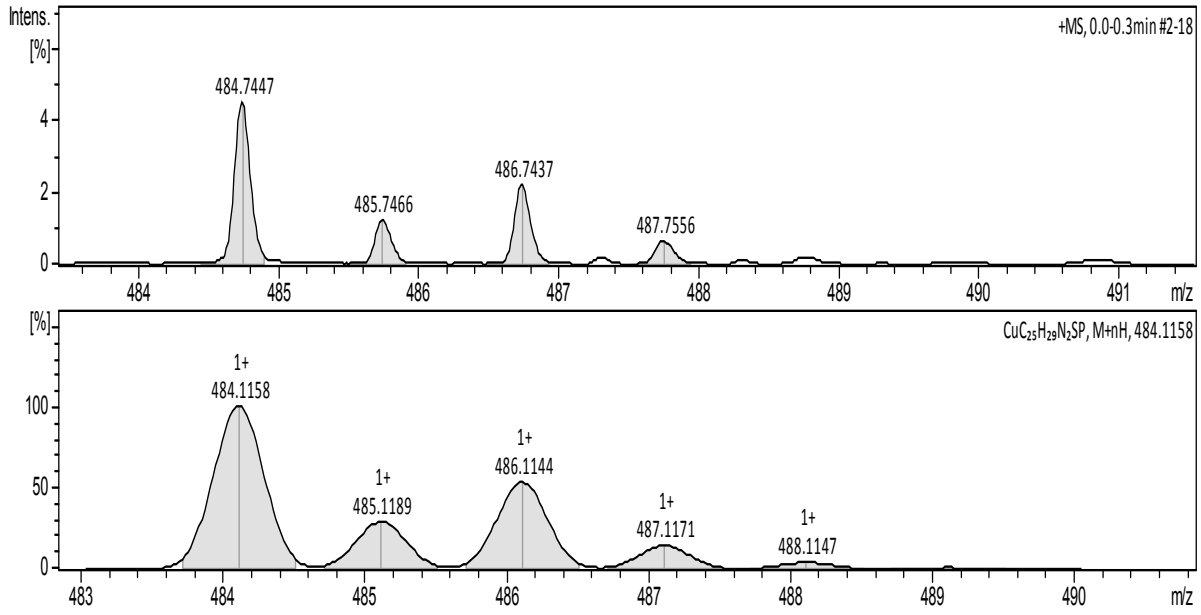

Fig. S12. ESI-mass spectrum due to [Cu(L-NBu^n)(PPh_3) + H]$^+$, species (**B + H$^+$)** ($CuC_{25}H_{29}N_2SP$; m/z = calcd, 484.11, obsd 484.74) with isotopic pattern (complex **4**).

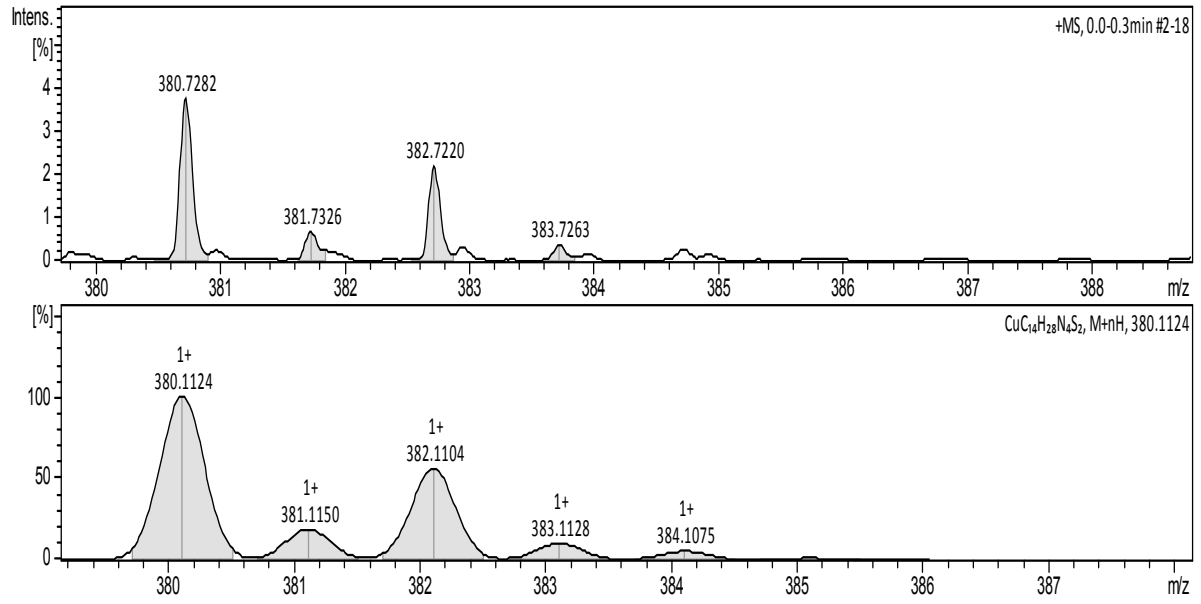

Fig. S13. ESI-mass spectrum due to [Cu(L-NBu^n)$_2$ + H]$^+$, species (**C + H$^+$)** ($CuC_{14}H_{29}N_4S_2$; m/z = calcd, 380.11, obsd 380.72) with isotopic pattern (complex **4**).

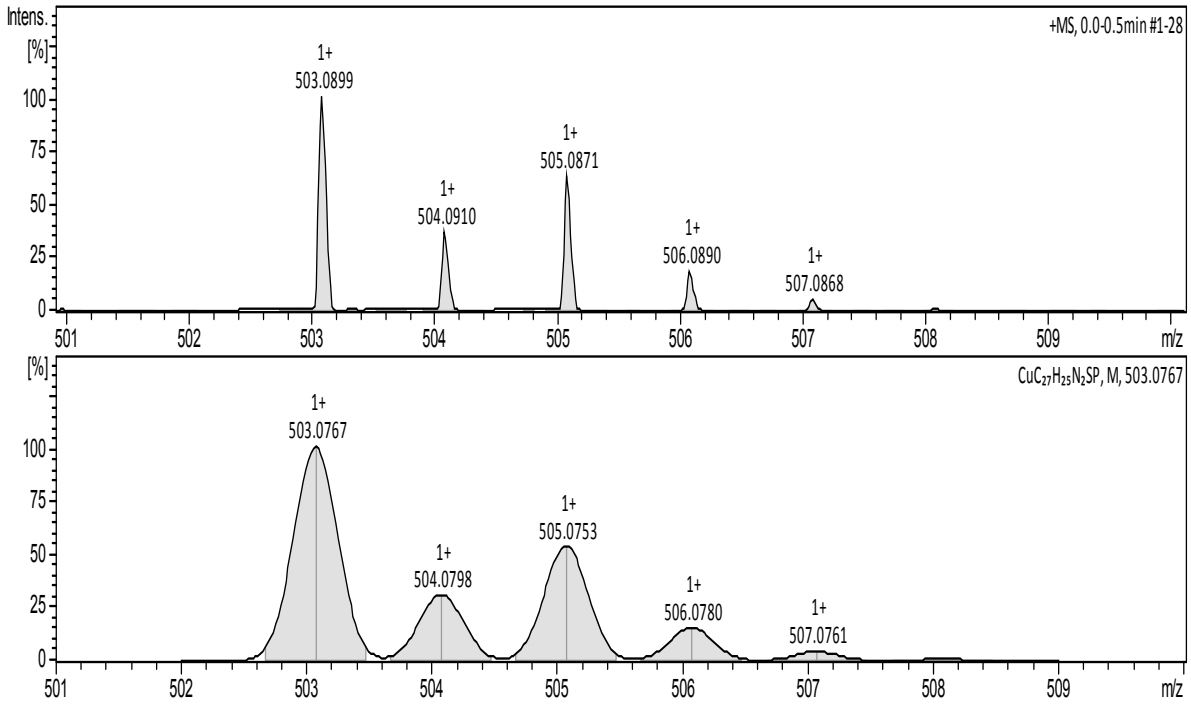

Fig. S14. ESI-mass spectrum due to $[Cu(L\text{-}NPh)(PPh_3)]^+$, species (**B**) ($CuC_{27}H_{25}N_2SP$; m/z = calcd, 503.07, obsd 503.08) with isotopic pattern (complex **5**).

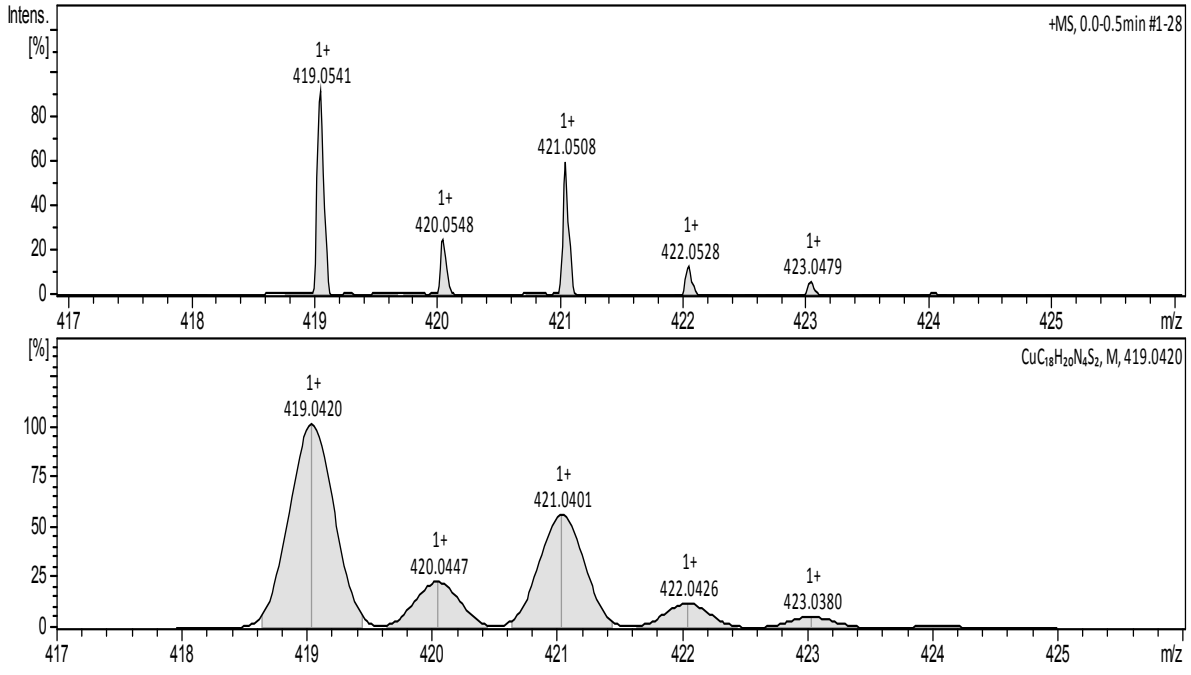

Fig. S15. ESI-mass spectrum due to $[Cu(L\text{-}NPh)_2]^+$, species (**C**) ($CuC_{18}H_{20}N_4S_2$; m/z = calcd, 419.04, obsd 419.05) with isotopic pattern (complex **5**).

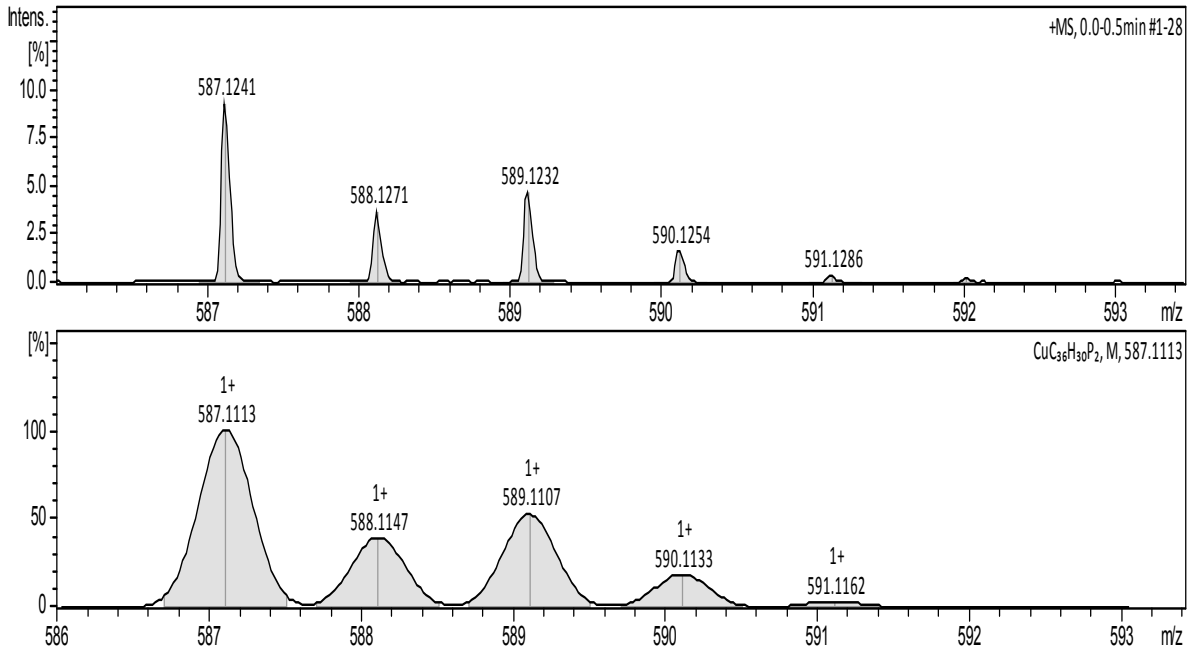

Fig. S16. ESI-mass spectrum due to $[Cu(PPh_3)_2]^+$, species (**D**) ($CuC_{36}H_{30}P_2$; m/z = calcd, 587.11, obsd 587.12) with isotopic pattern (complex **5**).

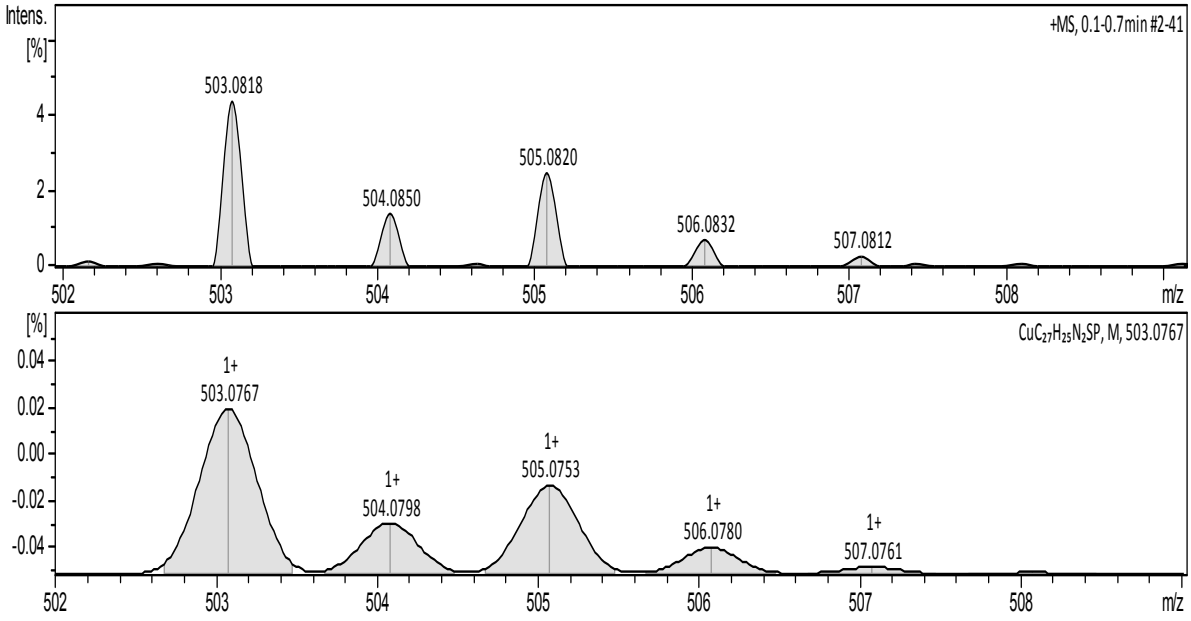

Fig. S17. ESI-mass spectrum due to $[Cu(L\text{-}NPh)(PPh_3)]^+$, species (**B**) ($CuC_{27}H_{25}N_2SP$; m/z = calcd, 503.07, obsd 503.08) with isotopic pattern (complex **6**).

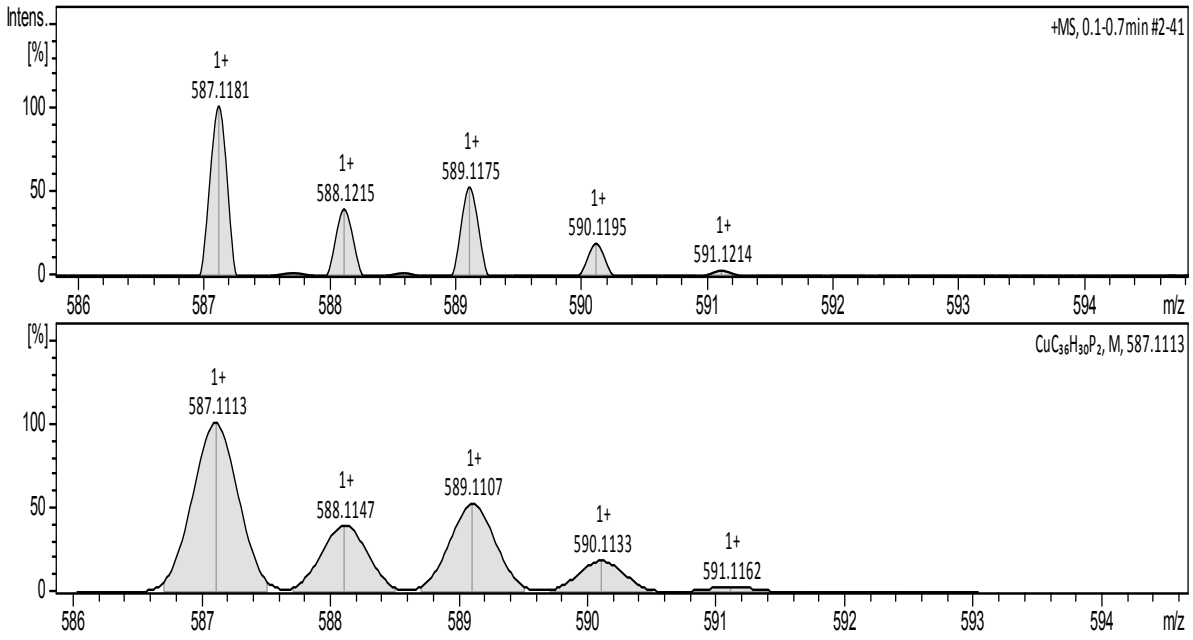

Fig. S18. ESI-mass spectrum due to $[Cu(PPh_3)_2]^+$, species (**D**) ($CuC_{36}H_{30}P_2$; m/z = calcd, 587.11, obsd 587.11) with isotopic pattern (complex **6**).

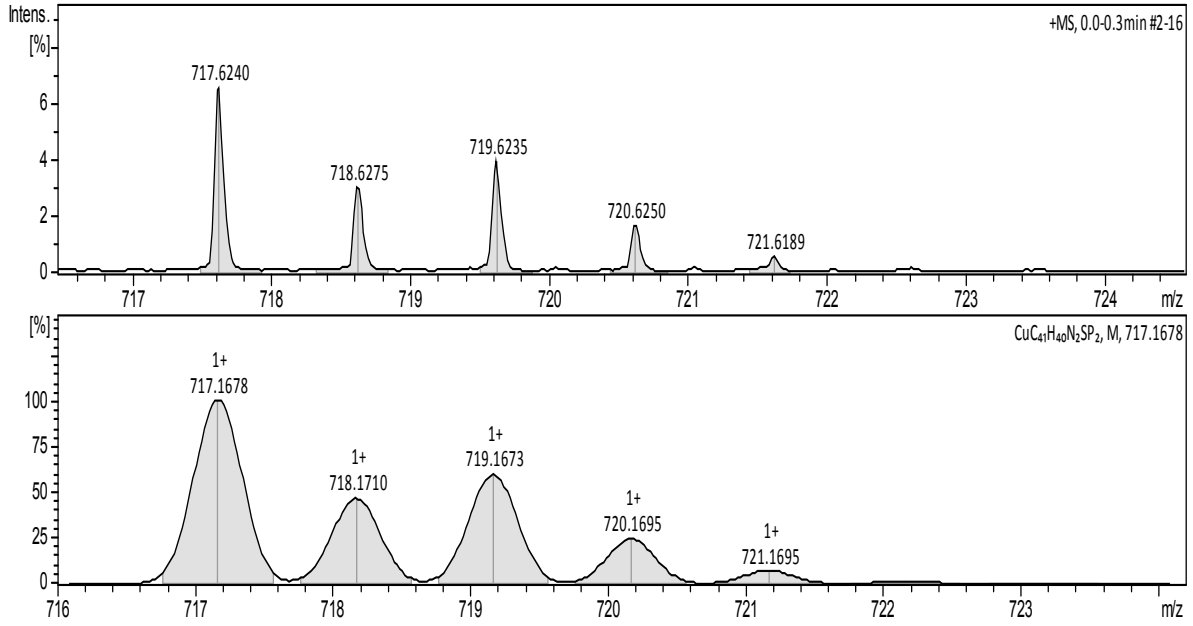

Fig. S19. ESI-mass spectrum due to $[Cu(L\text{-}NEt)(PPh_3)_2]^+$, species (**A**) ($CuC_{41}H_{40}N_2SP_2$; m/z = calcd, 717.16, obsd 717.62) with isotopic pattern (complex **7**).

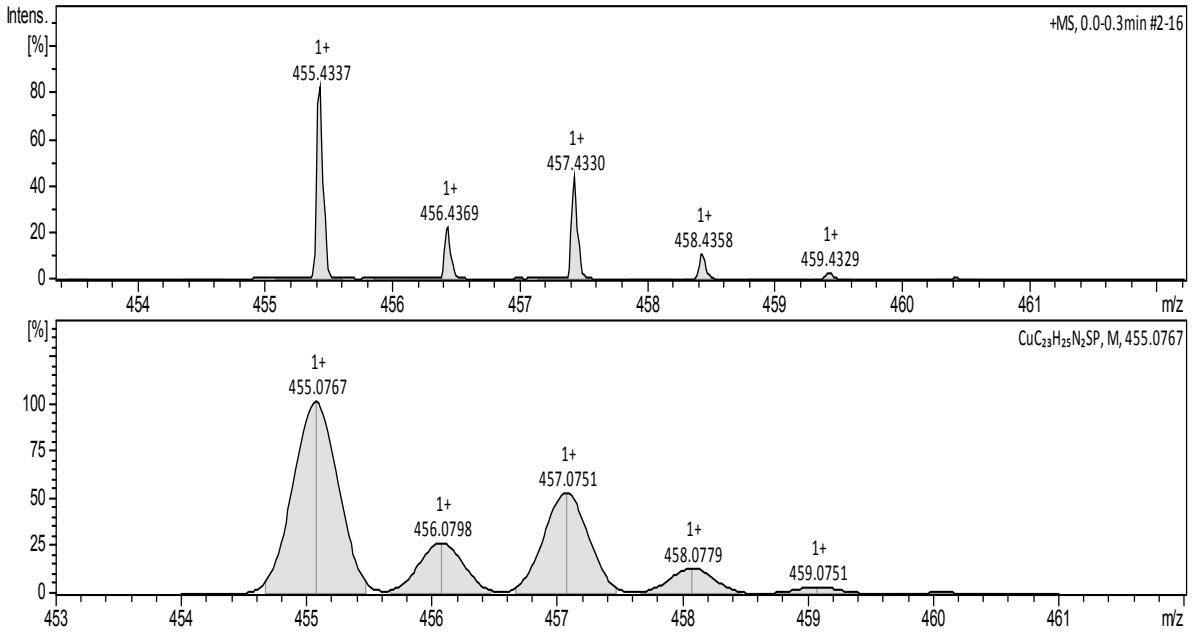

Fig. S20. ESI-mass spectrum due to $[Cu(L\text{-}NEt)(PPh_3)]^+$, species (**B**) ($CuC_{23}H_{25}N_2SP$; m/z = calcd, 455.07, obsd 455.43) with isotopic pattern (complex **7**).

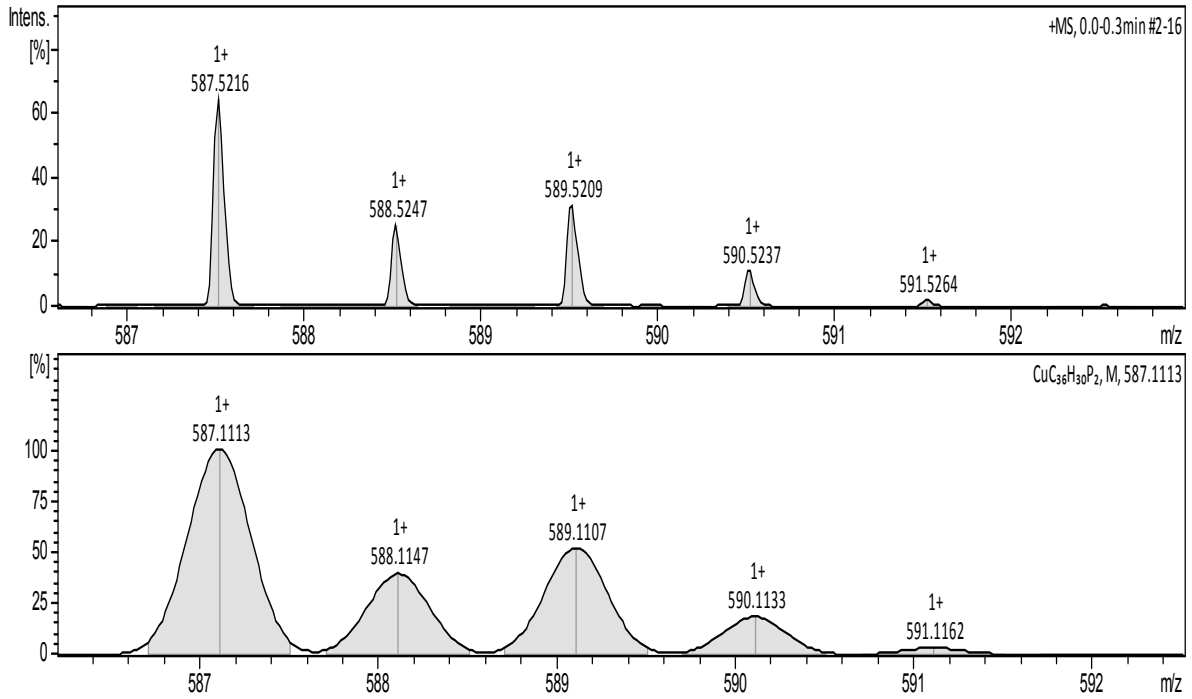

Fig. S21. ESI-mass spectrum due to $[Cu(PPh_3)_2]^+$, species (**D**) ($CuC_{36}H_{30}P_2$; m/z = calcd, 587.11, obsd 587.52) with isotopic pattern (complex **7**).

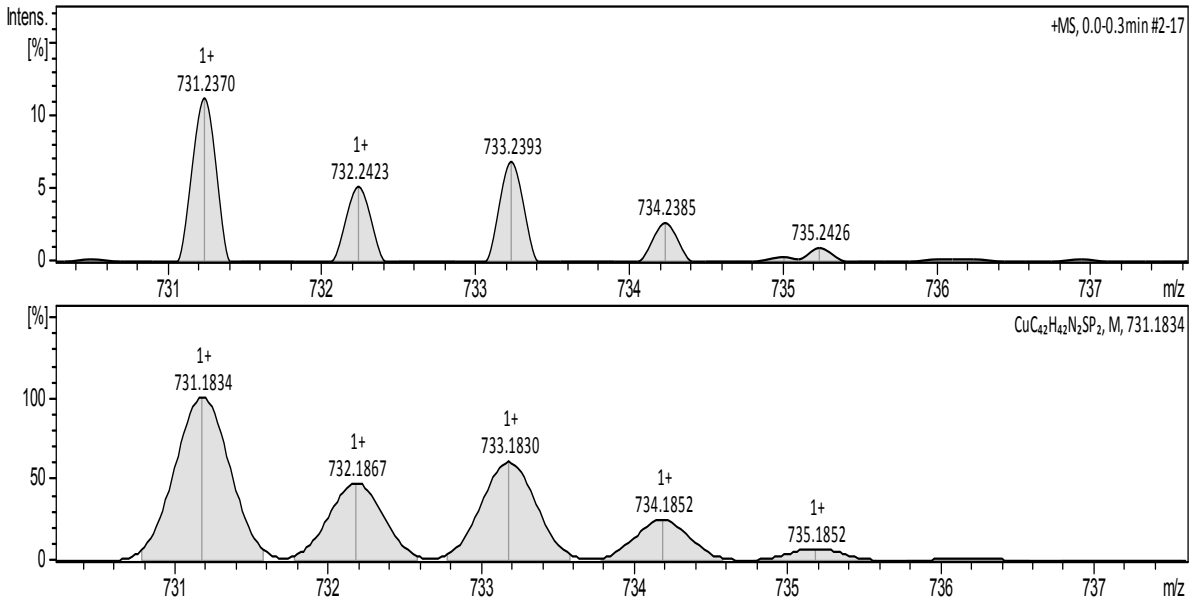

Fig. S22. ESI-mass spectrum due to $[Cu(L\text{-}NPr^n)(PPh_3)_2]^+$, species (**A**) ($CuC_{42}H_{42}N_2SP_2$; m/z = calcd, 731.18, obsd 731.23) with isotopic pattern (complex **9**).

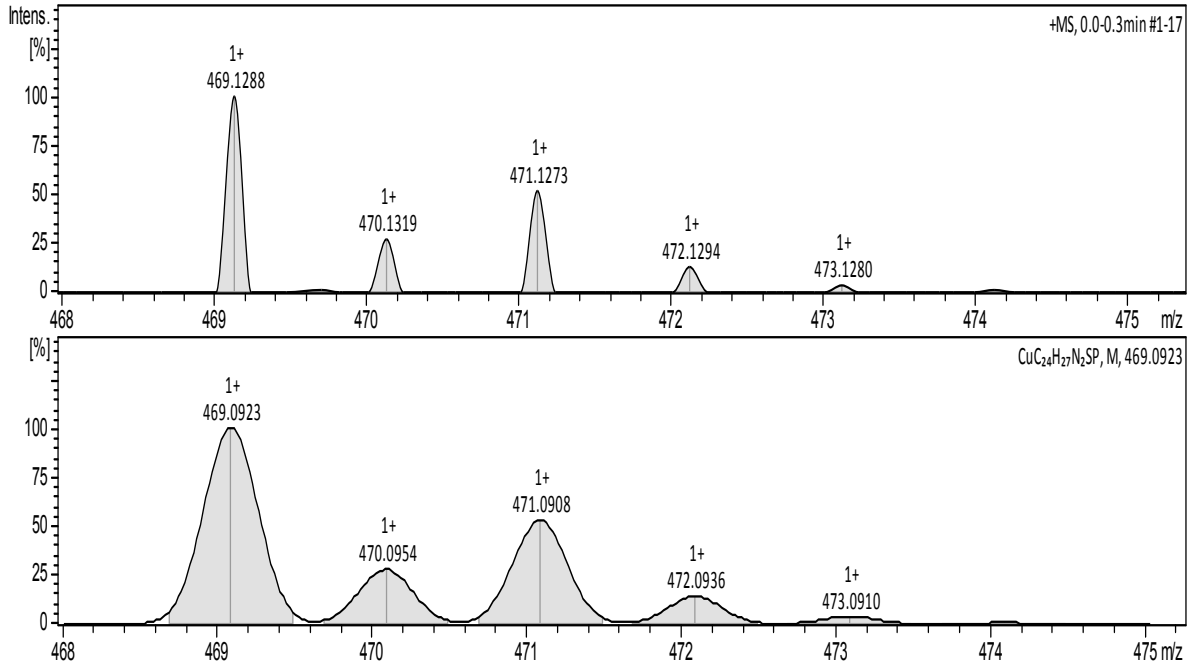

Fig. S23. ESI-mass spectrum due to $[Cu(L\text{-}NPr^n)(PPh_3)]^+$, species (**B**) ($CuC_{24}H_{27}N_2SP$; m/z = calcd, 469.09, obsd 469.12) with isotopic pattern (complex **9**).

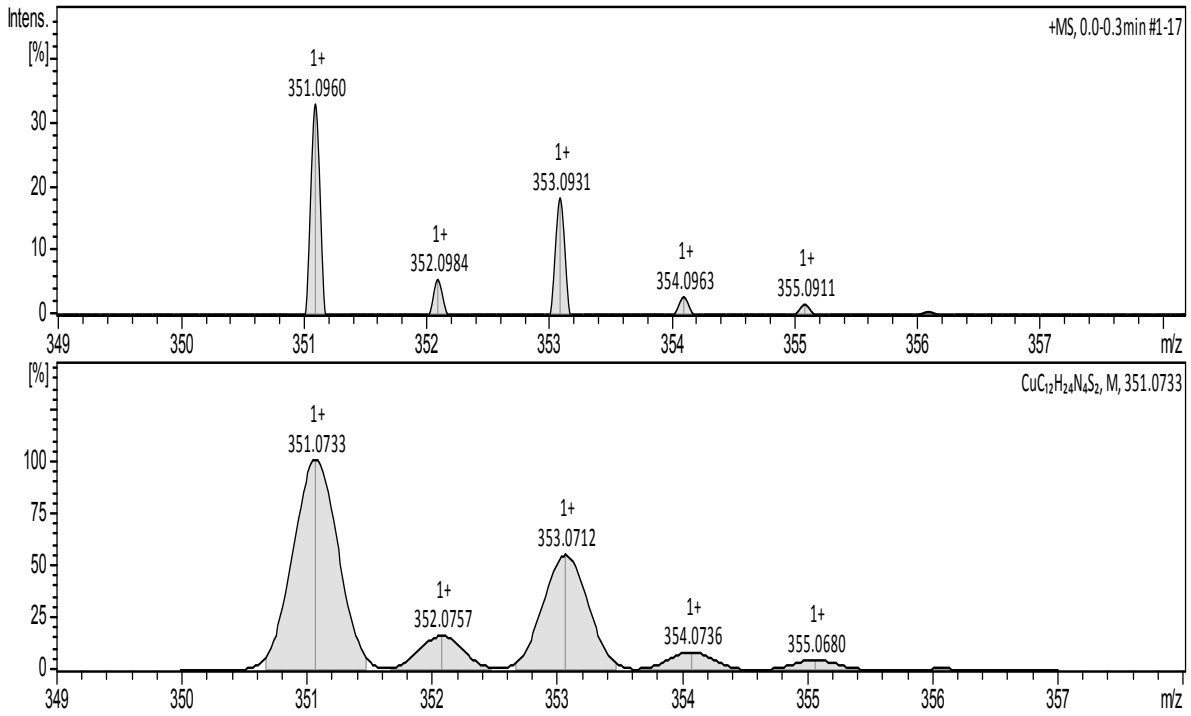

Fig. S24. ESI-mass spectrum due to $[Cu(L\text{-}NPr^n)_2]^+$, species (**C**) ($CuC_{12}H_{24}N_4S_2$; m/z = calcd, 351.07, obsd 351.09) with isotopic pattern (complex **9**).

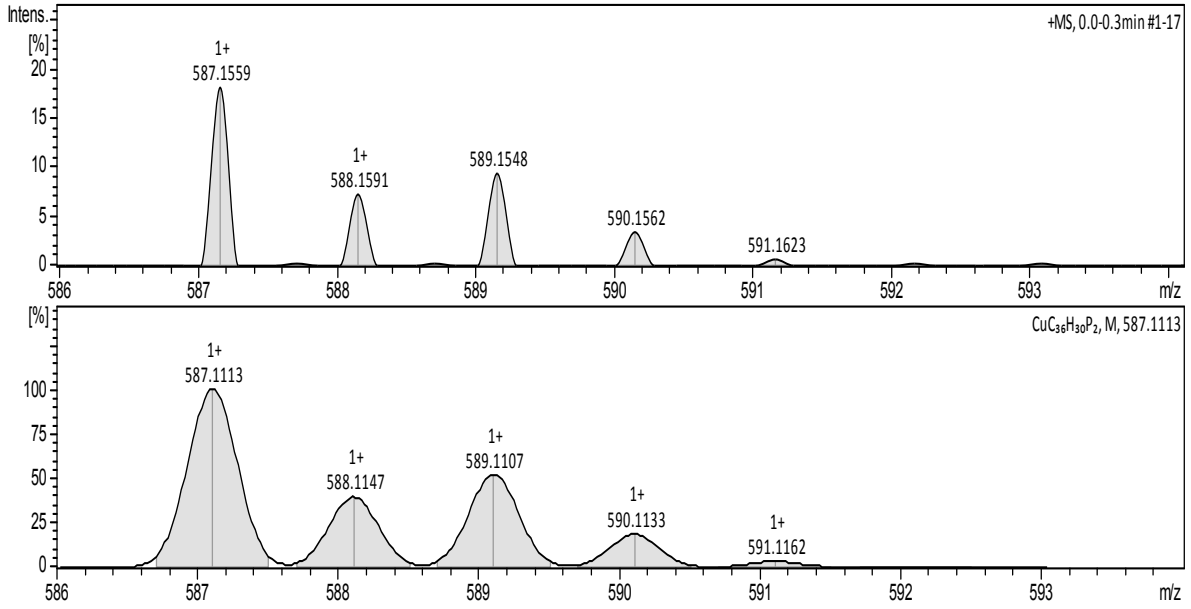

Fig. S25. ESI-mass spectrum due to $[Cu(PPh_3)_2]^+$, species (**D**) ($CuC_{36}H_{30}P_2$; m/z = calcd, 587.11, obsd 587.15) with isotopic pattern (complex **9**).

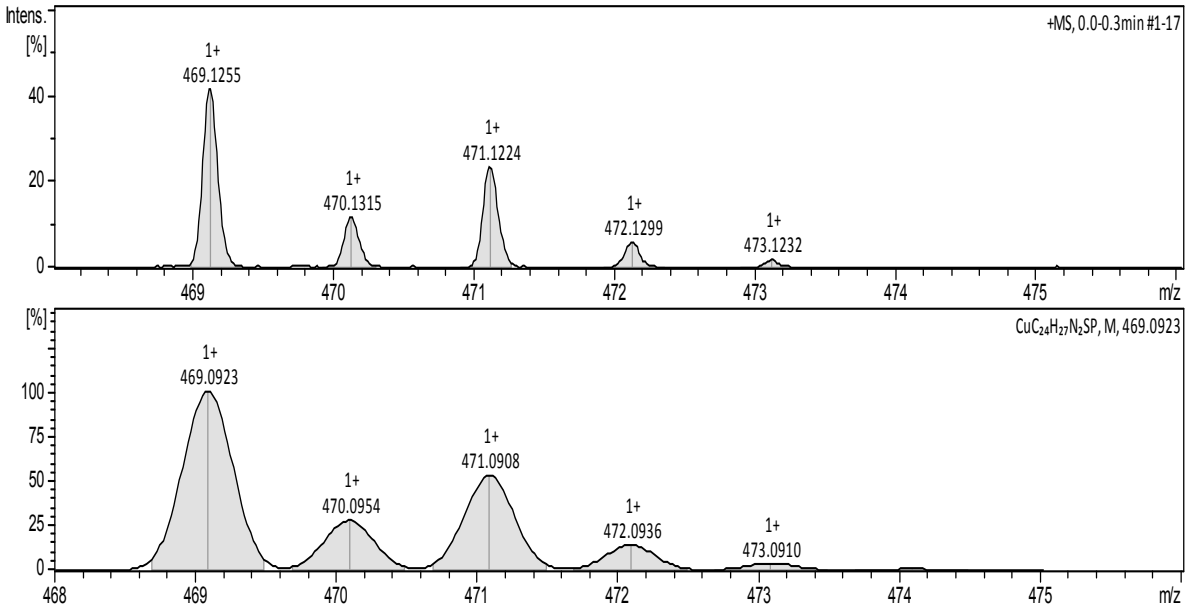

Fig. S26. ESI-mass spectrum due to $[Cu(L\text{-}NPr^n)(PPh_3)]^+$, species (**B**) ($CuC_{24}H_{27}N_2SP$; m/z = calcd, 469.09, obsd 469.12) with isotopic pattern (complex **10**).

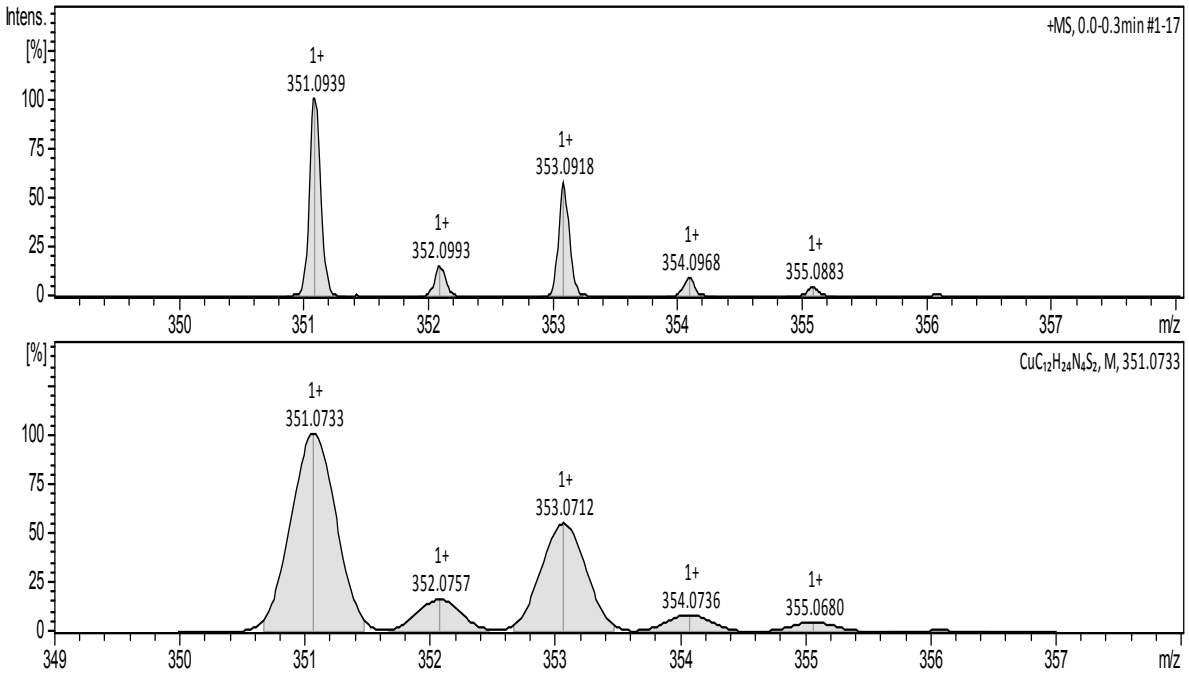

Fig. S27. ESI-mass spectrum due to $[Cu(L\text{-}NPr^n)_2)]^+$, species (**C**) ($CuC_{12}H_{24}N_4S_2$; m/z = calcd, 351.07, obsd 351.09) with isotopic pattern (complex **10**).

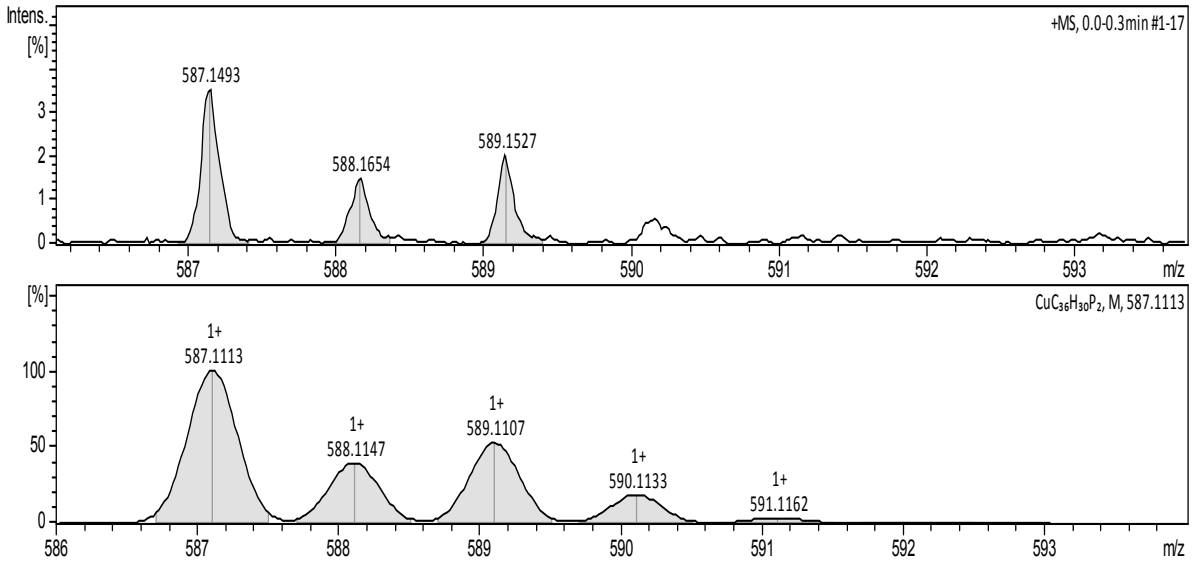

Fig. S28. ESI-mass spectrum due to $[Cu(PPh_3)_2)]^+$, species (**D**) ($CuC_{36}H_{30}P_2$; m/z = calcd, 587.11, obsd 587.14) with isotopic pattern (complex **10**).

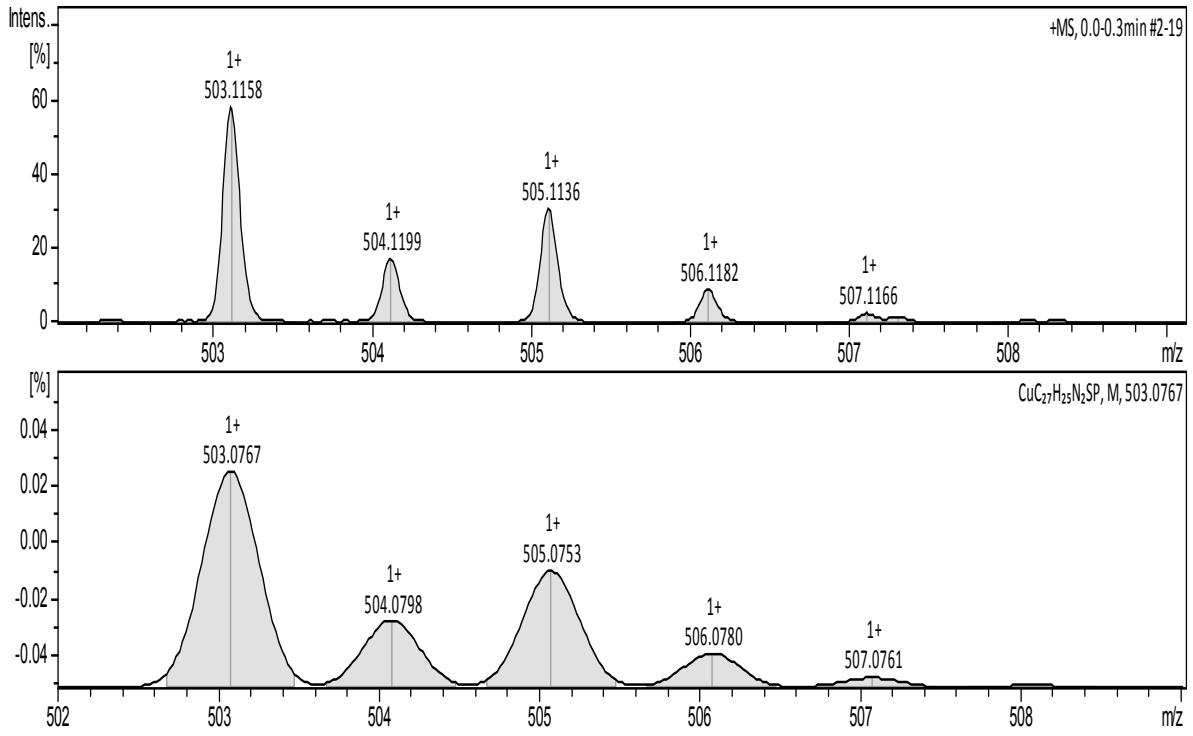

Fig. S29. ESI-mass spectrum due to $[Cu(L\text{-}NPh)(PPh_3)]^+$, species (**B**) ($CuC_{27}H_{25}N_2SP$; m/z = calcd, 503.07, obsd 503.11) with isotopic pattern (complex **11**).

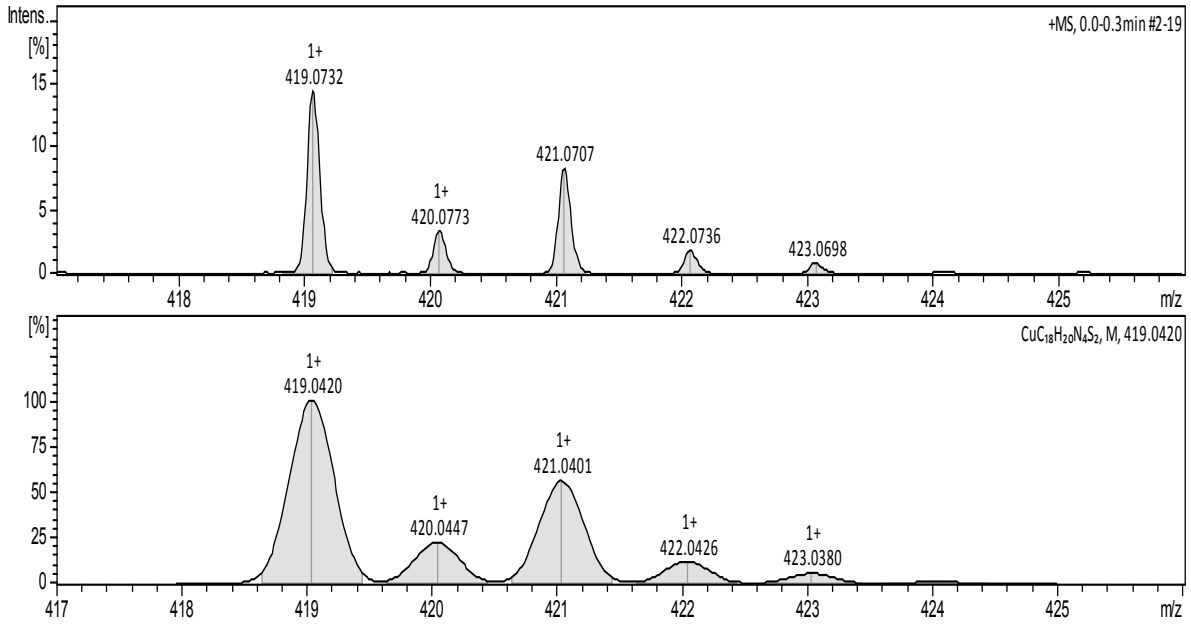

Fig. S30. ESI-mass spectrum due to $[Cu(L\text{-}NPh)_2]^+$, species (**C**) ($CuC_{18}H_{20}N_4S_2$; m/z = calcd, 419.04, obsd 419.07) with isotopic pattern (complex **11**).

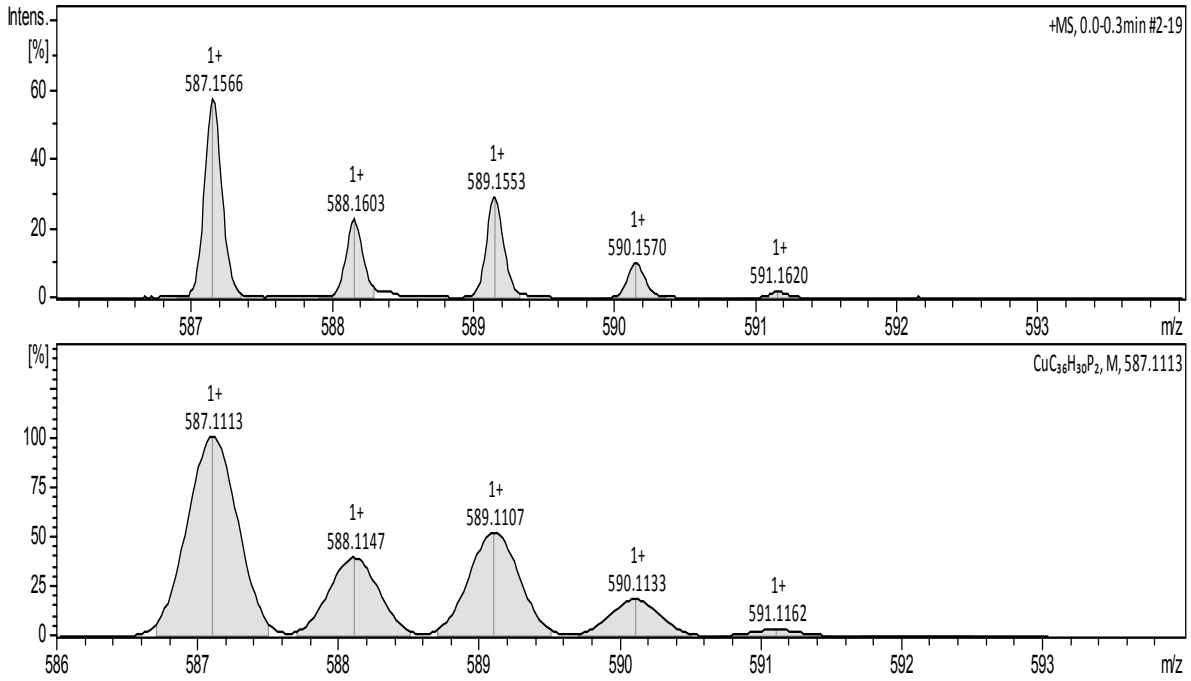

Fig. S31. ESI-mass spectrum due to $[Cu(PPh_3)_2]^+$, species (**D**) ($CuC_{36}H_{30}P_2$; m/z = calcd, 587.11, obsd 587.15) with isotopic pattern (complex **11**).

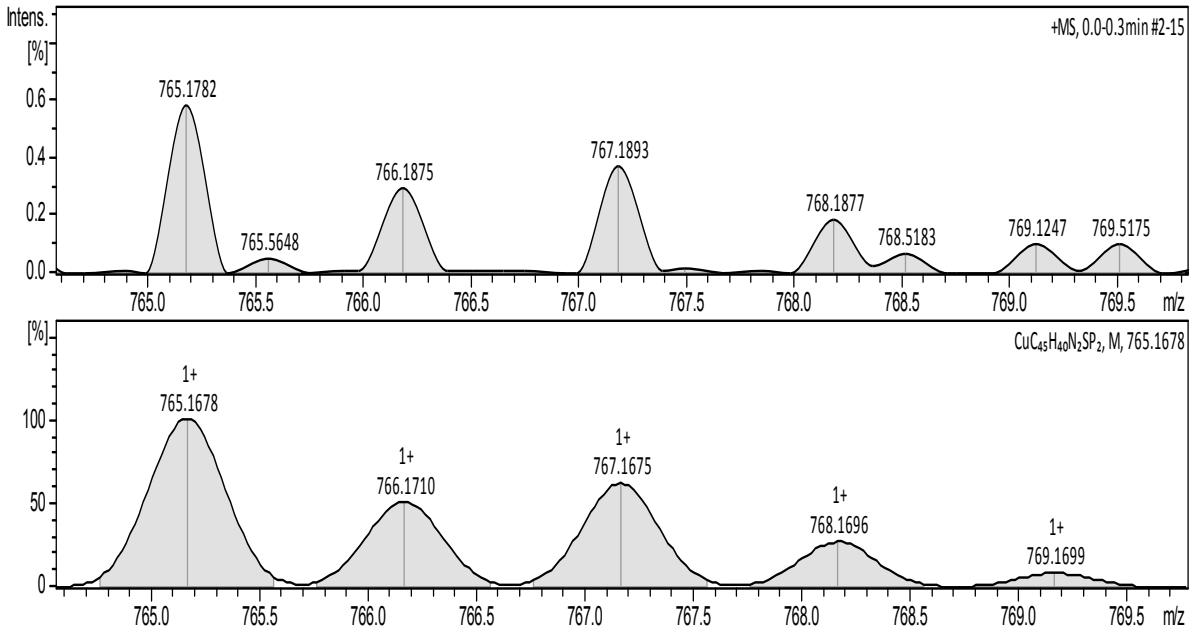

Fig. S32. ESI-mass spectrum due to $[Cu(L\text{-}NPh)(PPh_3)_2]^+$, species (**A**) ($CuC_{45}H_{40}N_2SP_2$; m/z = calcd, 765.16, obsd 765.17) with isotopic pattern (complex **12**).

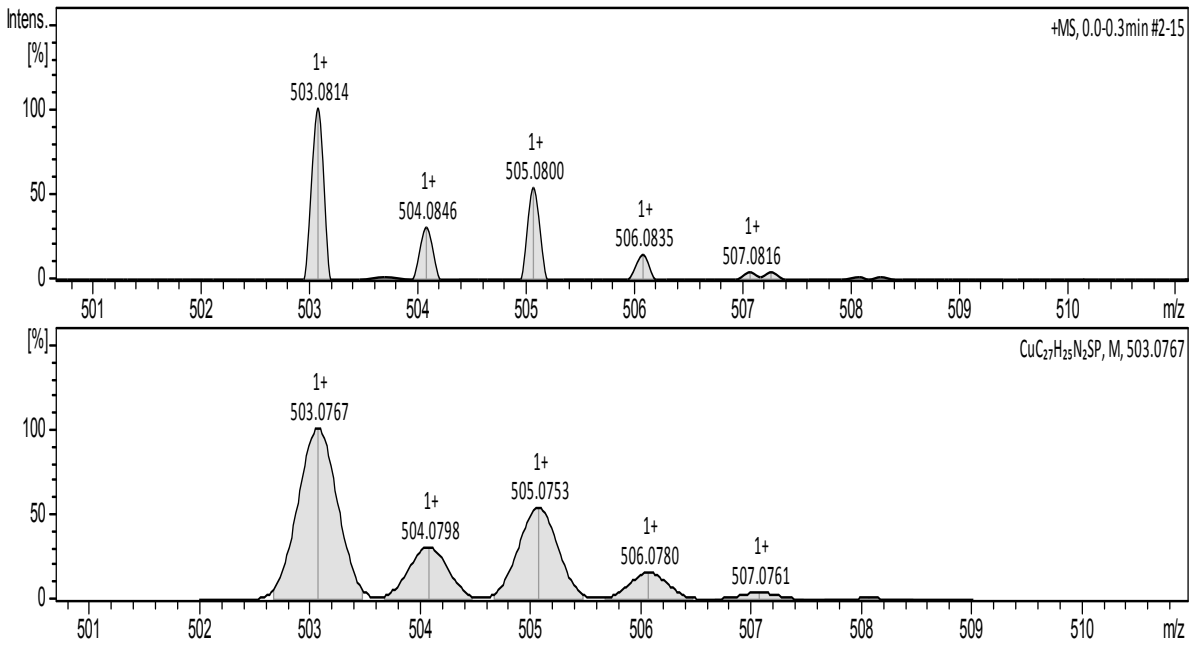

Fig. S33. ESI-mass spectrum due to $[Cu(L\text{-}NPh)(PPh_3)]^+$, species (**B**) ($CuC_{27}H_{25}N_2SP$; m/z = calcd, 503.07, obsd 503.08) with isotopic pattern (complex **12**).

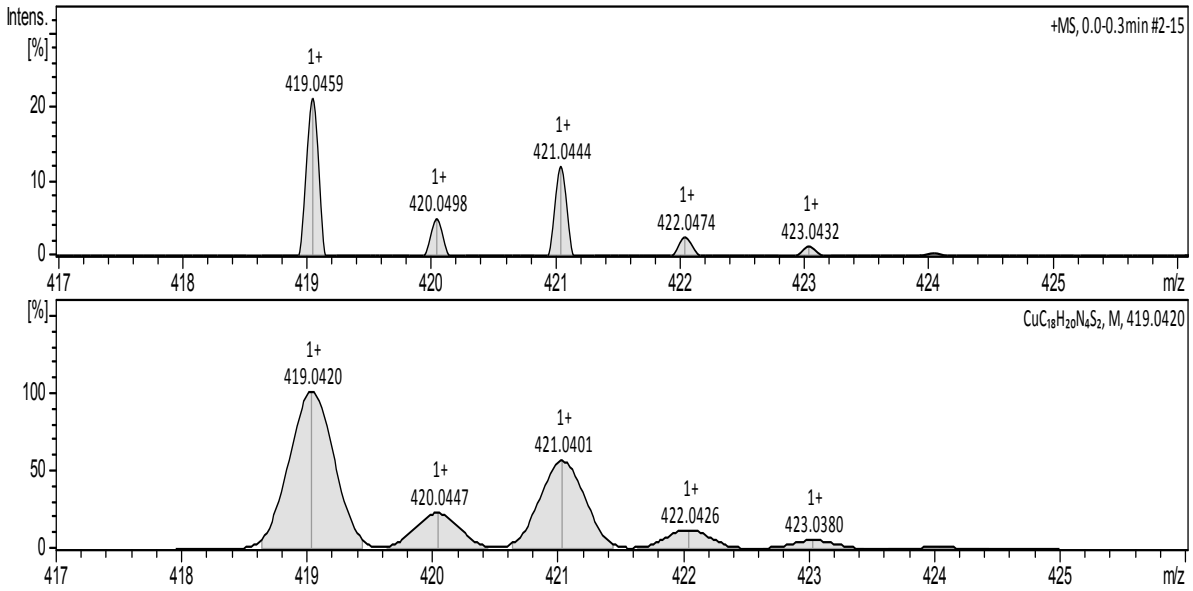

Fig. S34. ESI-mass spectrum due to $[Cu(L\text{-}NPh)_2]^+$, species (**C**) ($CuC_{18}H_{20}N_4S_2$; m/z = calcd, 419.04, obsd 419.04) with isotopic pattern (complex **12**).

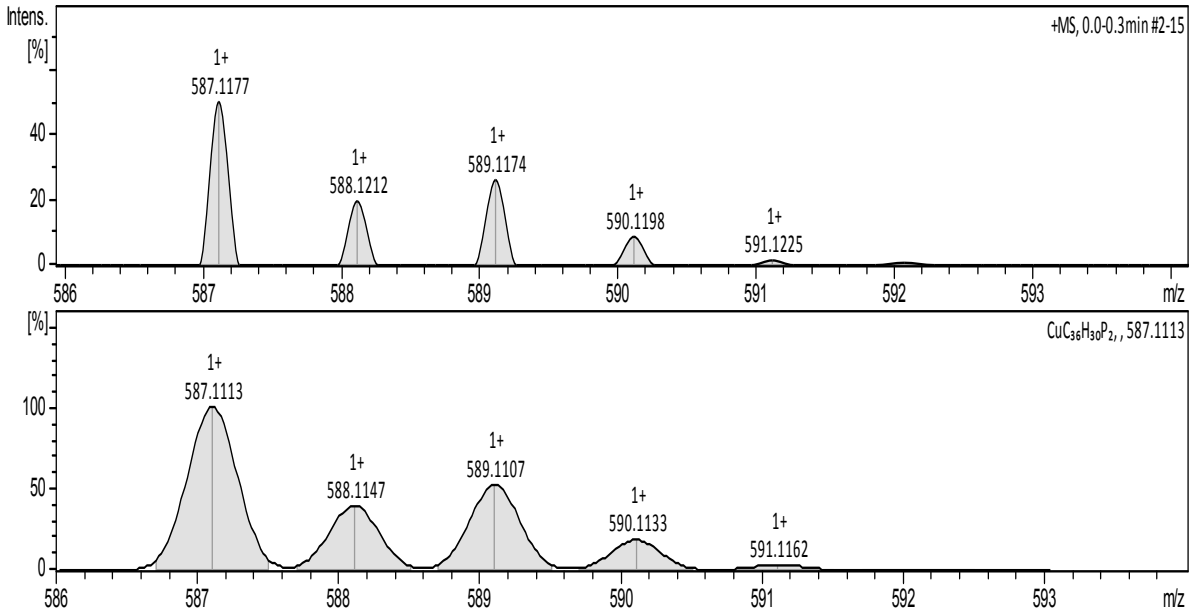

Fig. S35. ESI-mass spectrum due to $[Cu(PPh_3)_2]^+$, species (**D**) ($CuC_{36}H_{30}P_2$; m/z = calcd, 587.11, obsd 587.11) with isotopic pattern (complex **12**).

2S. IR spectra.

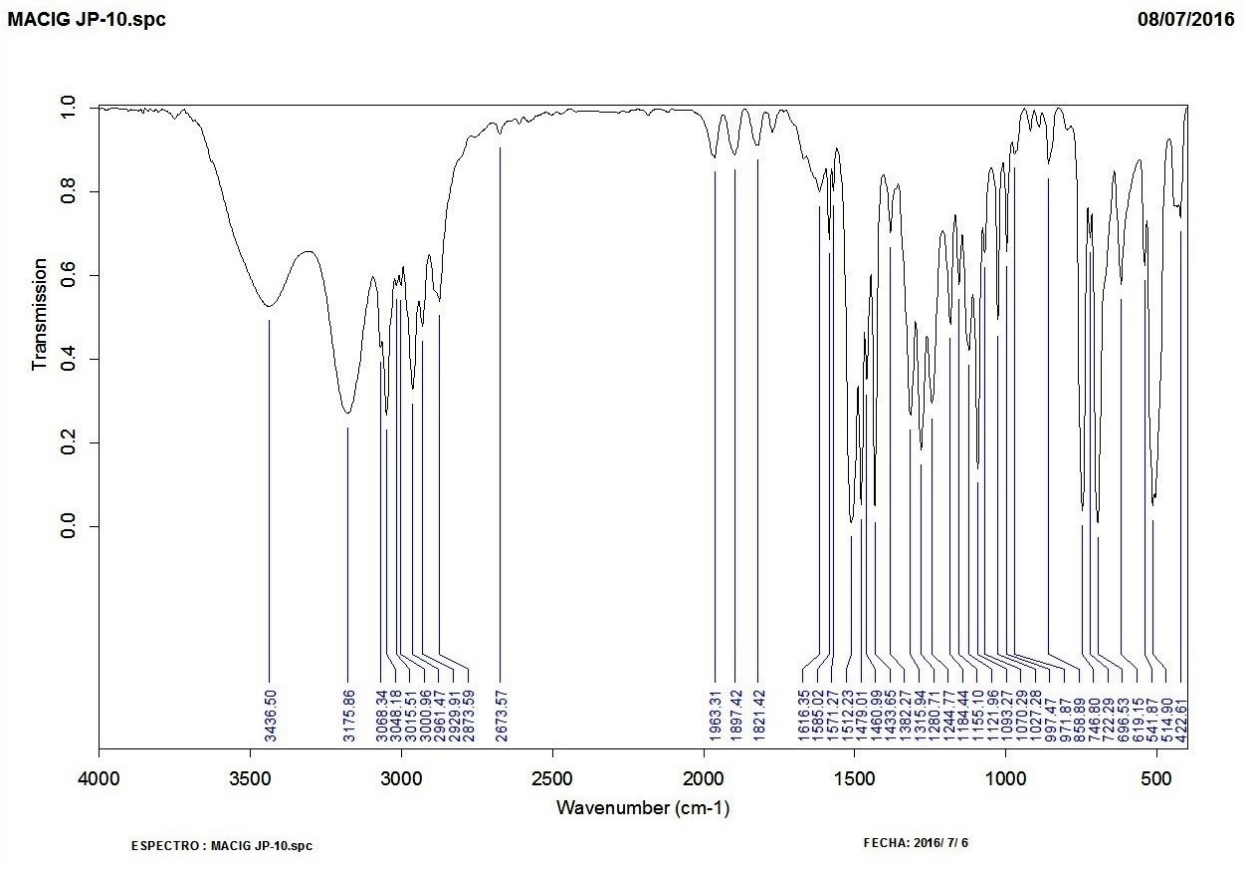

Fig. S36. IR spectrum of complex $[CuCl(L\text{-}NPr^n)(PPh_3)_2]$ **(1)**.

IR (KBr, absorption bands): 3176 s, 3068 m, 3048 s, 3016 w, 3001 w, 2961 s, 2930 w, 2874 w, 1616 w, 1585 w, 1571 w, 1512 s, 1479 s, 1461 m, 1434 s, 1382 w, 1316 s, 1281 s, 1245 m, 1184 m, 1155 w, 1122 m, 1093 s, 1070 w, 1027 m, 997 w, 972 w, 859 w, 747 s, 722 w, 696 s, 619 w, 542 w, 515 s, 423 w cm^{-1}.

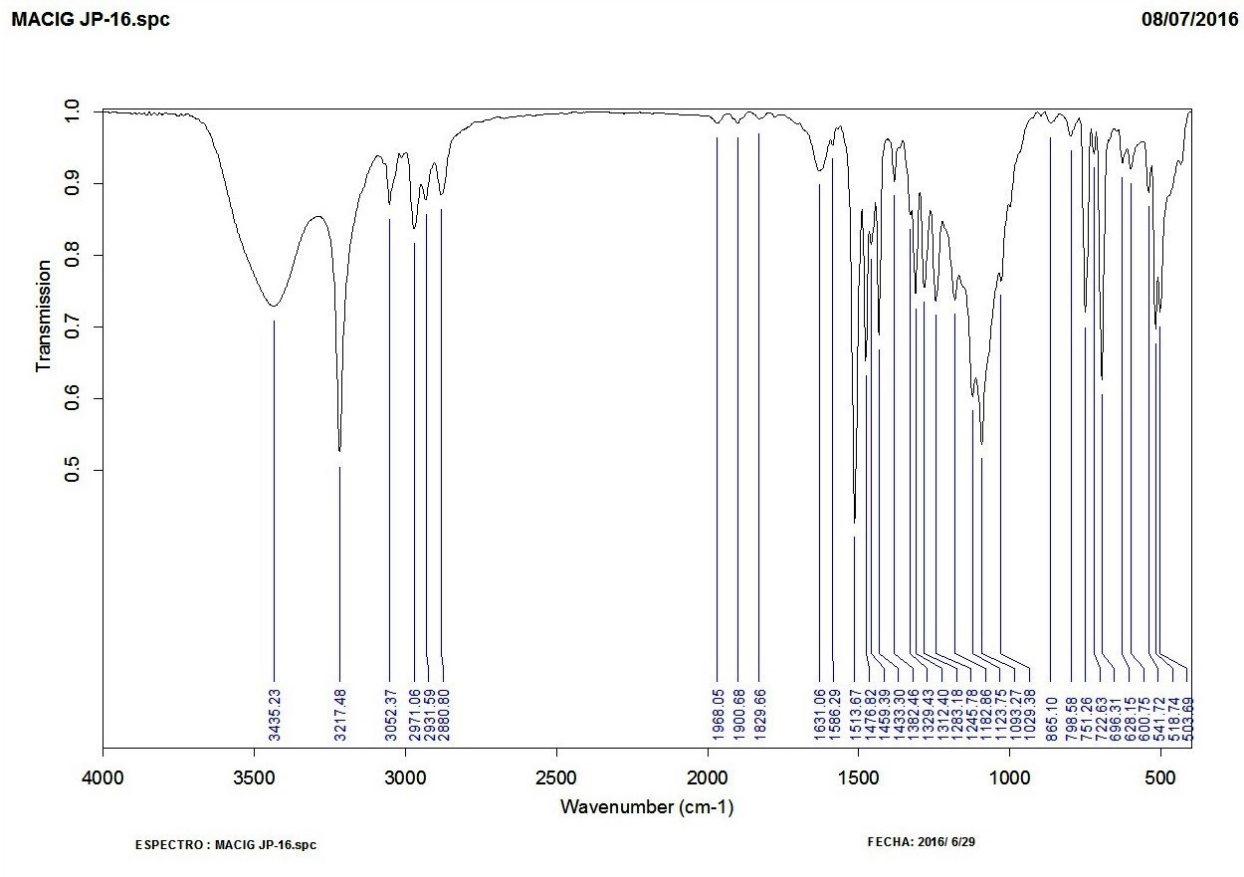

Fig. S37. IR spectrum of complex [CuBr(L-NPr^n)(PPh$_3$)$_2$] **(2)**.

IR (KBr, absorption bands) : 3217 s, 3052 w, 2971 w, 2932 w, 2888 w, 1631 w, 1586 w, 1514 s, 1477 m, 1459 w, 1433 m, 1382 w, 1312 m,1283 m, 1246 m, 1183 w, 1124 m, 1093 s, 1029 w, 865 w, 799 w, 751 m, 723 m, 696 m, 628 w, 601 w, 542 w, 519 m, 504 m cm^{-1}.

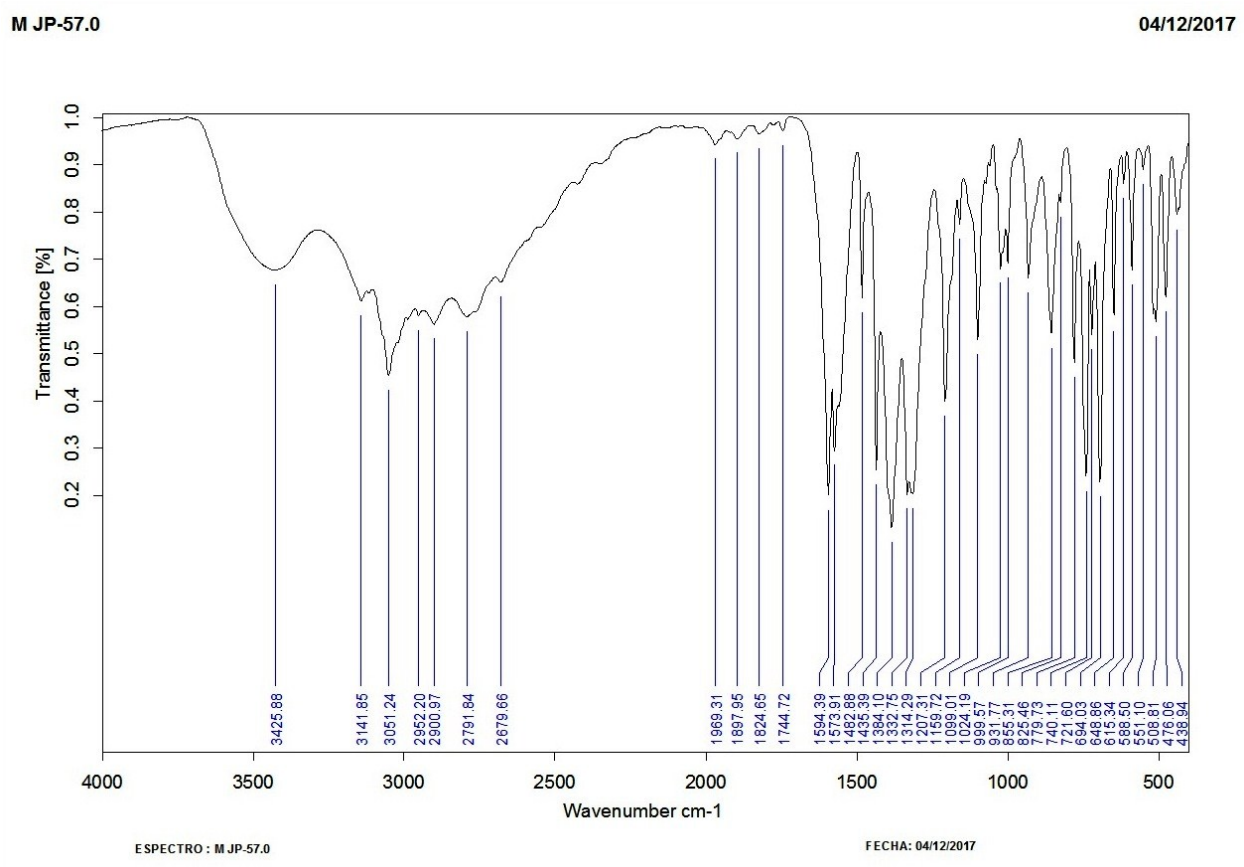

Fig. S38. IR spectrum of complex [CuCl(L-NBu^n)(PPh_3)$_2$] **(3)**.

IR (KBr, absorption bands): 3142 w, 3051 m, 2952 w, 2901 w, 2888 w, 1631 w, 1574 s, 1483 m, 1435 s, 1384 s, 1332 s, 1314 s, 1207 s, 1160 w, 1099 m, 1024 m, 999 m, 932 m, 855 m, 825 w, 780 m, 740 s, 722 m, 694 s, 649 m, 615 w, 588 m, 509 m, 476 w cm^{-1}.

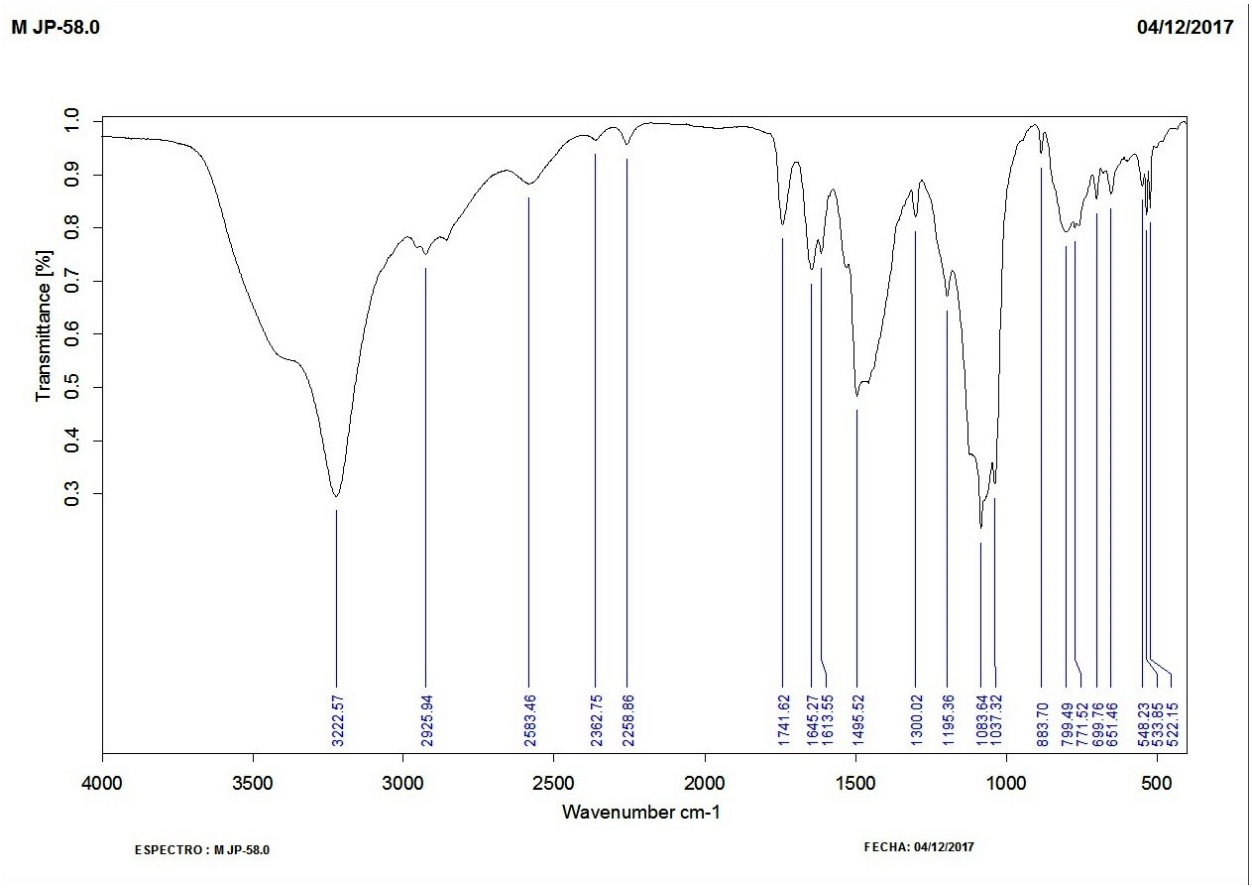

Fig. S39. IR spectrum of complex $[CuI(L\text{-}NBu^n)(PPh_3)_2]$**(4)**.

IR (KBr, absorption bands): 3222 s, 2926 w, 1614 w, 1496 s, 1300 w, 1332 s, 1314 s, 1207 s, 1155 w, 1084 s, 1037 m, 884 w, 799 w, 771 w, 700 w, 651 w, 548 w, 534 w, 522 w cm^{-1}.

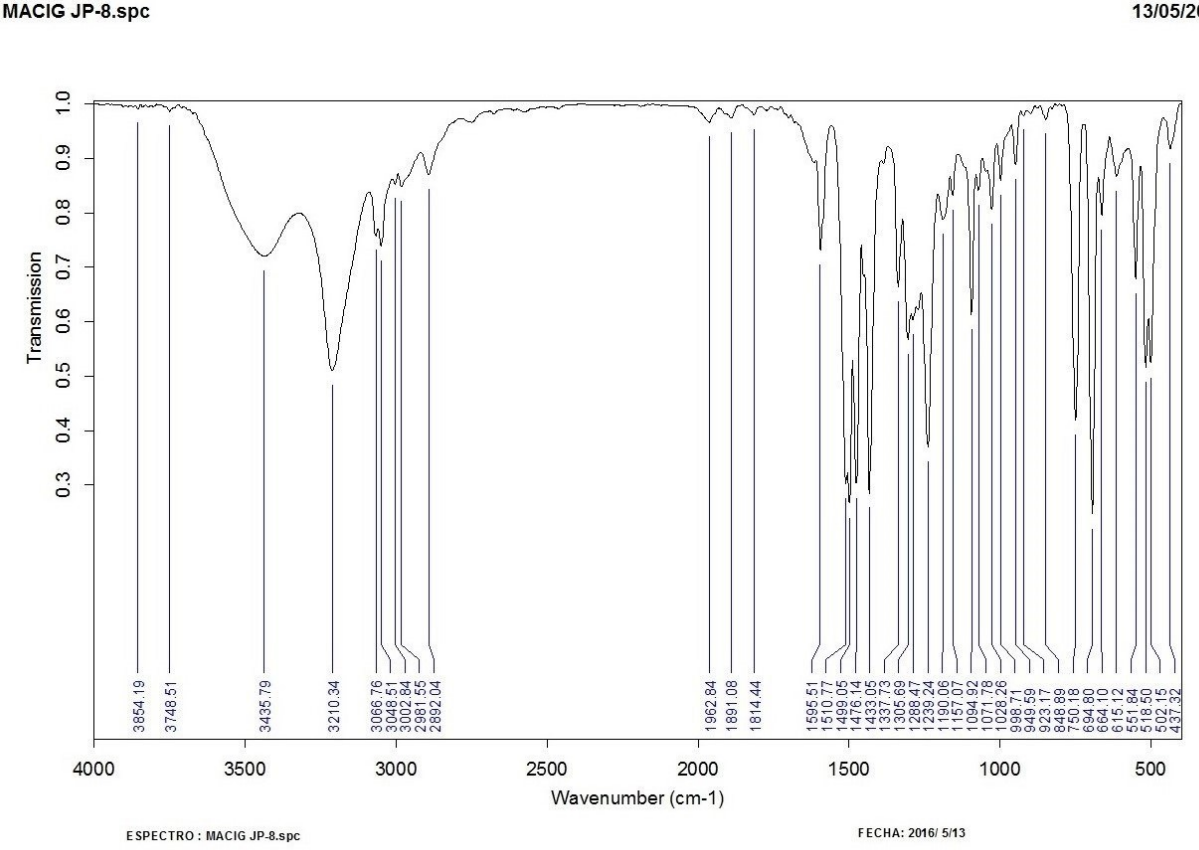

Fig. S40. IR spectrum of complex $[CuBr(L\text{-}NPh)_2(PPh_3)]$ **(5)**.

IR (KBr, absorption bands): 3210 s, 3067 w, 3048 w, 3003 w, 2982 w, 2892 w, 1596 w, 1510 s, 1499 s, 1476 s, 1433 s, 1338 m, 1306 m, 1288 m, 1239 m, 1190 w, 1157 w, 1095 m, 1072 w, 1028 w, 999 w, 950 w, 923 w, 849 w, 750 s, 695 s, 615 w, 552 w, 518 w, 502 m, 437 w cm^{-1}.

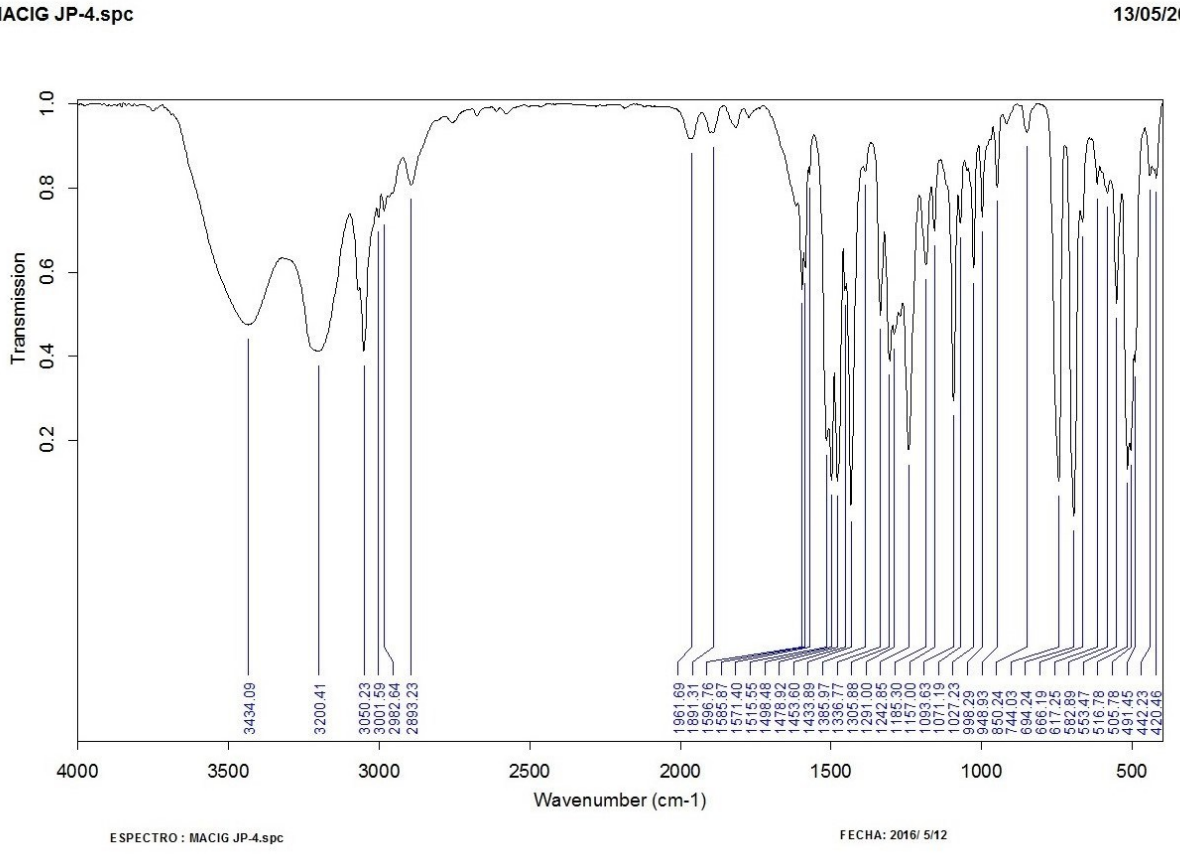

Fig. S41. IR spectrum of complex [CuI(L-NPh)(PPh_3)$_2$] **(6)**.

IR (KBr, absorption bands): 3200 s, 3050 s, 3002 w, 2983 w, 2893 w, 1597 m, 1586 m, 1571 w, 1515 s, 1498 s, 1479 s, 1454 w, 1434 s, 1386 w, 1337 s, 1306 s, 1291 s, 1243 s, 1185 w, 1157 w, 1094 s, 1071 w, 1027 m, 998 w, 949 w, 850 w, 744 s, 694 s, 666 s, 617 w, 583 w, 553 m, 517 s, 506 s, 491 m, 442 w, 420 w cm^{-1}.

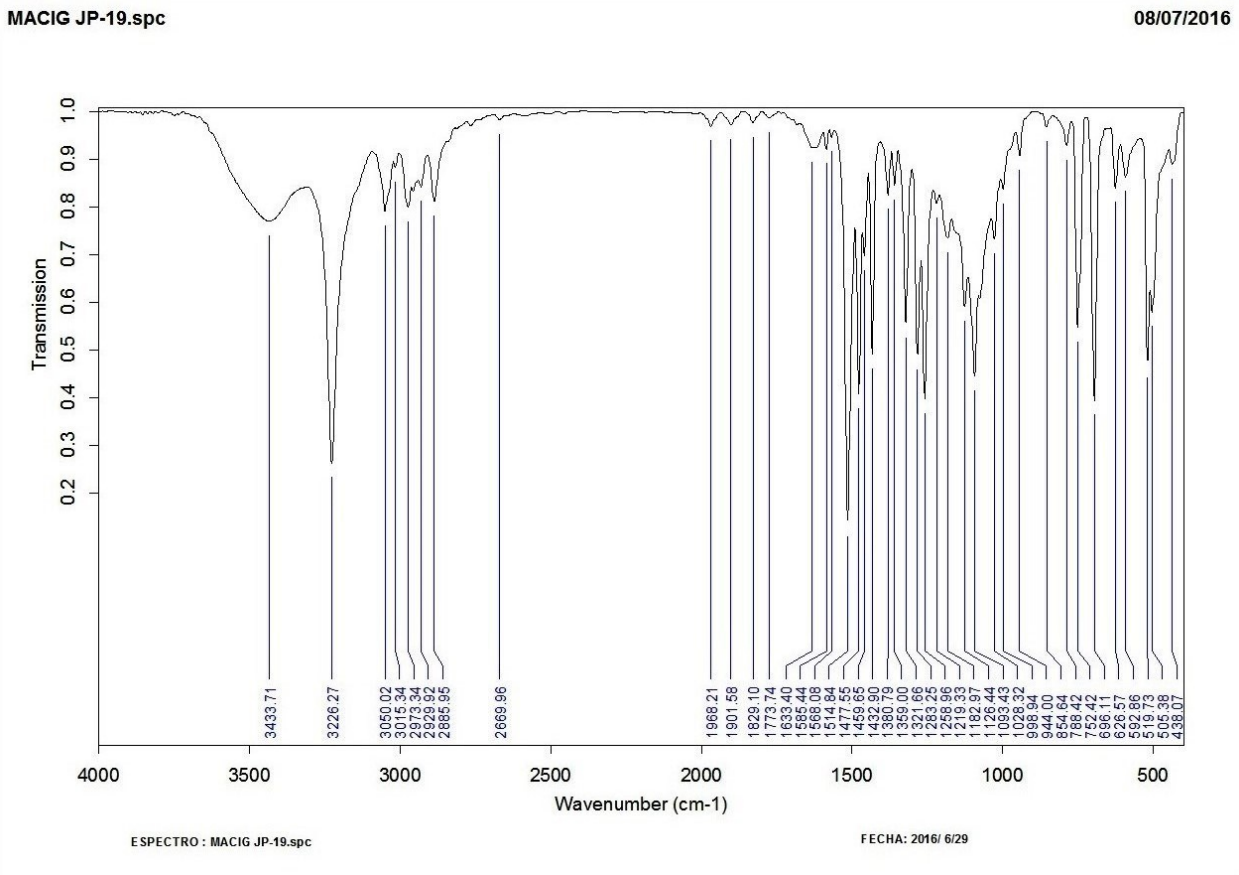

Fig. S42. IR spectrum of complex $[Cu_2(\mu\text{-}Br)_2(L\text{-}NEt)_2(PPh_3)_2]$ **(7)**.

IR (KBr, absorption bands): 3226 s, 3050 w, 3015 w, 2973 w, 2930 w, 2886 w, 1633 w, 1585 w, 1568 w, 1515 s, 1478 s, 1460 w, 1433 m, 1381 w, 1359 w, 1322 m, 1283 m, 1259 m, 1219 w, 1183 w, 1126 w, 1093 m, 1028 w, 999 w, 944 w, 855 w, 788 w, 752 m, 696 s, 626 w, 593 w, 520 m, 505 m, 438 w cm^{-1}.

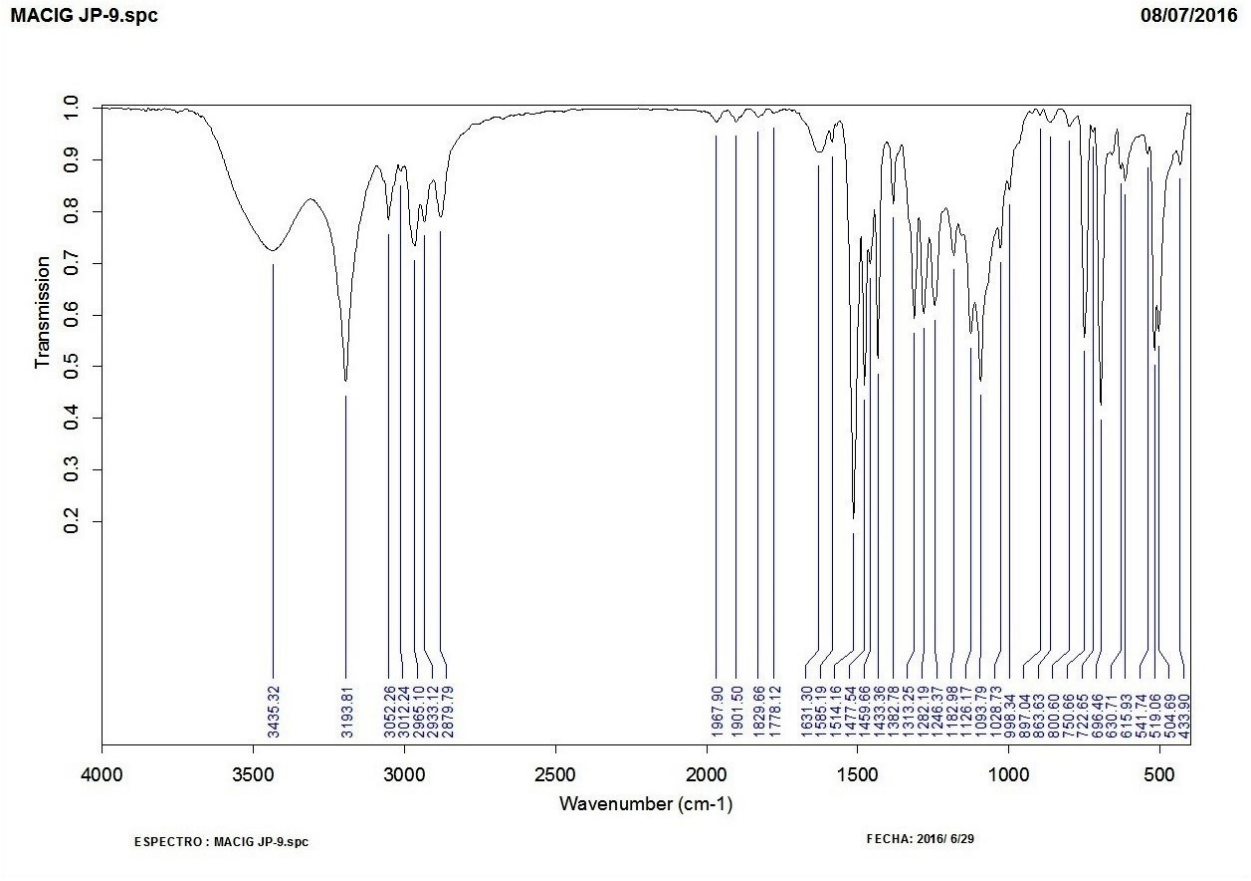

Fig. S43. IR spectrum of complex $[Cu_2(\mu\text{-}Cl)_2(L\text{-}NPr^n)_2(PPh_3)_2]$ **(8).**

IR (KBr, absorption bands): 3194 s, 3052 w, 3012 w, 2965 w, 2933 w, 2880 w, 1631 w, ν1585 s, 1514 s, 1478 s, 1460 w, 1433 s, 1383 w, 1313 m, 1282 m, 1246m, 1183 w, 1126m, 1094 s, 1029 w, 998 w, 897 w, 864 w, 801 w, 751 s, 723 w, 696 s, 630 w, 616 w, 542 w, 519 s, 505 s, 434 w cm^{-1}.

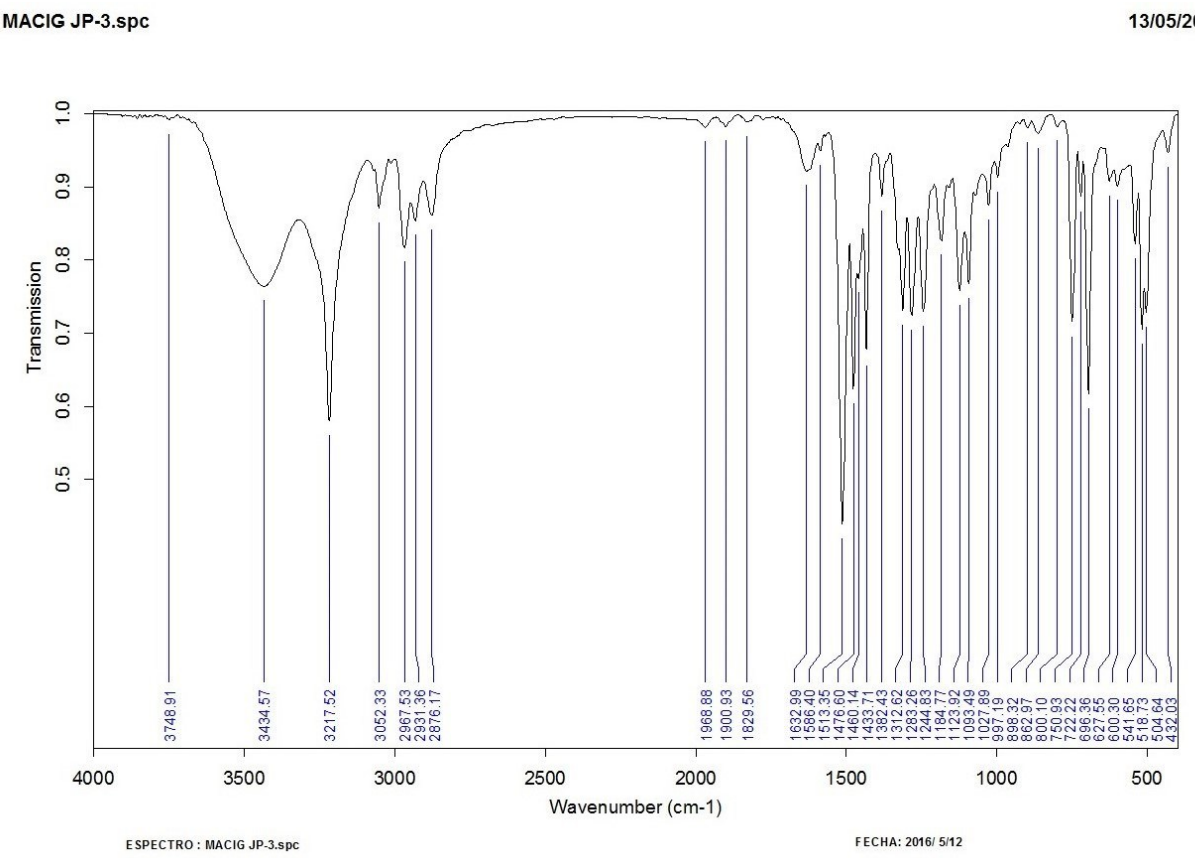

Fig. S44. IR spectrum of complex $[Cu_2(\mu\text{-}Br)_2(L\text{-}NPr^n)_2(PPh_3)_2]$ **(9).**

IR (KBr, absorption bands): 3218 s, 3052 w, 2968 w, 2931 w, 2876 w, 1633 w, ν1585 w, 1513 s, 1477 m, 1460 w, 1434 m, 1382 w, 1313 m, 1283 m, 1245 w, 1185 w, 1124 m, 1093 m, other 1028 w, 997 w, 898 w, 863 w, 800 w, 751 m, 722 w, 696 s, 628 w, 600 w, 592 w, 519 m, 505 m, 432 w cm^{-1}.

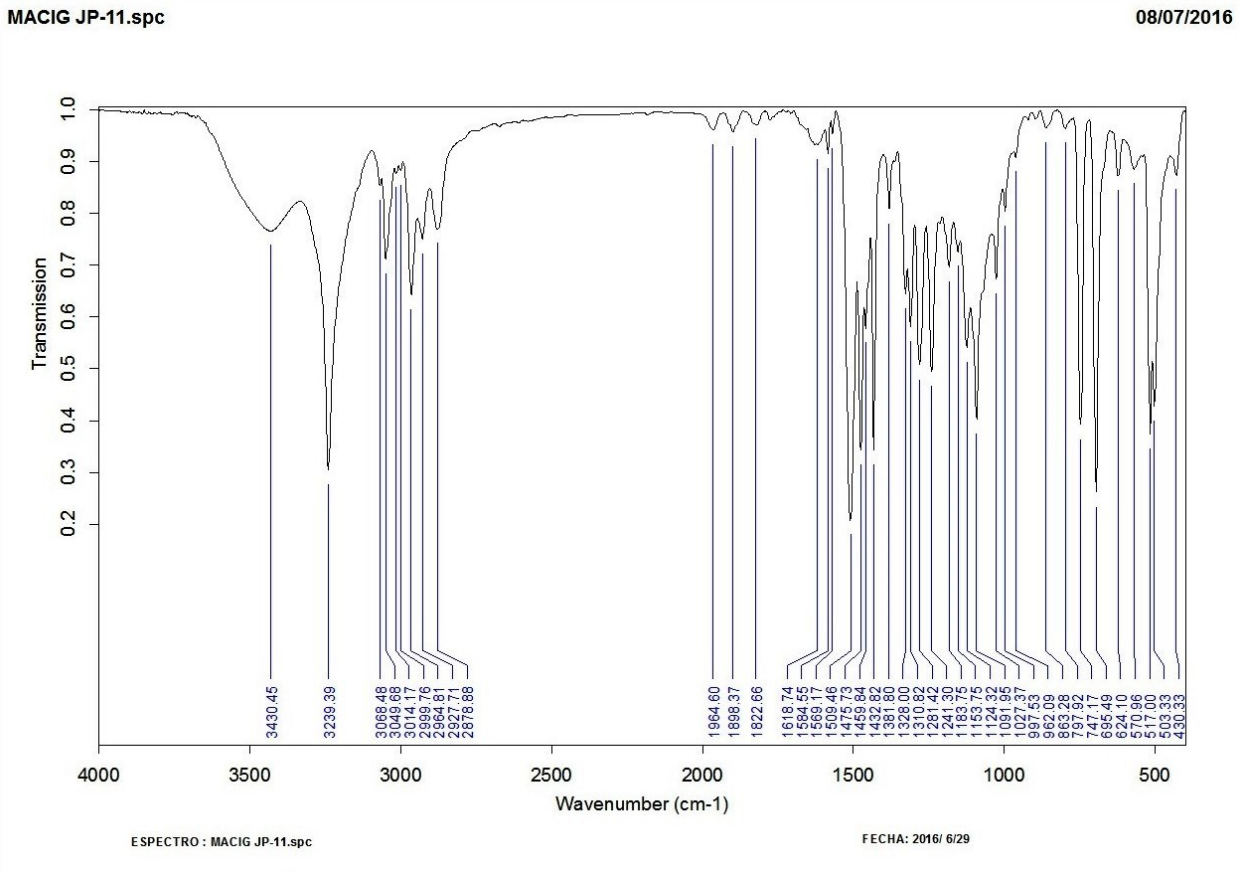

Fig. S45. IR spectrum of complex $[Cu_2(\mu\text{-}I)_2(L\text{-}NPr^n)_2(PPh_3)_2]$ **(10)**.

IR (KBr, absorption bands): 3239 s, 3068 w, 3050 m, 3014 w, 3000 w, 2965 m, 2928 w, 2879 w, 1619 w, 1584 w, 1569 w, 1510 s, 1476 s, 1460 w, 1433 s, 1382 w, 1311 m, 1281 m, 1241 m, 1184 w, 1154 w, 1124 w, 1092 m, 1027 w, 998 w, 962 w, 863 w, 798 w, 747 s, 695 s, 624 w, 571 w, 517 s, 503 s, 430 w cm^{-1}.

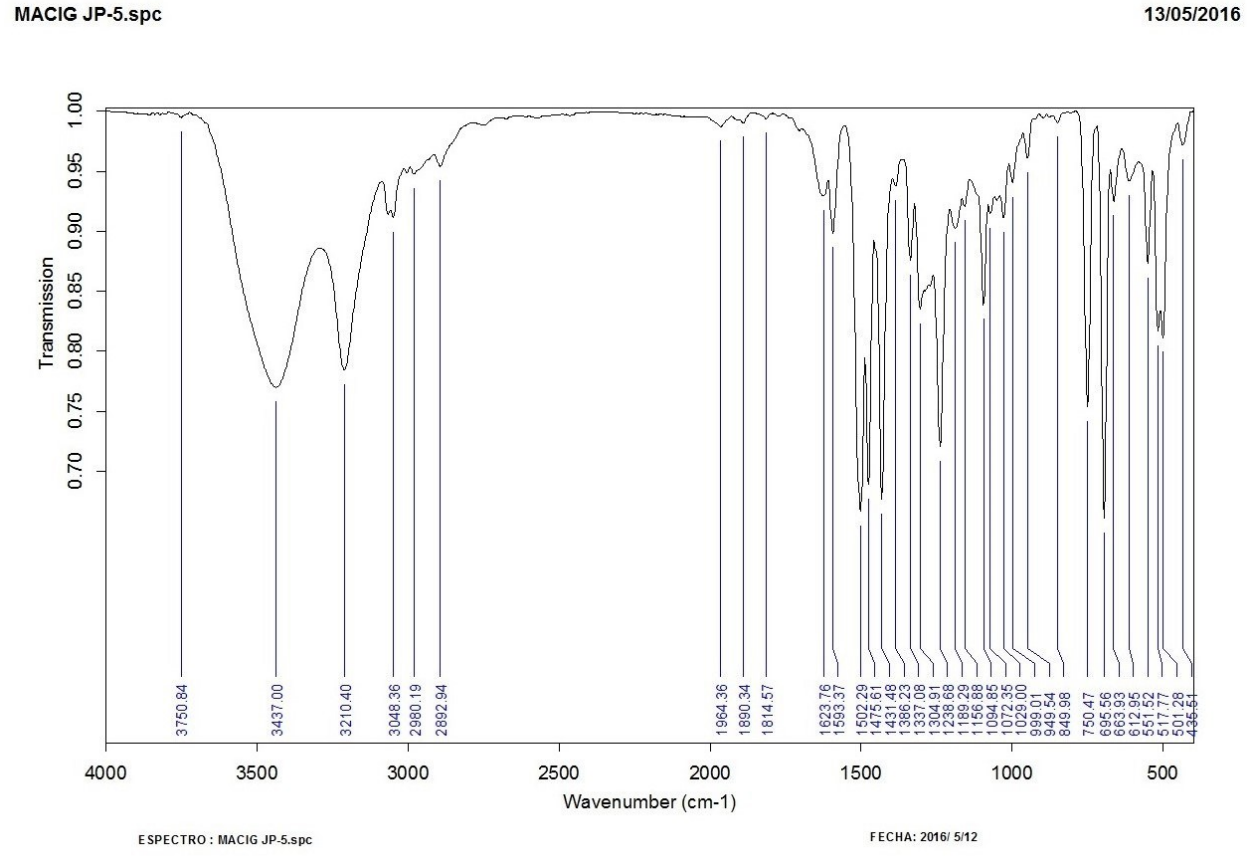

Fig. S46. IR spectrum of complex $[Cu_2(\mu\text{-}Br)_2(L\text{-}NPh)_2(PPh_3)_2]$ **(11)**.

IR (KBr, absorption bands): 3210 m, 3048 w, 2980 w, 2893 w, 1624 w, 1593 w, 1502 s, 1431 s, 1386 w, 1337 w, 1305 w, 1239 s, 1189 w, 1157 w, 1095 m, 1072 w, 1029 w, 999 w, 950 w, 850 w, 750 s, 696 s, 664 w, 613 w, 552 w, 518 s, 501 s, 436 w cm^{-1}.

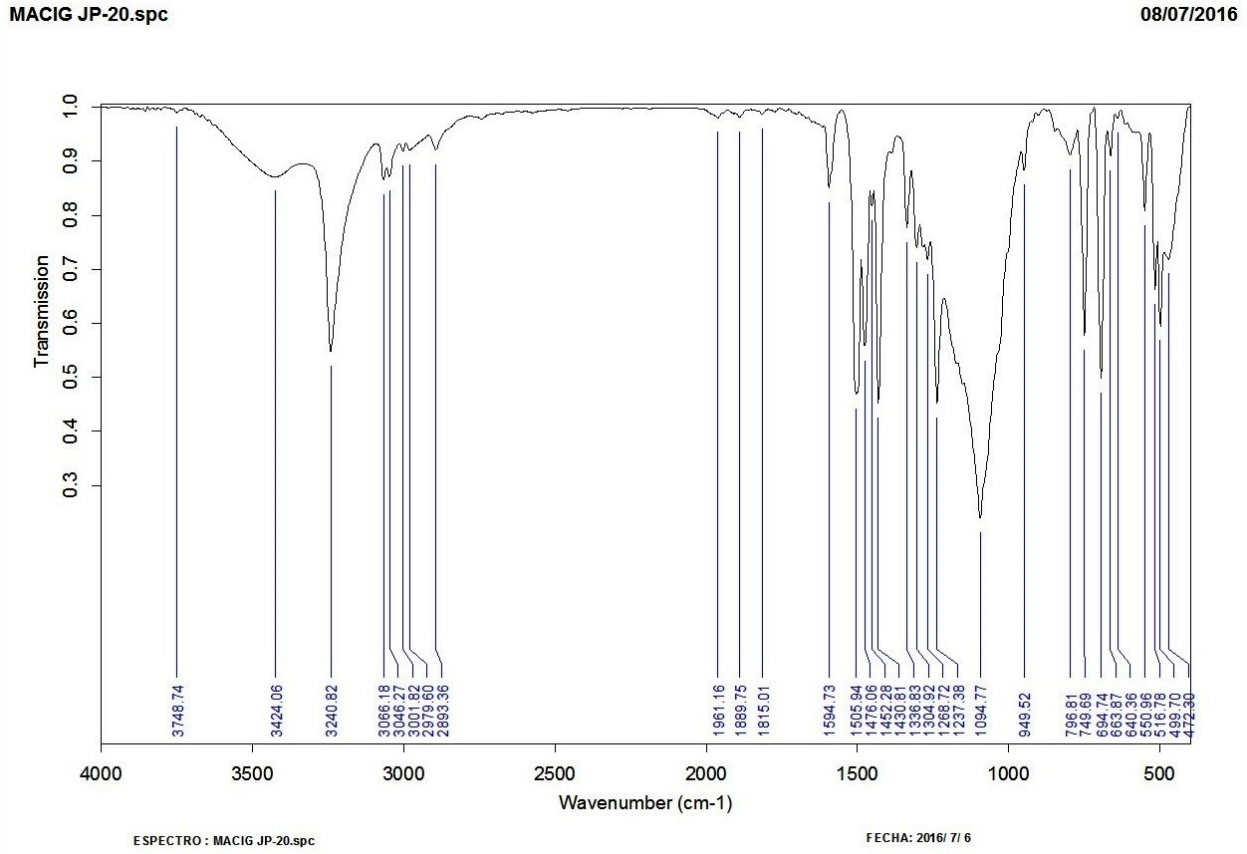

Fig. S47. IR spectrum of complex $[Cu_2(\mu\text{-}I)_2(L\text{-}NPh)_2(PPh_3)_2]$ **(12)**.

IR (KBr, absorption bands): 3241 s, 3066 w, 3046 w, 3002 w, 2980 w, 2893 w, 1595 w, 1506 s, 1476 s, 1452 s, 1431 s, 1337 w, 1305 w, 1269 w, 1095 s, 950 w, 797 w, 750 s, 695 s, 664 w, 640 w, 551 w, 517 w, 500 m, 472 m cm^{-1}.

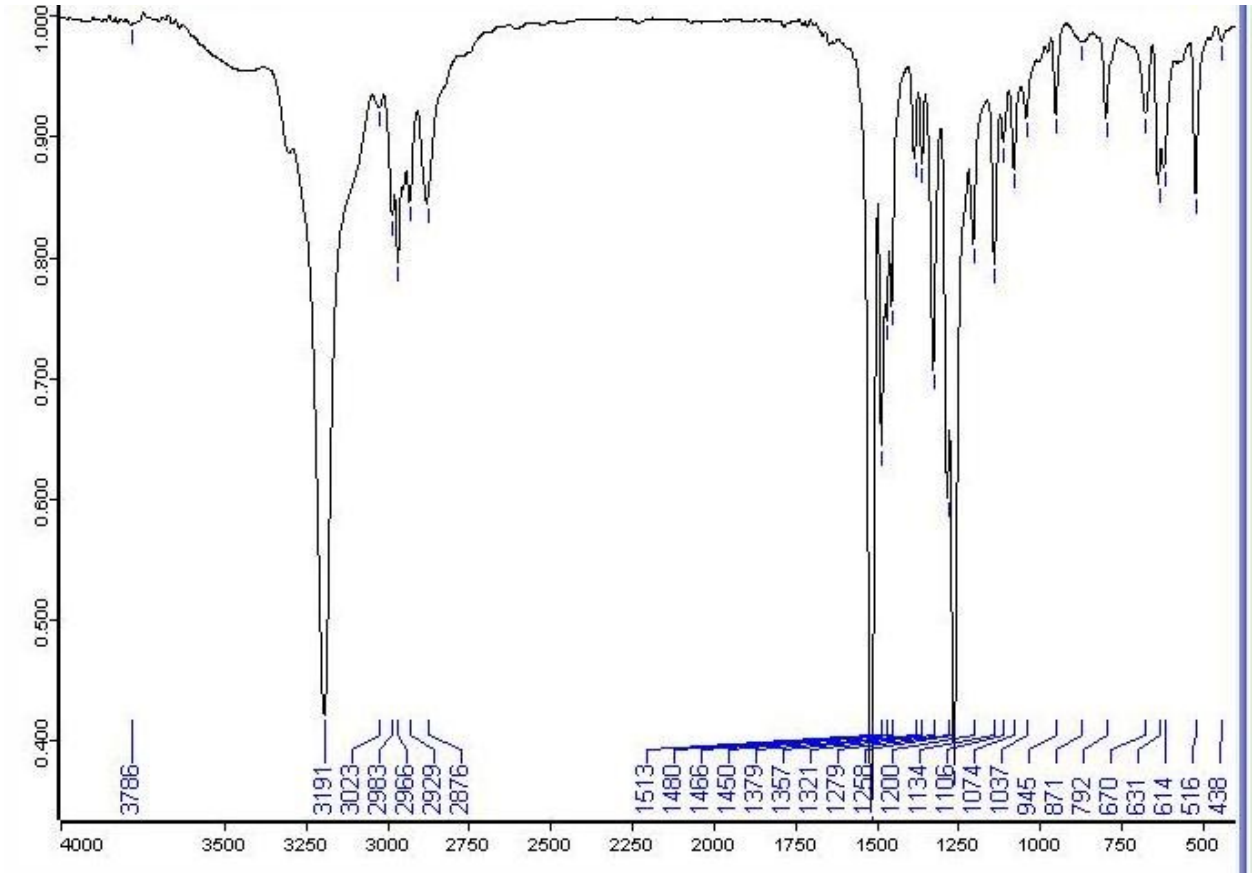

Fig. S48. IR spectrum of ligand L-NEt.

IR (KBr, absorption bands): 3191 s, 3023 w, 2983 m, 2966 m, 2929 m, 2876 m, 1513 s, 1480 m, 1466 m, 1450 m, 1379 w, 1357 w, 1321 m, 1279 m, 1258 m, 1200 m, 1134 m, 1106 m, 1074 m; 1037 m, 945 w, 871 w, 792 m, 670 m, 631 m, 614 m, 516 m, 438 w cm^{-1}.

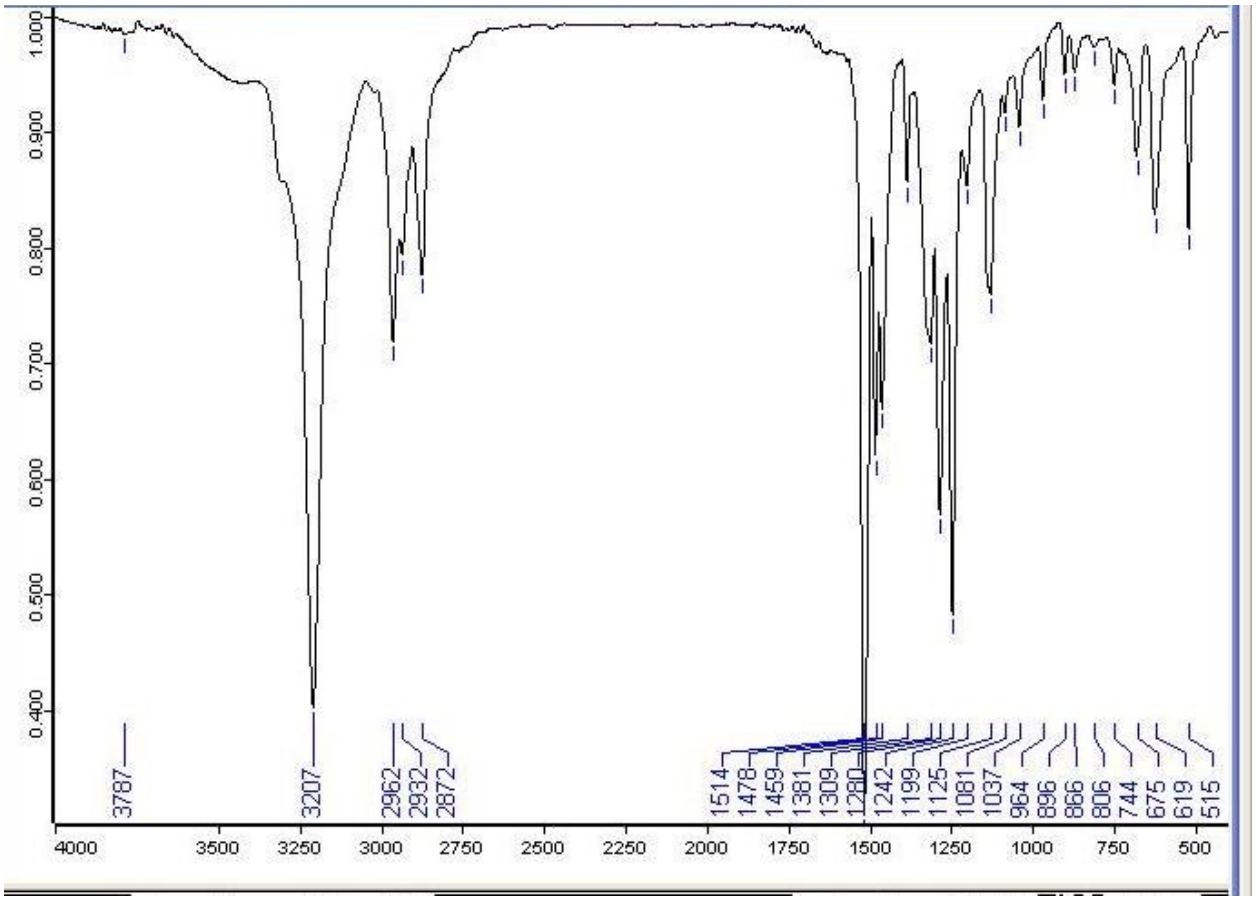

Fig. S49. IR spectrum of ligand L-NPr^{n}.

IR (KBr, absorption bands): 3207 s, 2962 m, 2932 m, 2872 m, 1514 s, 1478 m, 1459 m, 1381 w, 1309 m, 1280 s, 1242 s, 1199 w, 1125 m, 1081 w, 1037 w, 964 w, 896 w, 866 w, 806 w, 744 w, 675 w, 619 m, 515 m cm^{-1}.

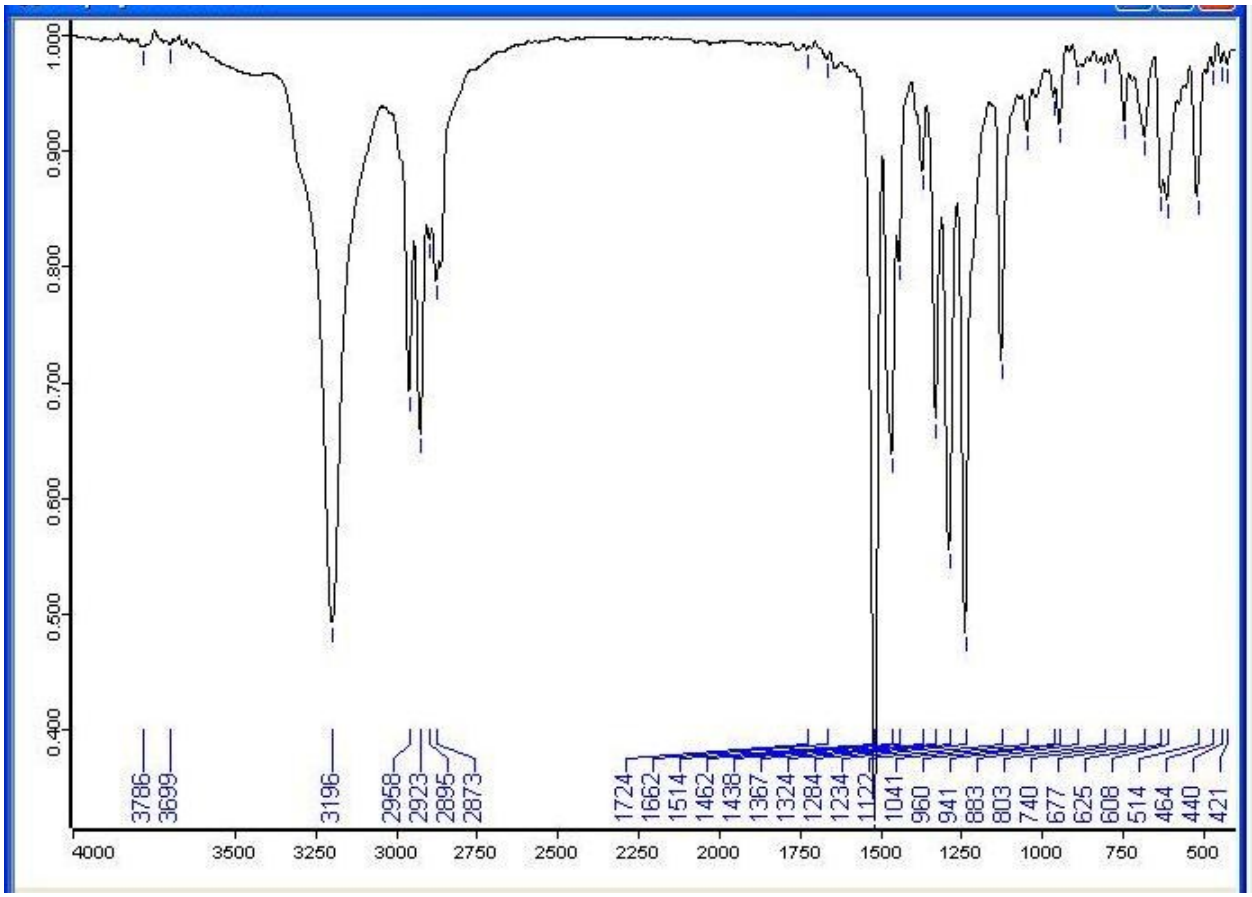

Fig. S50. IR spectrum of ligand L-NBu^{n}.

IR (KBr, absorption bands): 3196 s, 2958 m, 2923 m, 2895 m, 2873 m, 1514 s, 1462 m, 1438 m; 1367 w, 1324 m, 1284 s, 1234 s, 1122 m, 1041 w, 960 w, 941 w, 883 w, 803 w, 740 w, 677 w, 625 w, 608 w, 514 w, 464 w, 440 w, 421 w cm^{-1}.

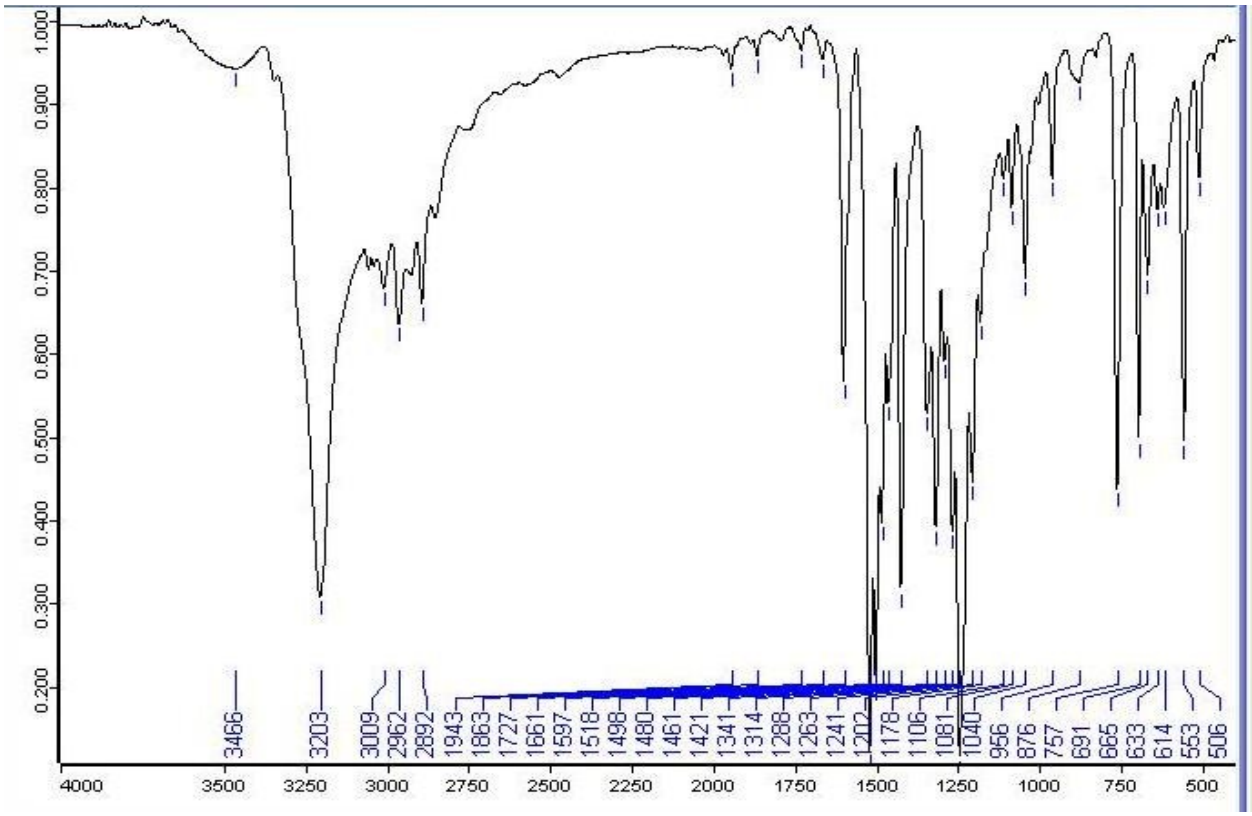

Fig. S51. IR spectrum of ligand L-NPh.

IR (KBr, absorption bands): 3203 s, 3009 m, 2962 m, 2892 m, 1597 s, 1518 s, 1498 s, 1480 s, 1461 s, 1421 s, 1341 m, 1314 s, 1288 m, 1263 s, 1241 s, 1202 m, 1178 m, 1106 w, 1081 m, 1040 m, 956 m, 876 w, 757 s, 691 s, 665 m, 633 m, 614 m, 553 s, 506 m cm^{-1}.

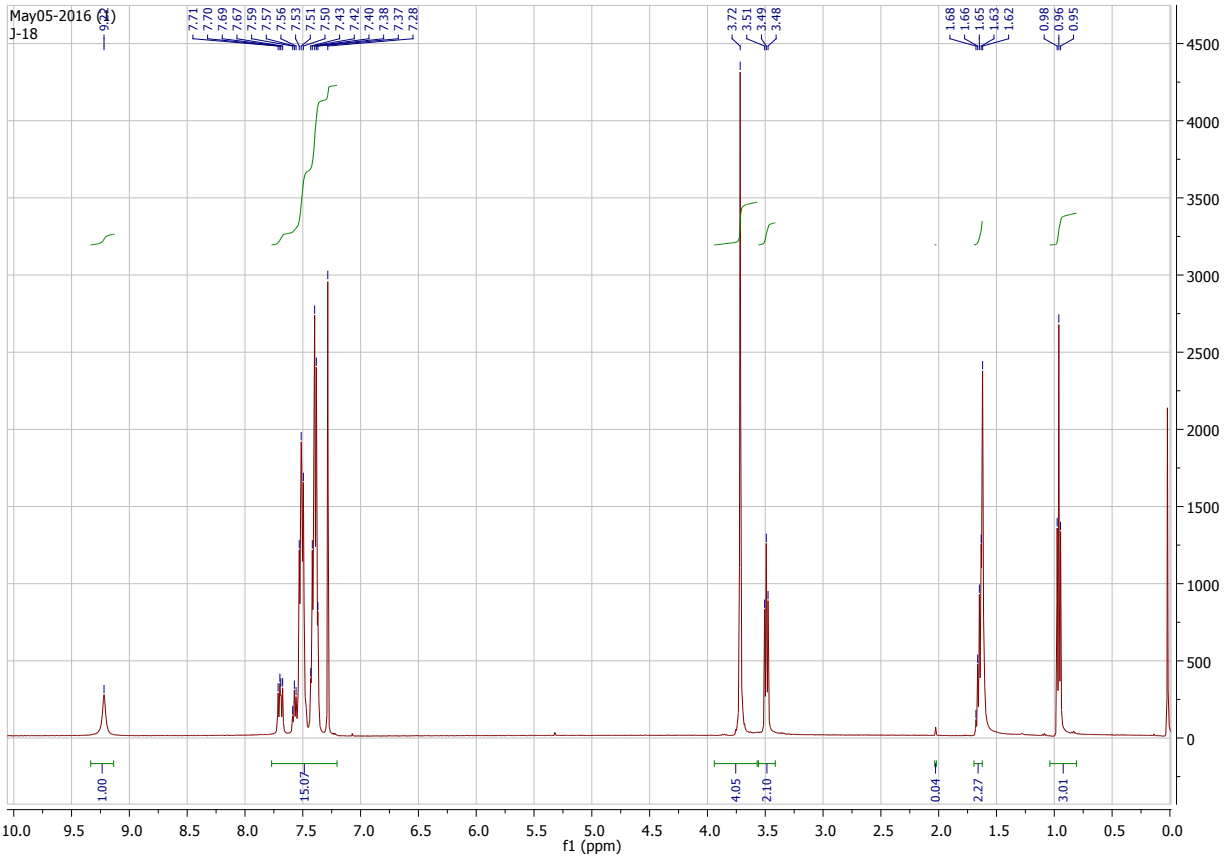

Fig. S52. ^{1}H-NMR spectrum of complex [CuCl(L-NPr^{n})(PPh$_3$)$_2$] **(1)**.

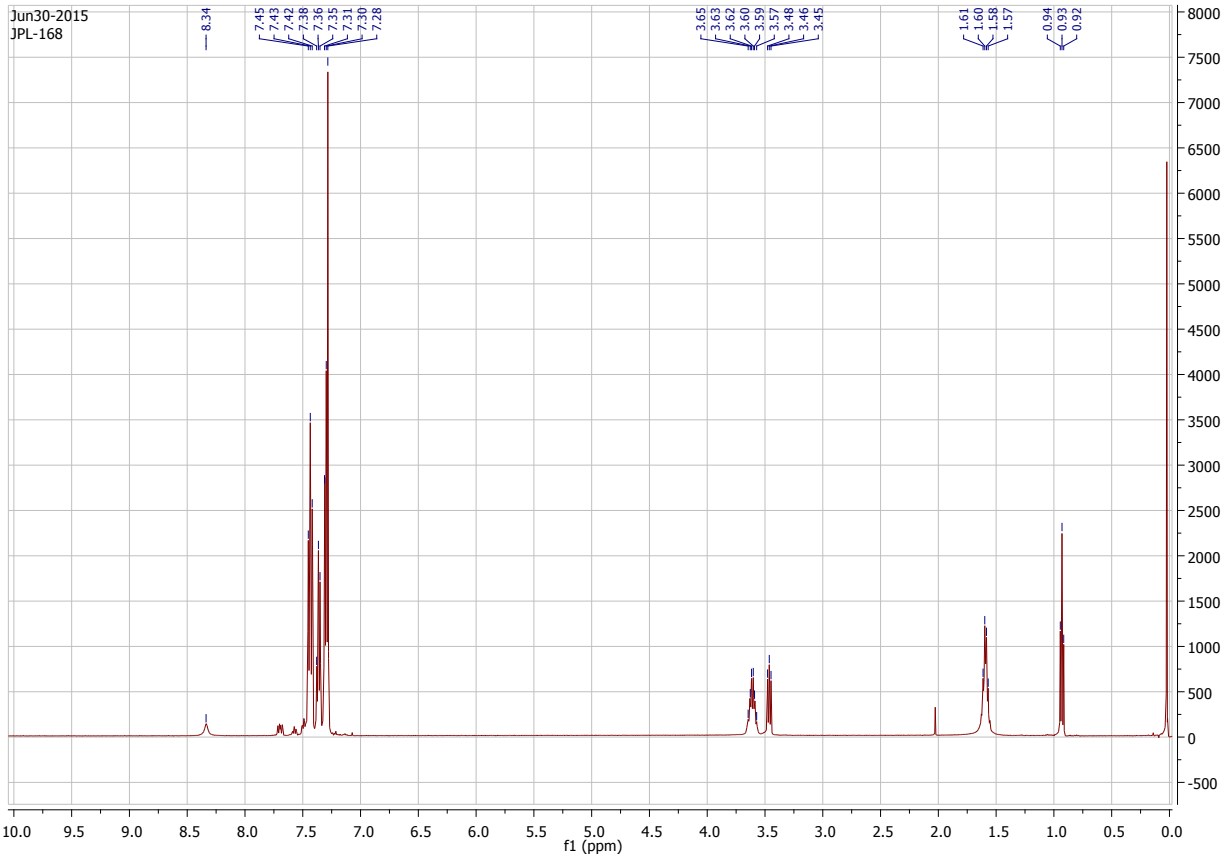

Fig. S53. ^{1}H-NMR spectrum of complex [CuBr(L-NPr^{n})(PPh$_3$)$_2$] **(2)**.

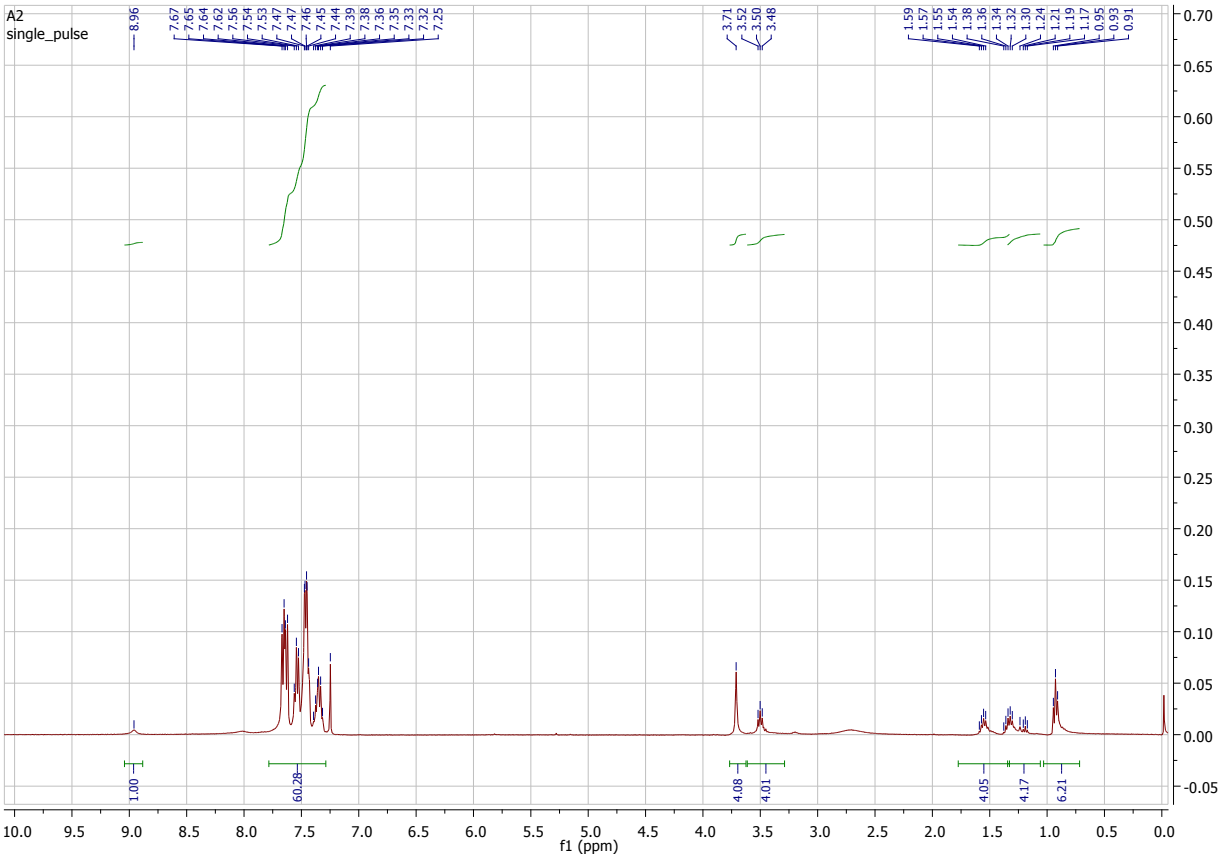

Fig. S54. ^{1}H-NMR spectrum of complex [CuCl(L-NBu^{n})(PPh_3)$_2$] **(3)**.

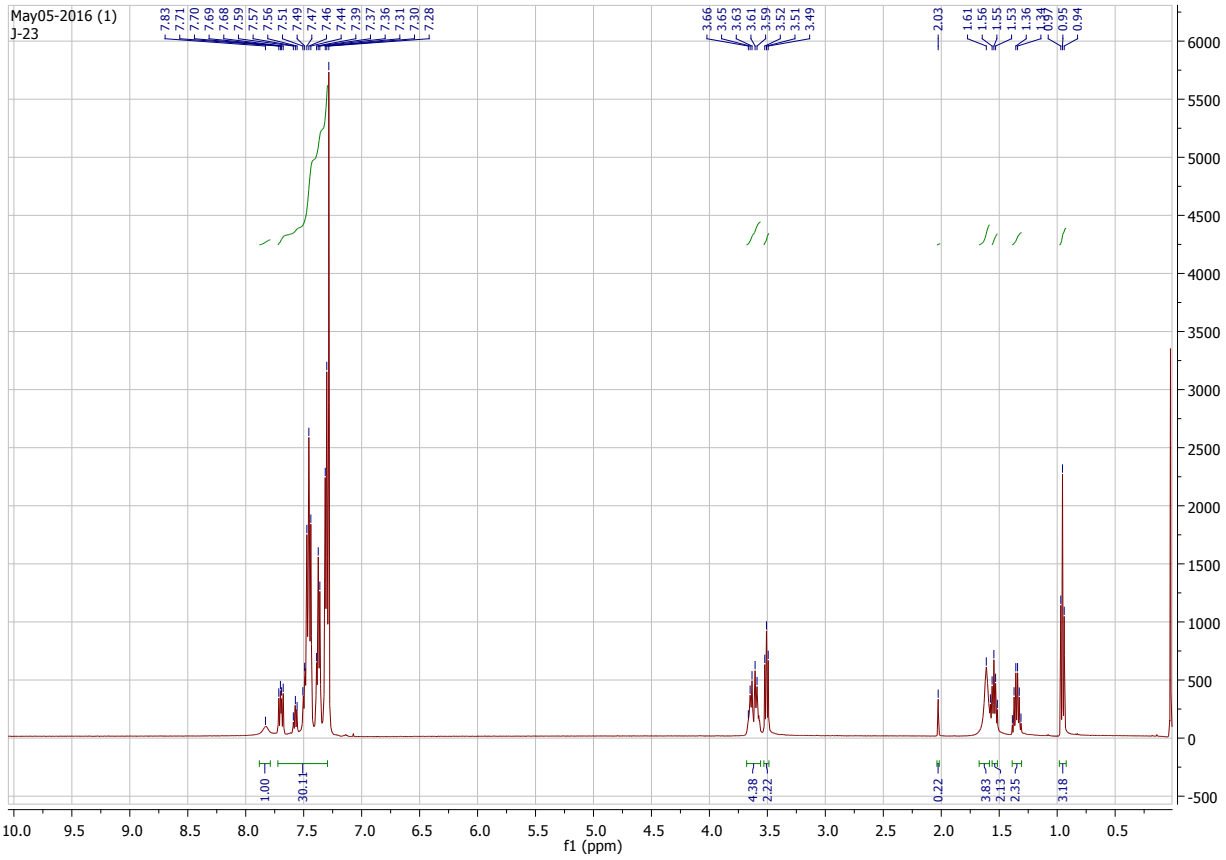

Fig. S55. ^{1}H-NMR spectrum of complex [CuI(L-NBu^{n})(PPh$_3$)$_2$] **(4)**.

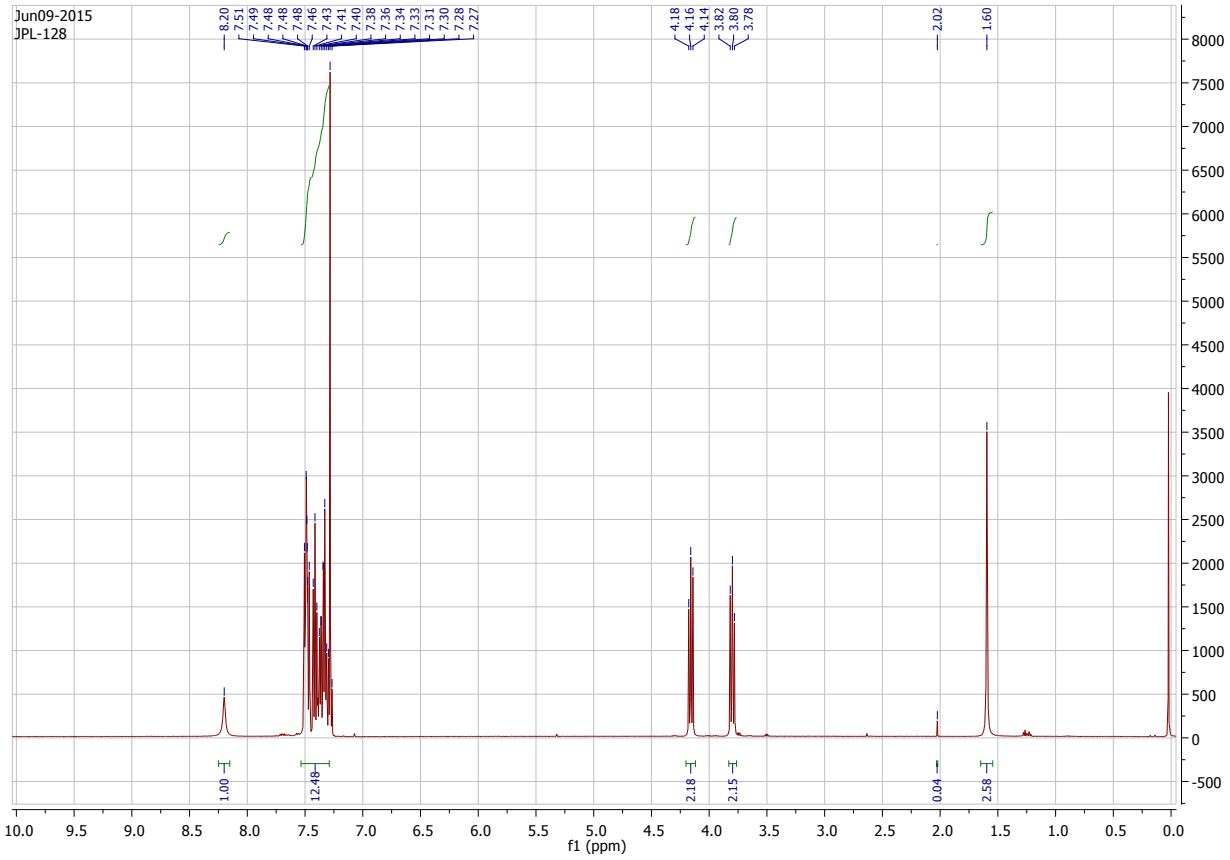

Fig. S56. ^{1}H-NMR spectrum of complex [CuBr(L-NPh)$_2$(PPh$_3$)] **(5)**.

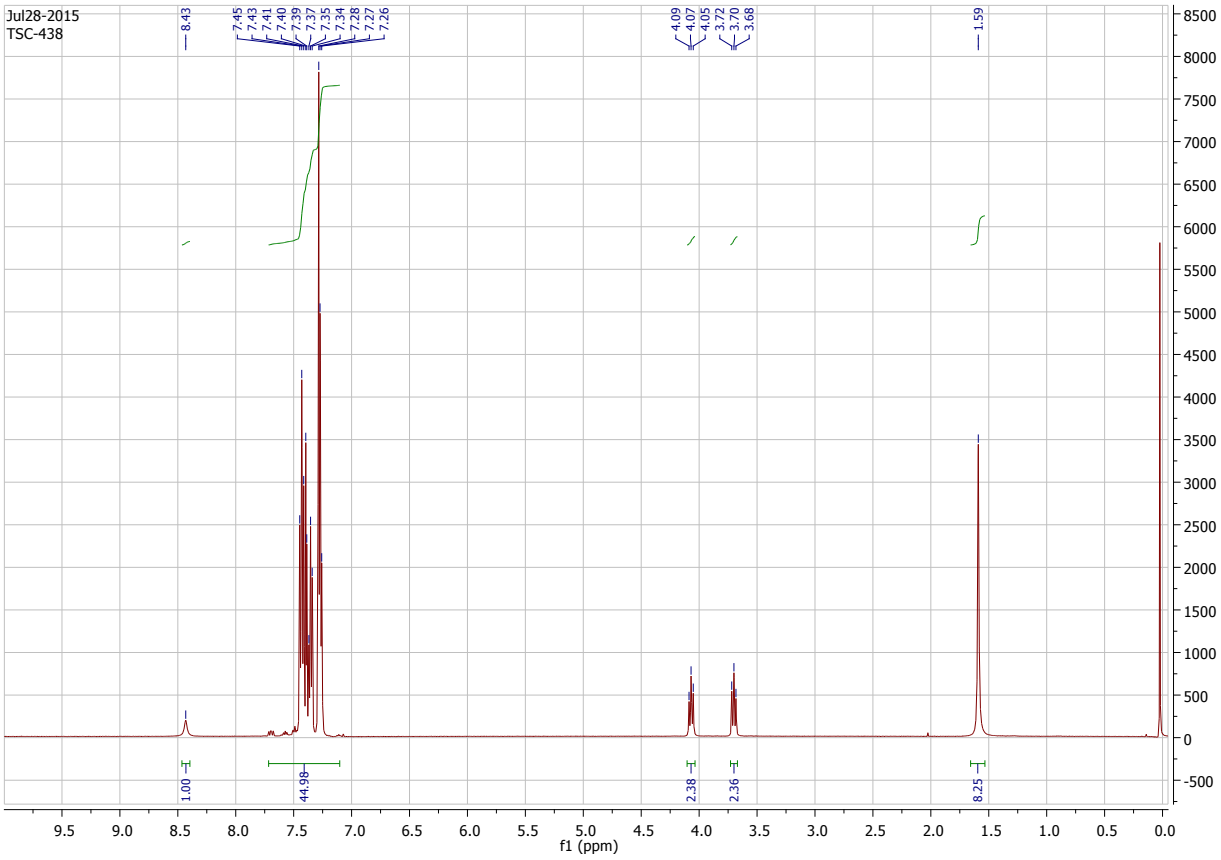

Fig. S57. ^{1}H-NMR spectrum of complex [CuI(L-NPh)(PPh_3)$_2$] **(6)**.

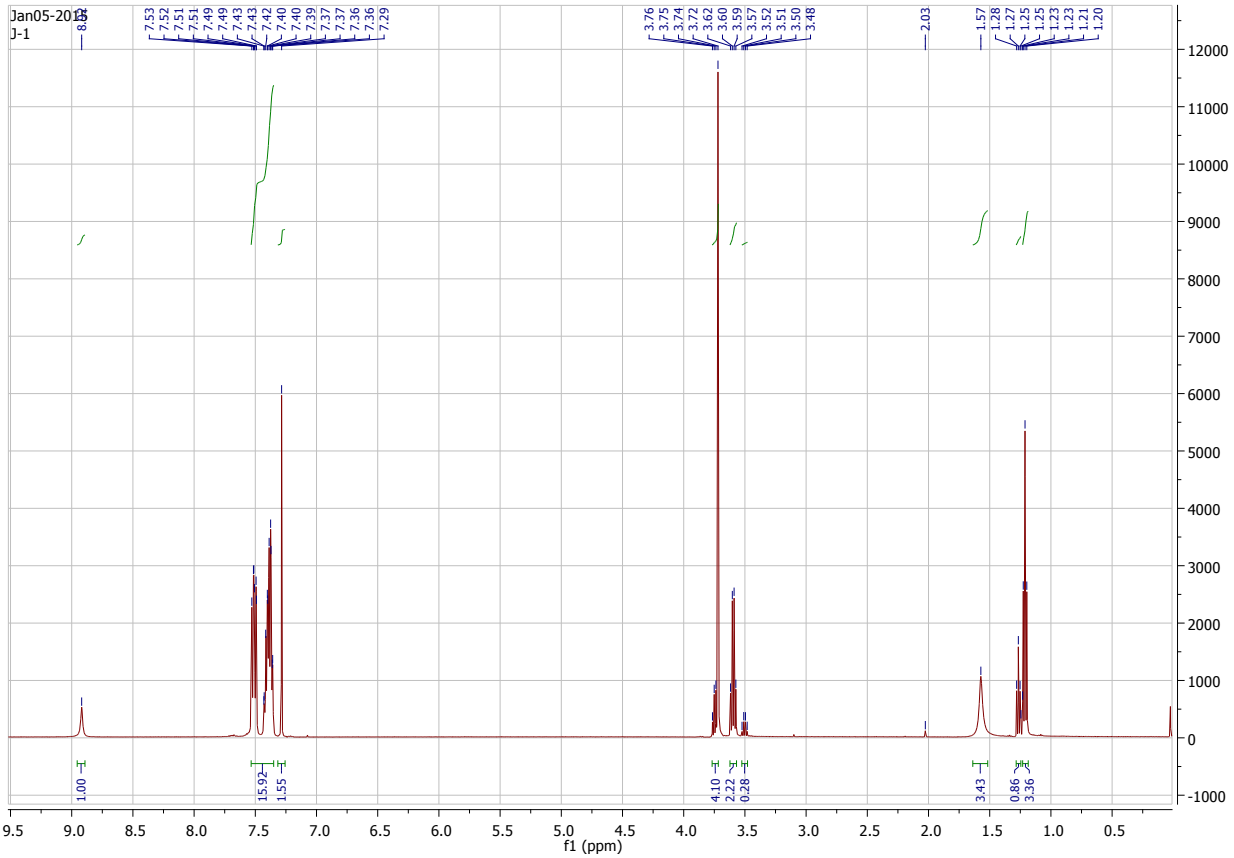

Fig. S58. ^{1}H-NMR spectrum of complex $[Cu_2(\mu\text{-}Br)_2(L\text{-}NEt)_2(PPh_3)_2]$ **(7)**.

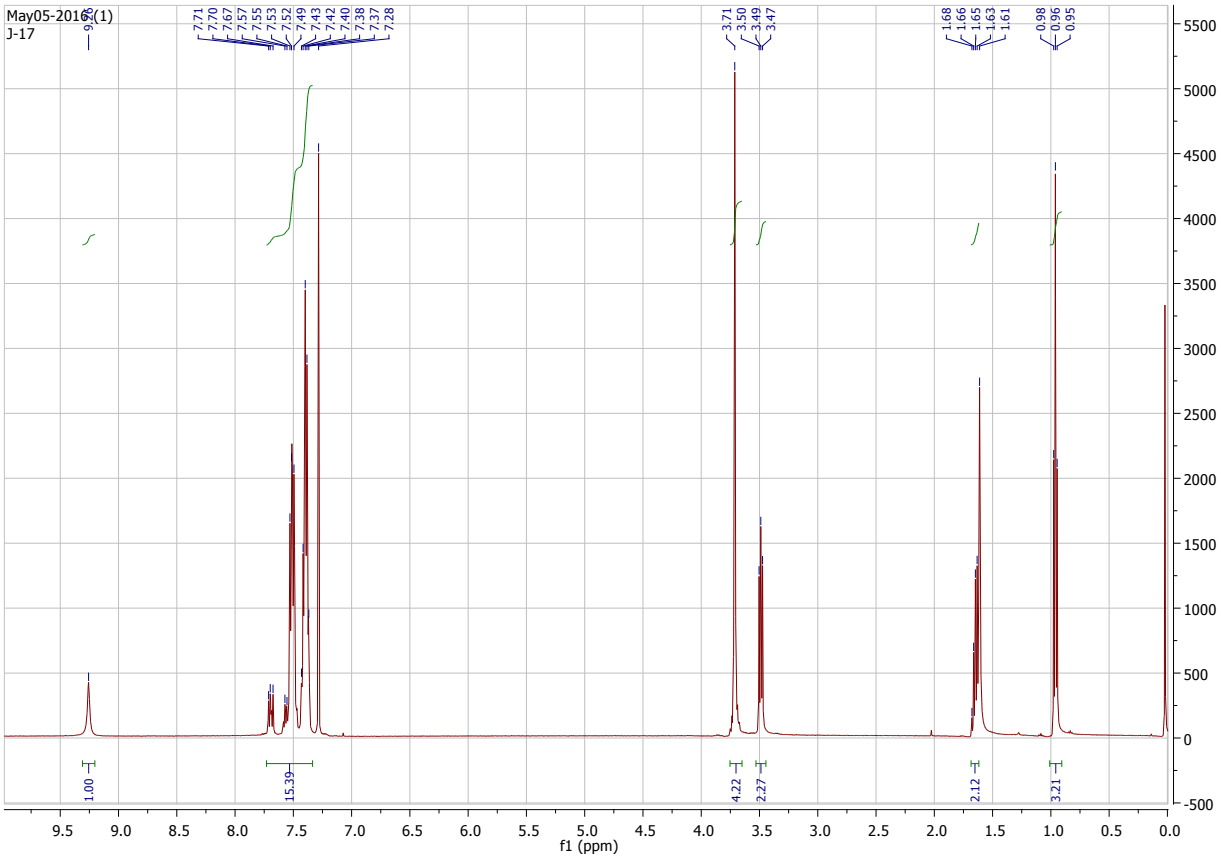

Fig. S59. ^{1}H-NMR spectrum of complex $[Cu_2(\mu\text{-}Cl)_2(L\text{-}NPr^n)_2(PPh_3)_2]$ **(8)**.

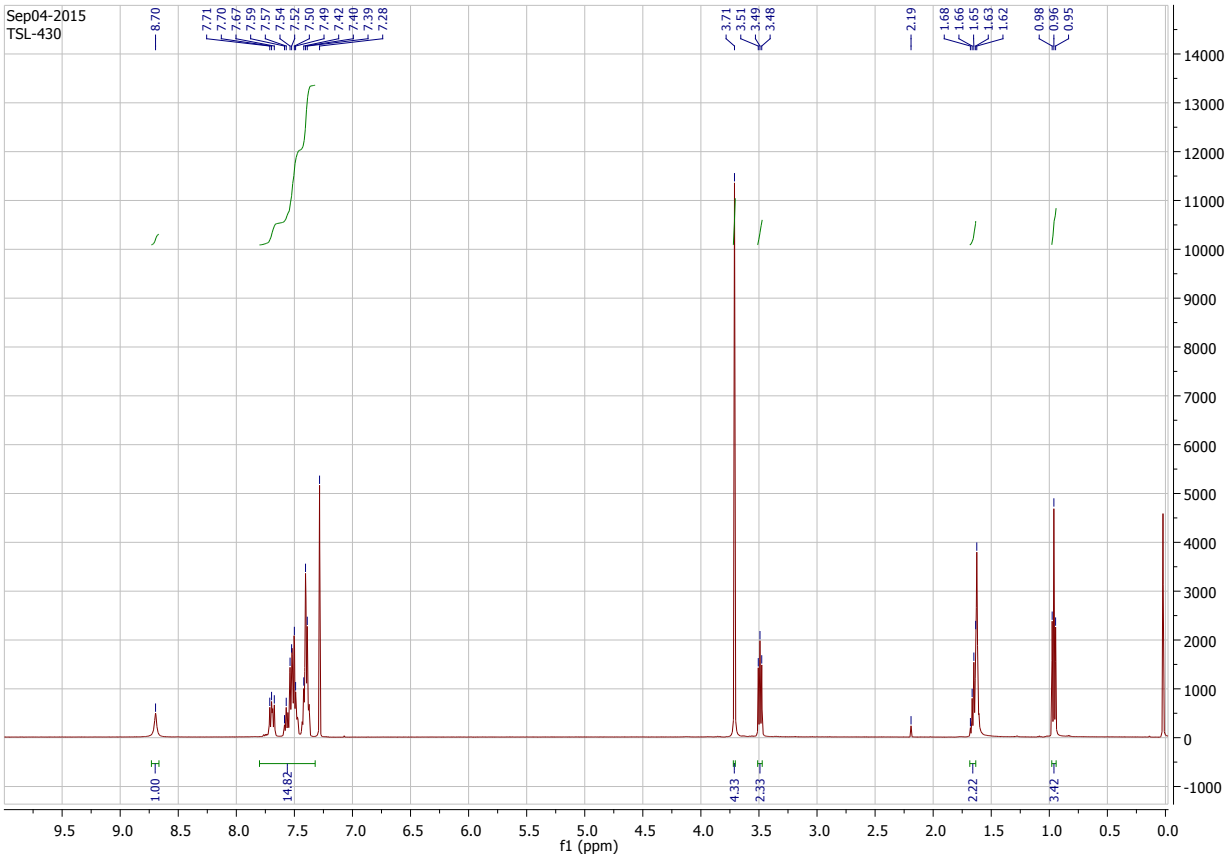

Fig. S60. ^{1}H-NMR spectrum of complex $[Cu_2(\mu\text{-}Br)_2(L\text{-}NPr^n)_2(PPh_3)_2]$ **(9)**.

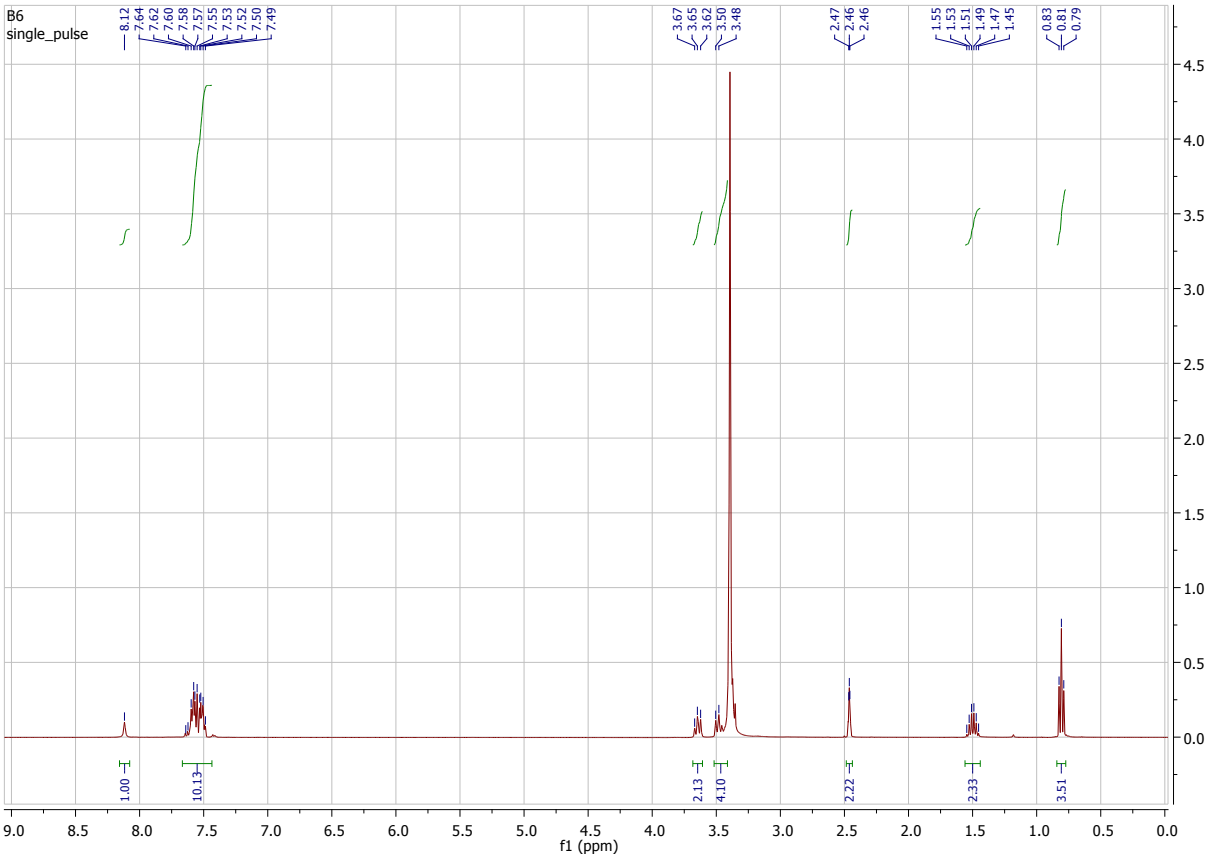

Fig. S61. ^{1}H-NMR spectrum of complex $[Cu_2(\mu\text{-}I)_2(L\text{-}NPr^n)_2(PPh_3)_2]$ **(10)**.

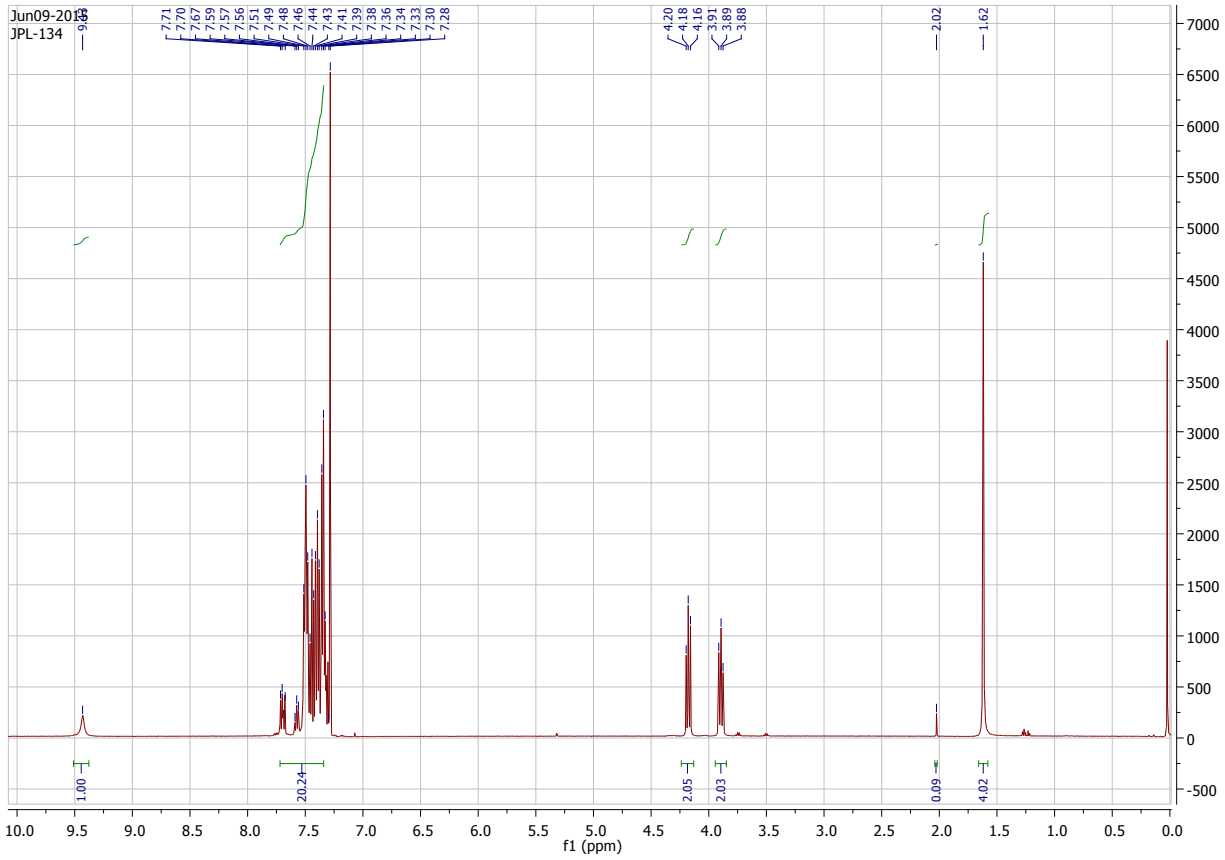

Fig. S62. ^{1}H-NMR spectrum of complex $[Cu_2(\mu\text{-}Br)_2(L\text{-}NPh)_2(PPh_3)_2]$ **(11)**.

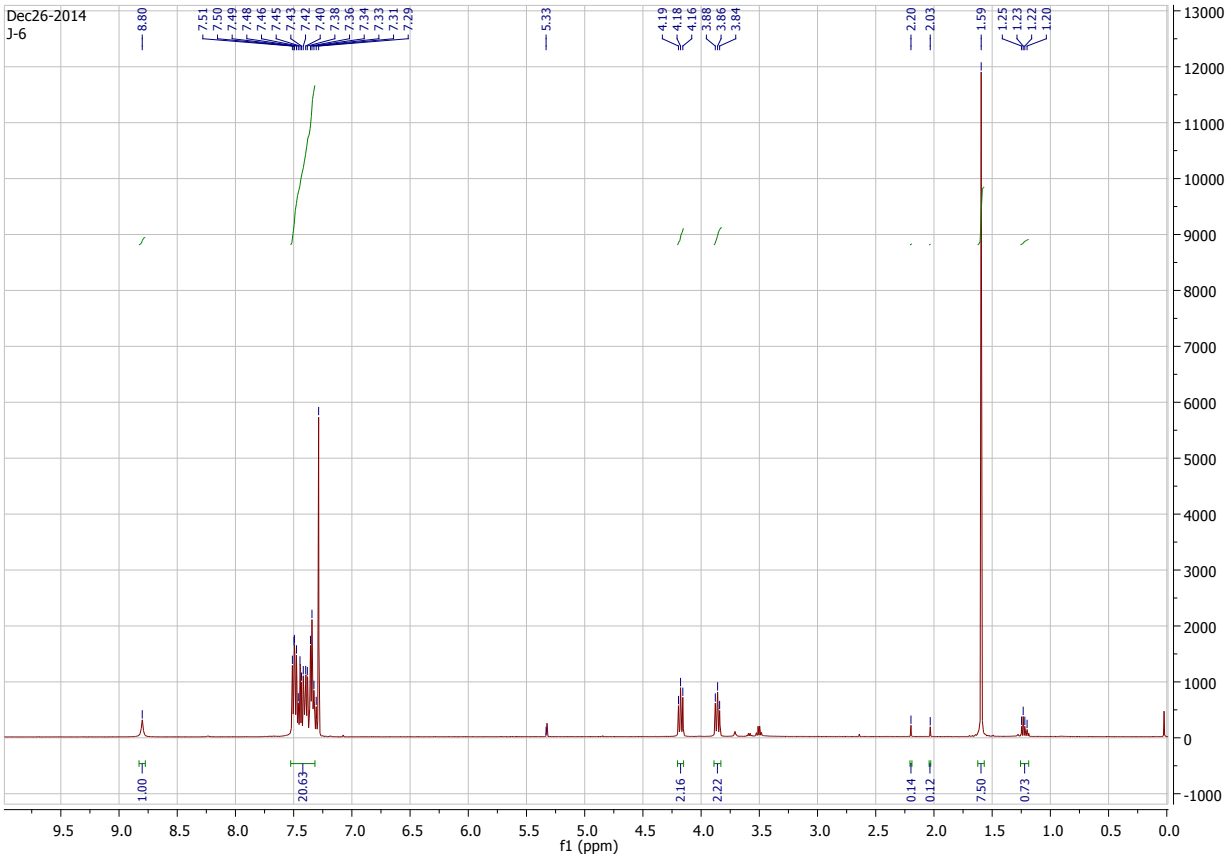

Fig. S63. ^{1}H-NMR spectrum of complex $[Cu_2(\mu\text{-}I)_2(L\text{-}NPh)_2(PPh_3)_2]$ **(12)**.

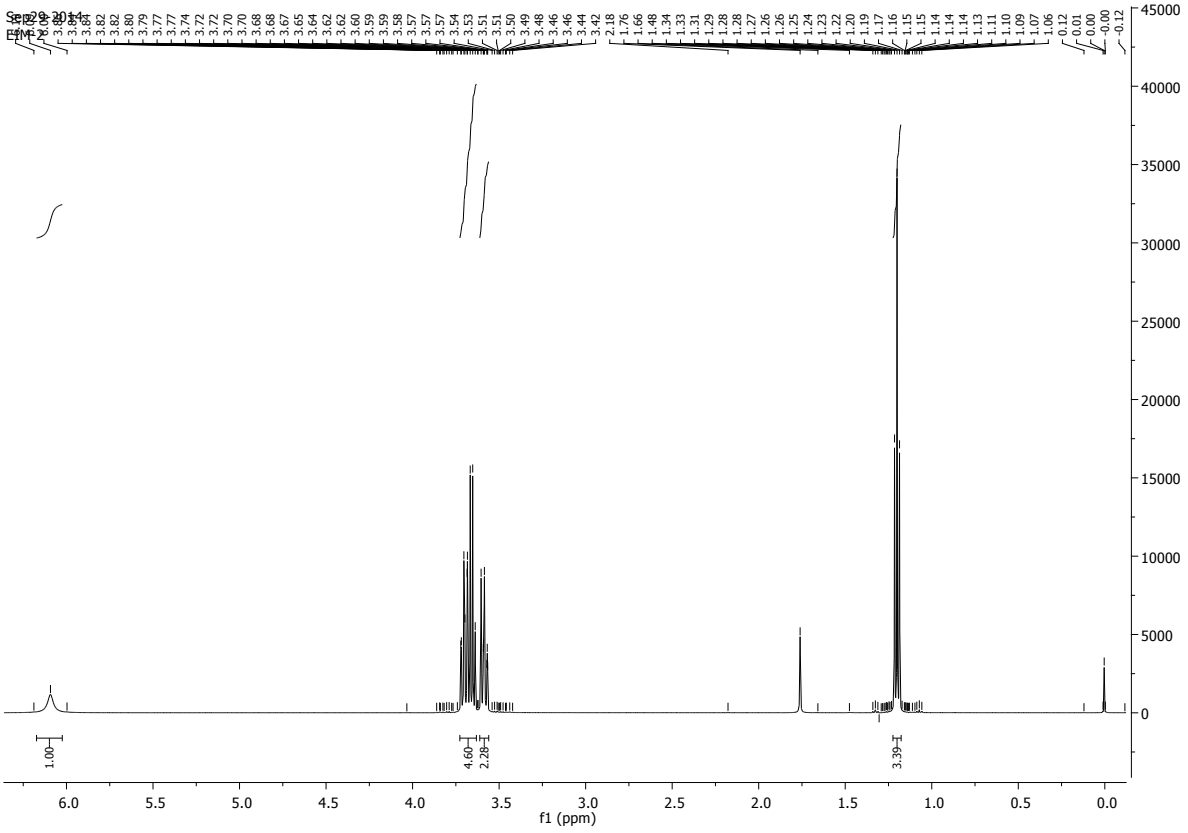

Fig. S64. ^{1}H-NMR spectrum of ligand L-NEt.

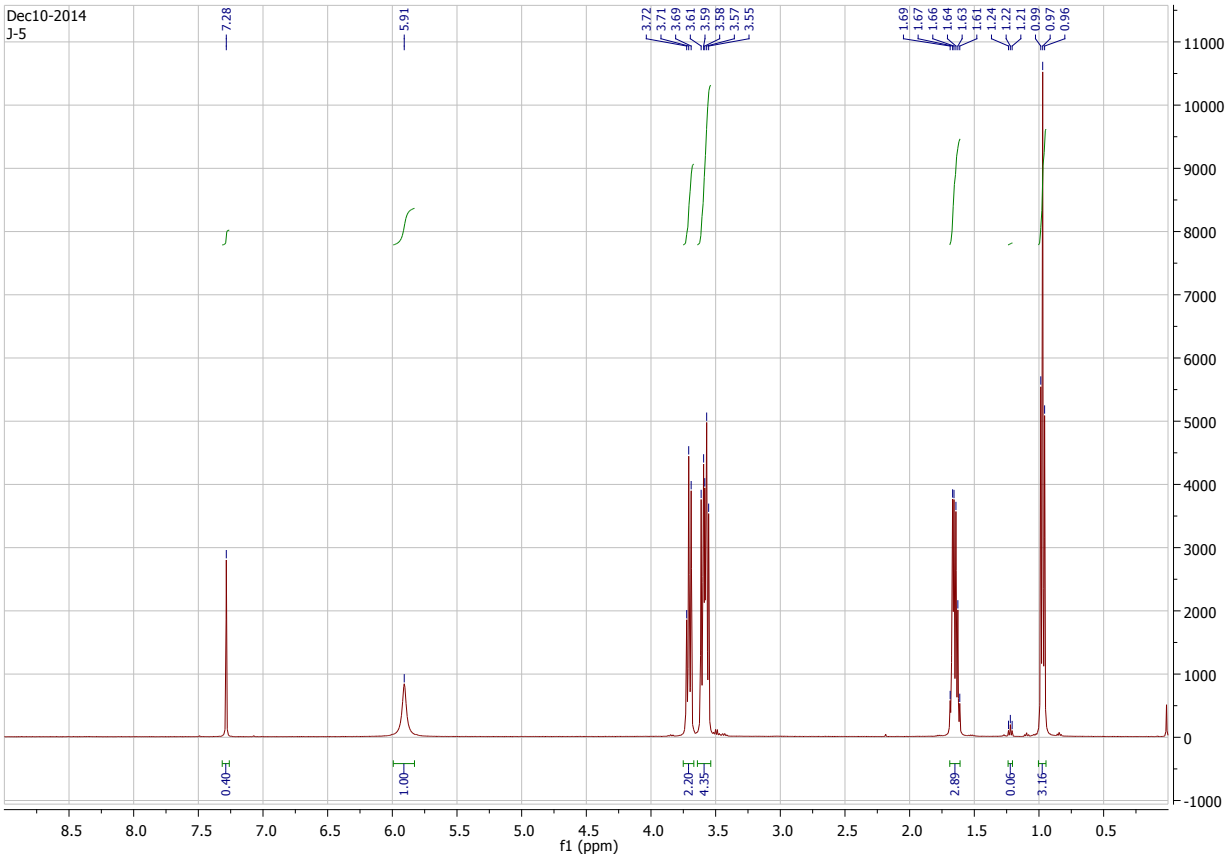

Fig. S65. ^{1}H-NMR spectrum of ligand L-NPr^{n}.

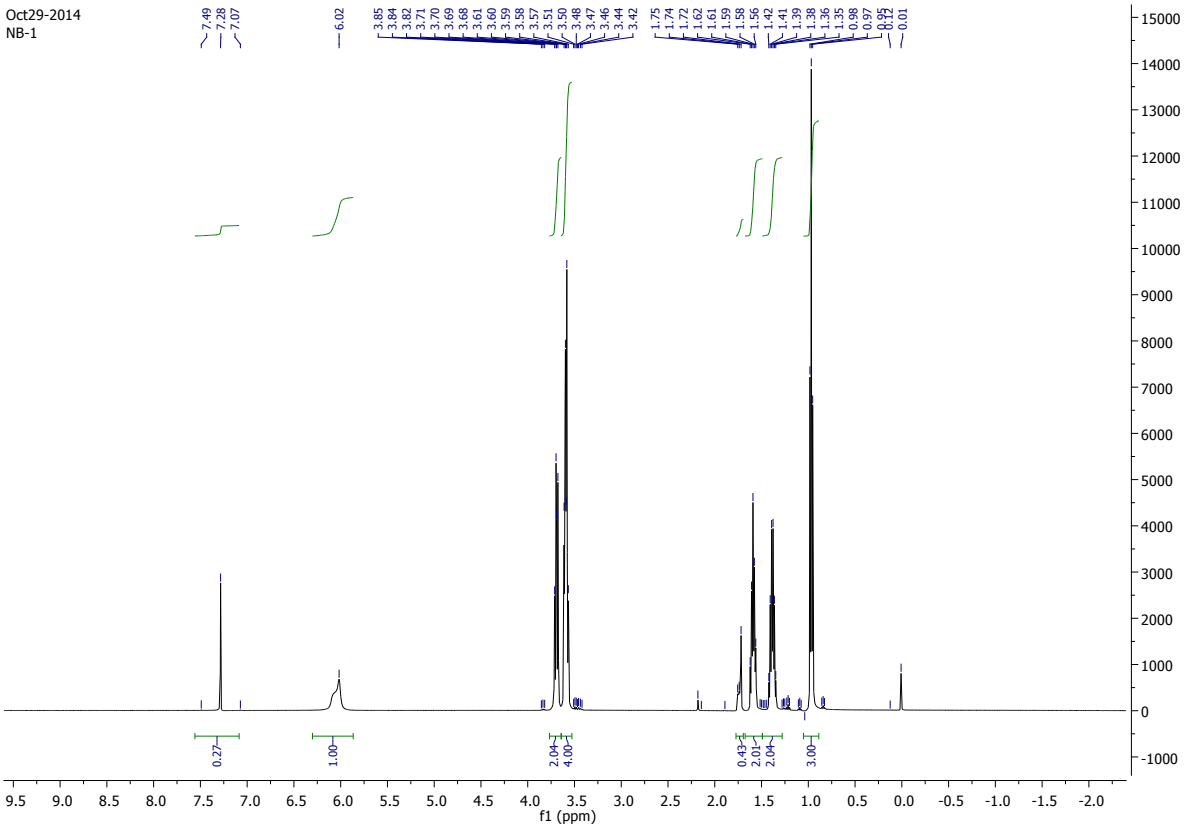

Fig. S66. ^{1}H-NMR spectrum of ligand L-NBu^{n}.

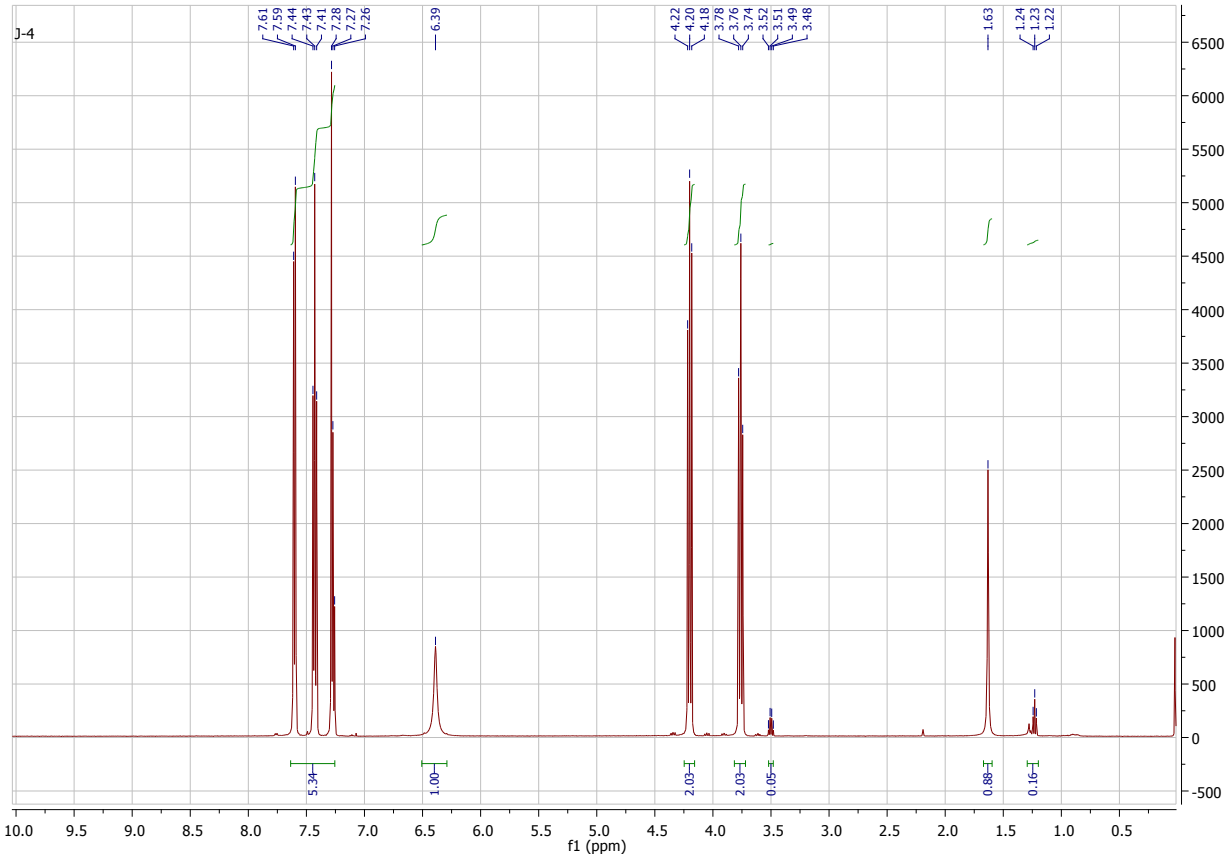

Fig. S67. ^{1}H-NMR spectrum of ligand L-NPh.

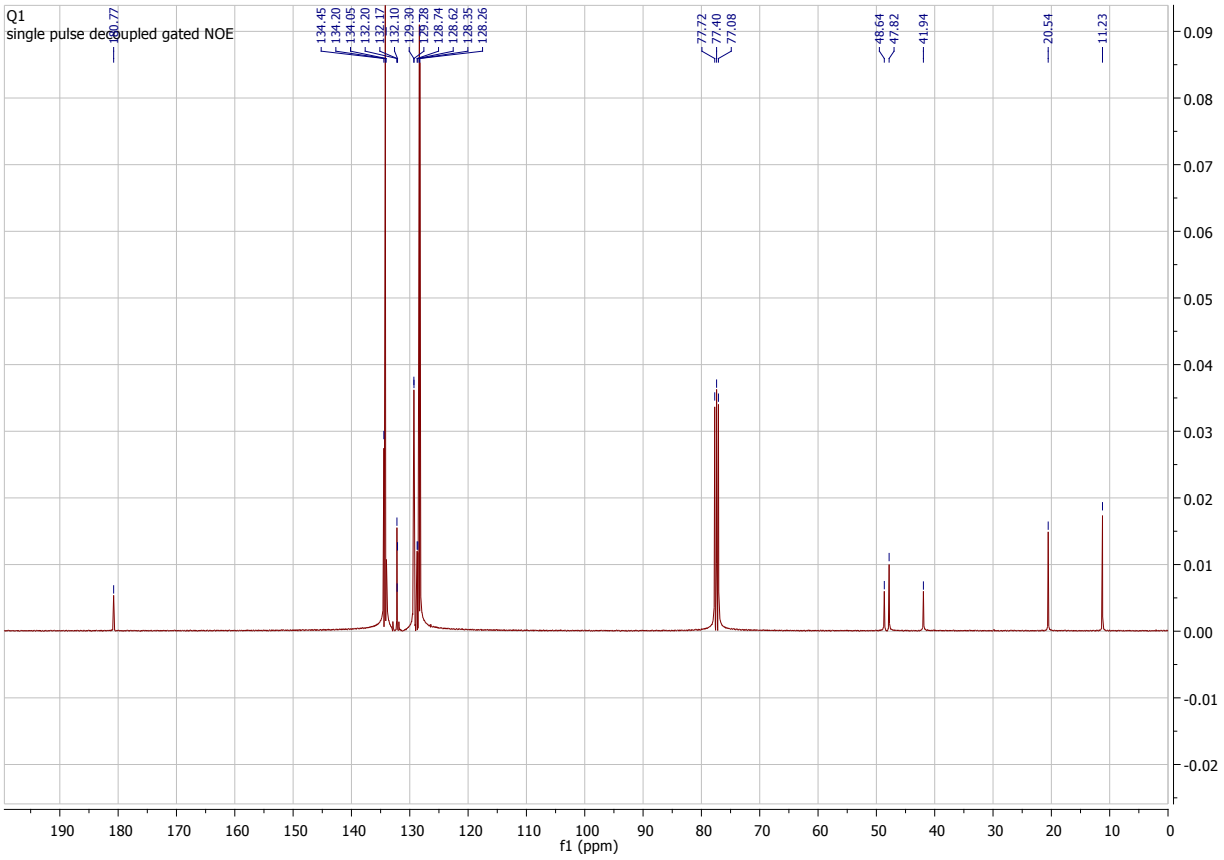

Fig. S68. ^{13}C-NMR spectrum of complex (**1**).

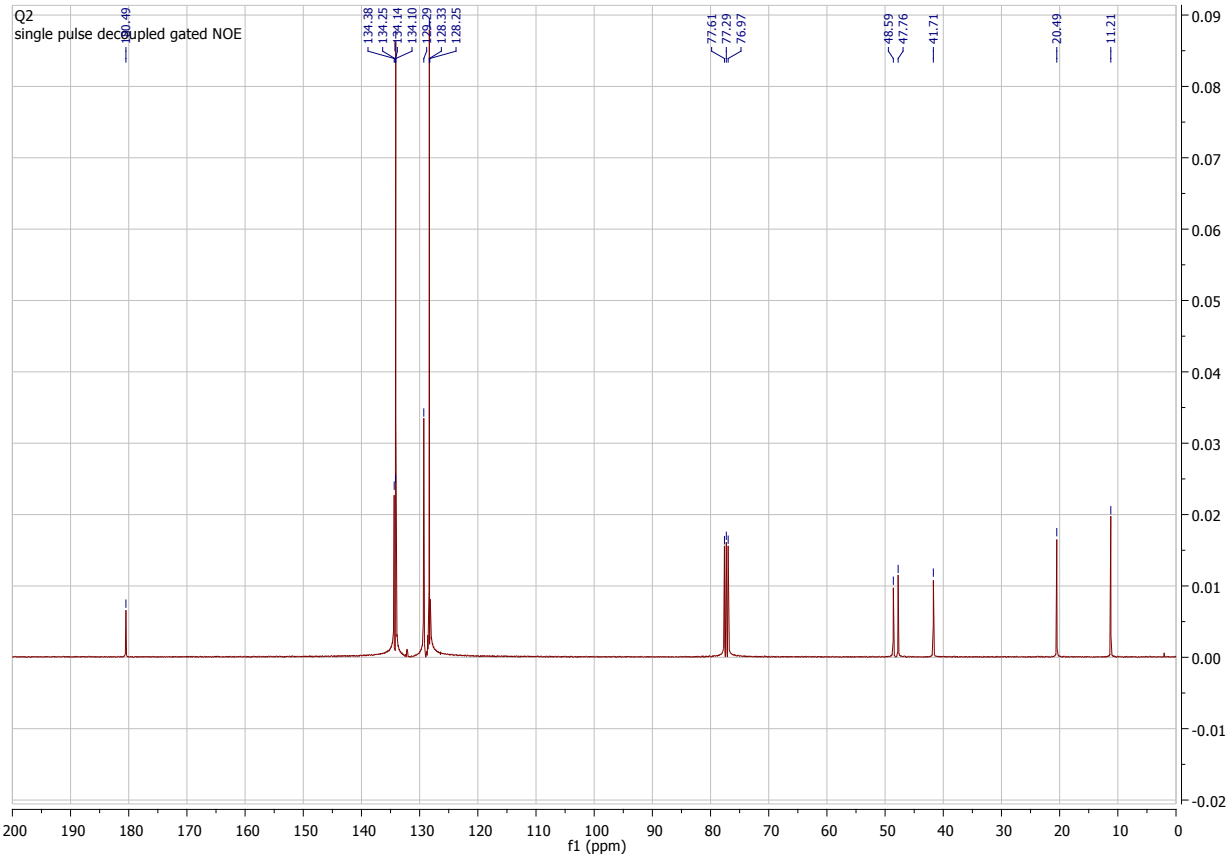

Fig. S69. ^{13}C-NMR spectrum of complex (**2**).

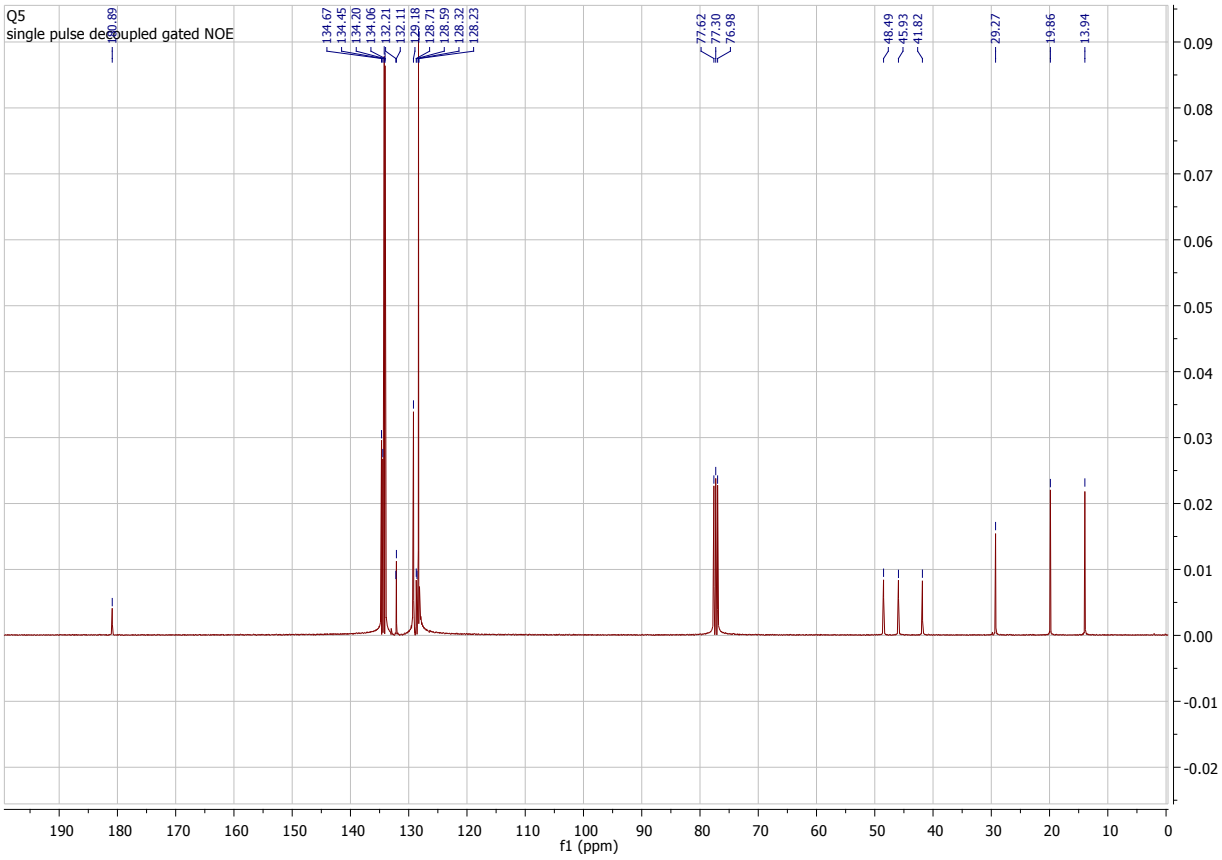

Fig. S70. ^{13}C-NMR spectrum of complex (**3**).

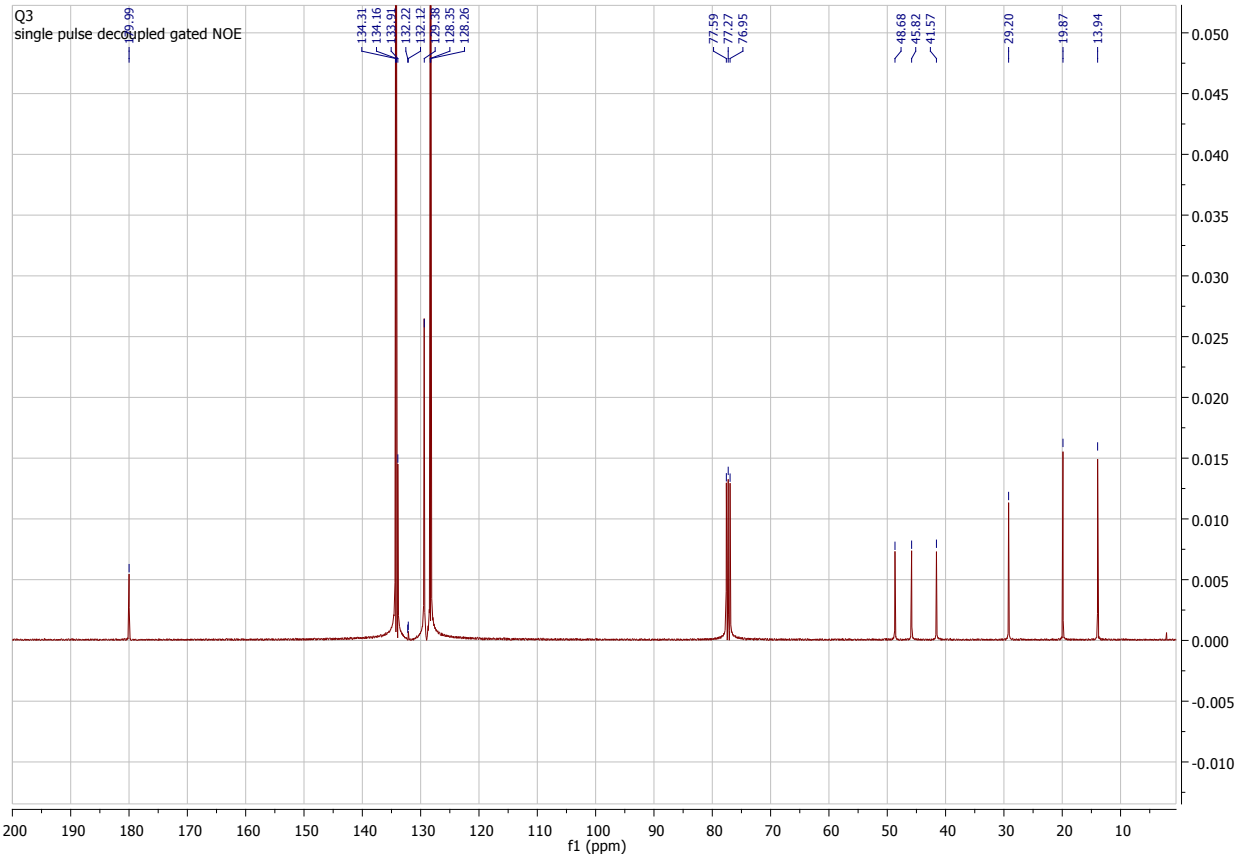

Fig. S71. ^{13}C-NMR spectrum of complex (**4**).

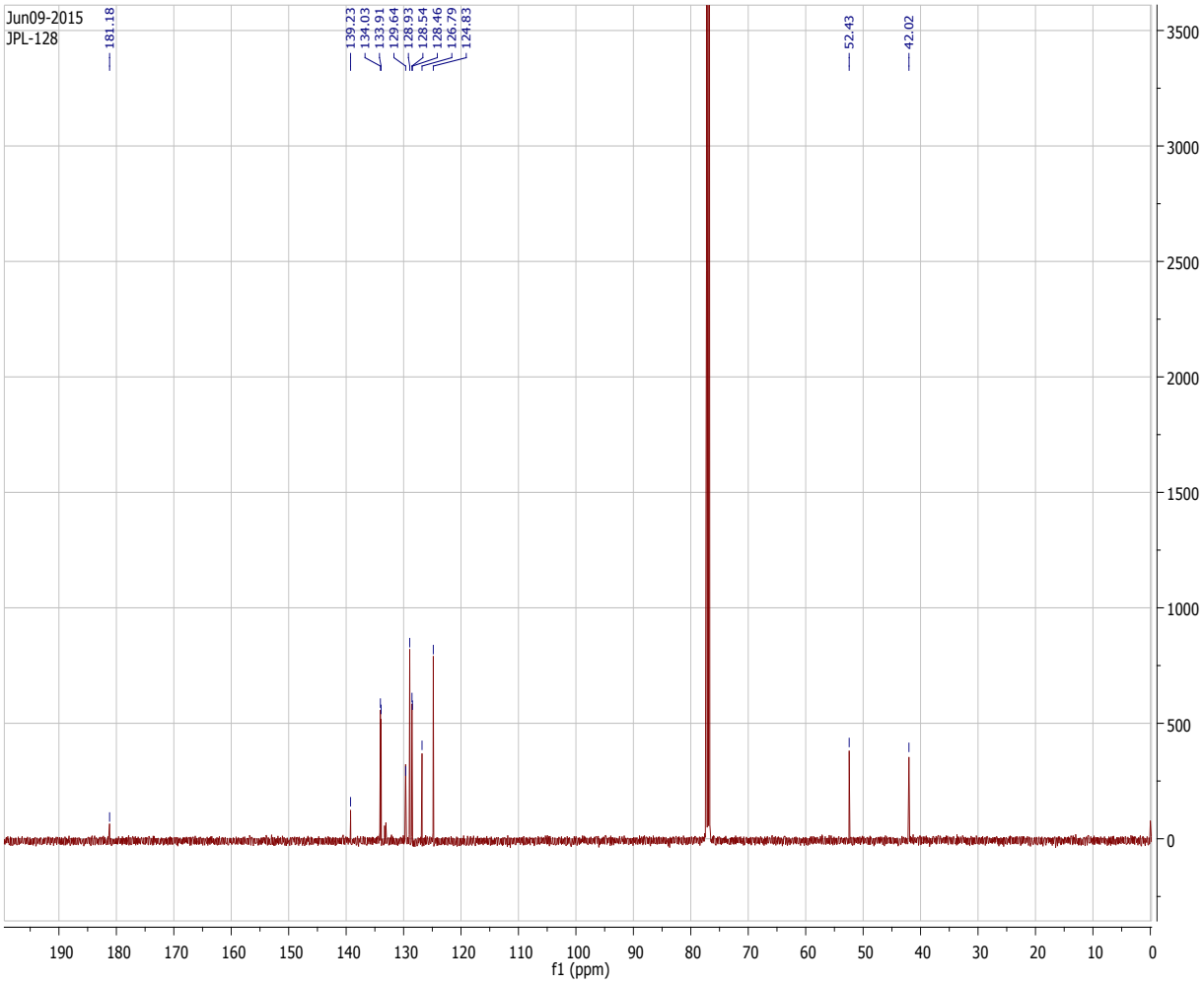

Fig. S72. ^{13}C-NMR spectrum of complex (**5**).

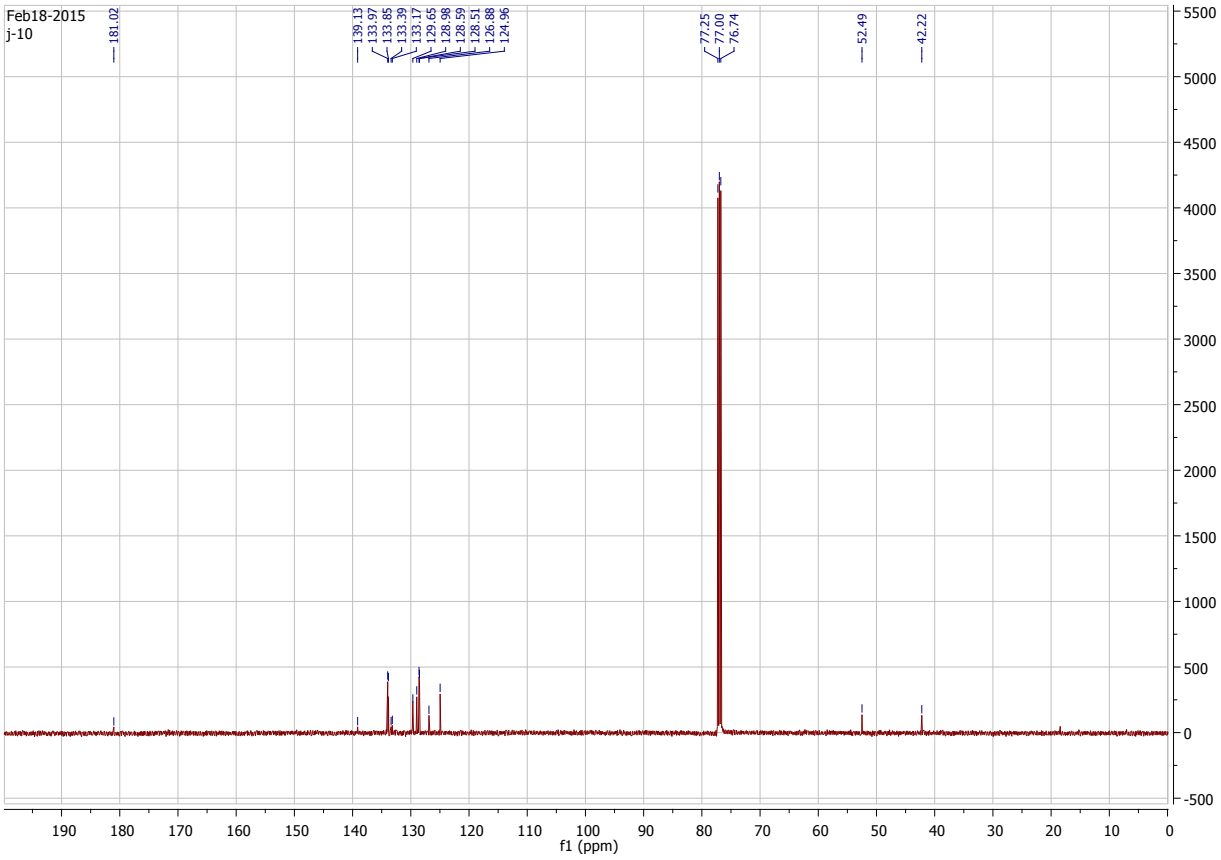

Fig. S73. ^{13}C-NMR spectrum of complex (**6**).

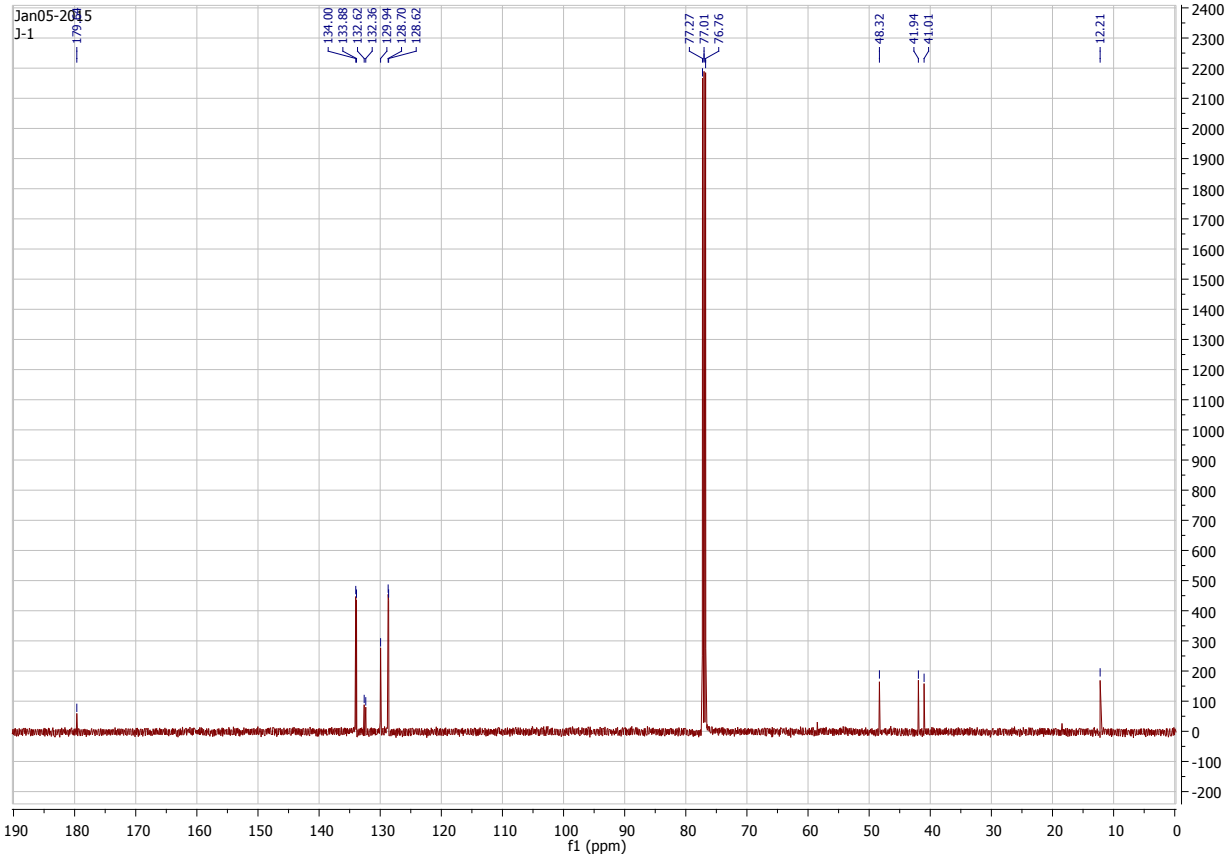

Fig. S74. ^{13}C-NMR spectrum of complex (**7**).

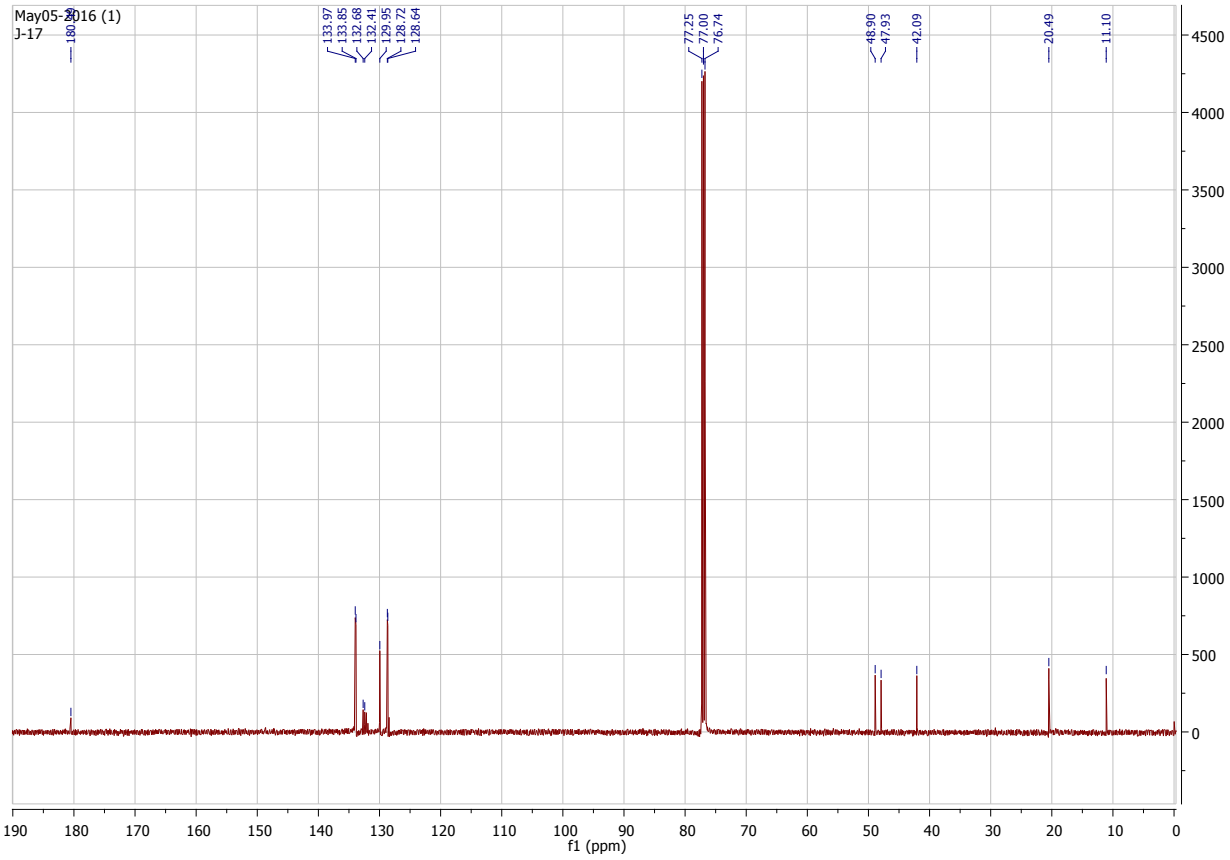

Fig. S75. ^{13}C-NMR spectrum of complex (**8**).

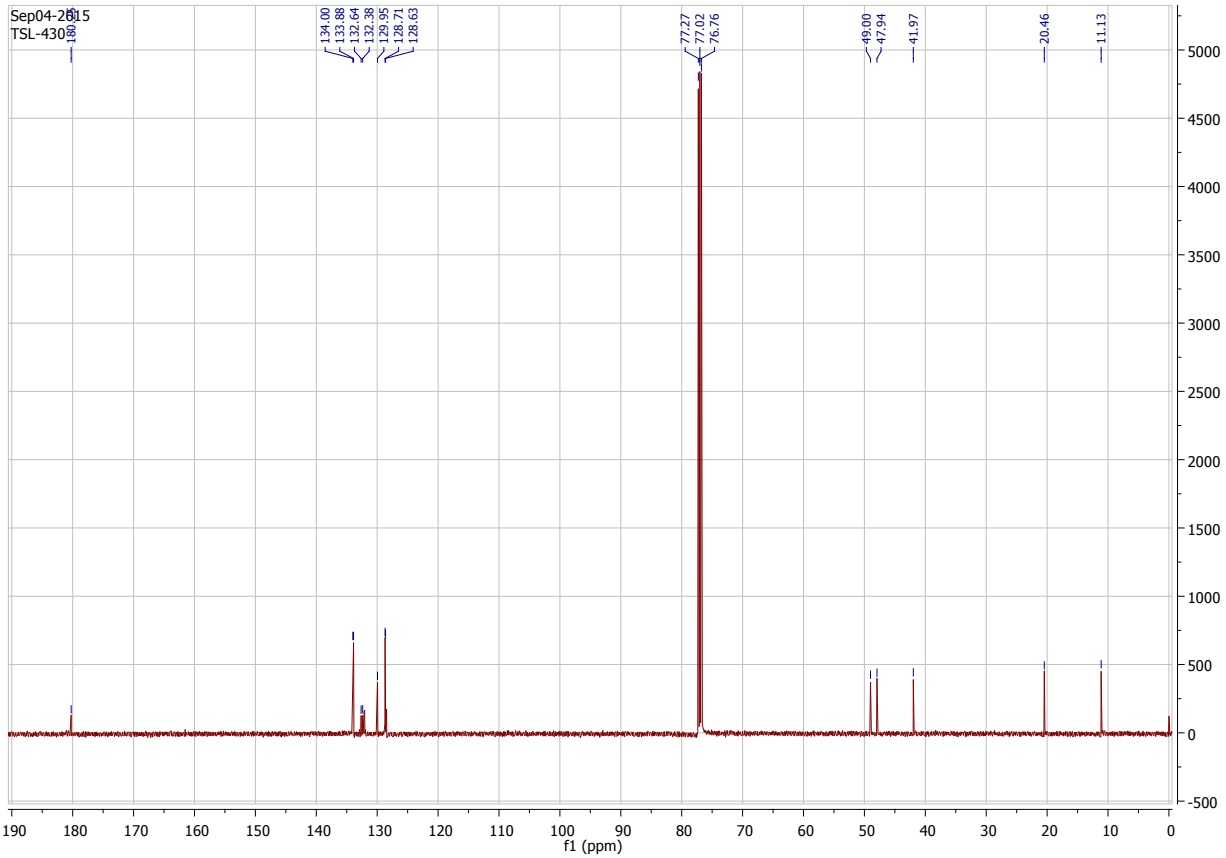

Fig. S76. ^{13}C-NMR spectrum of complex (**9**).

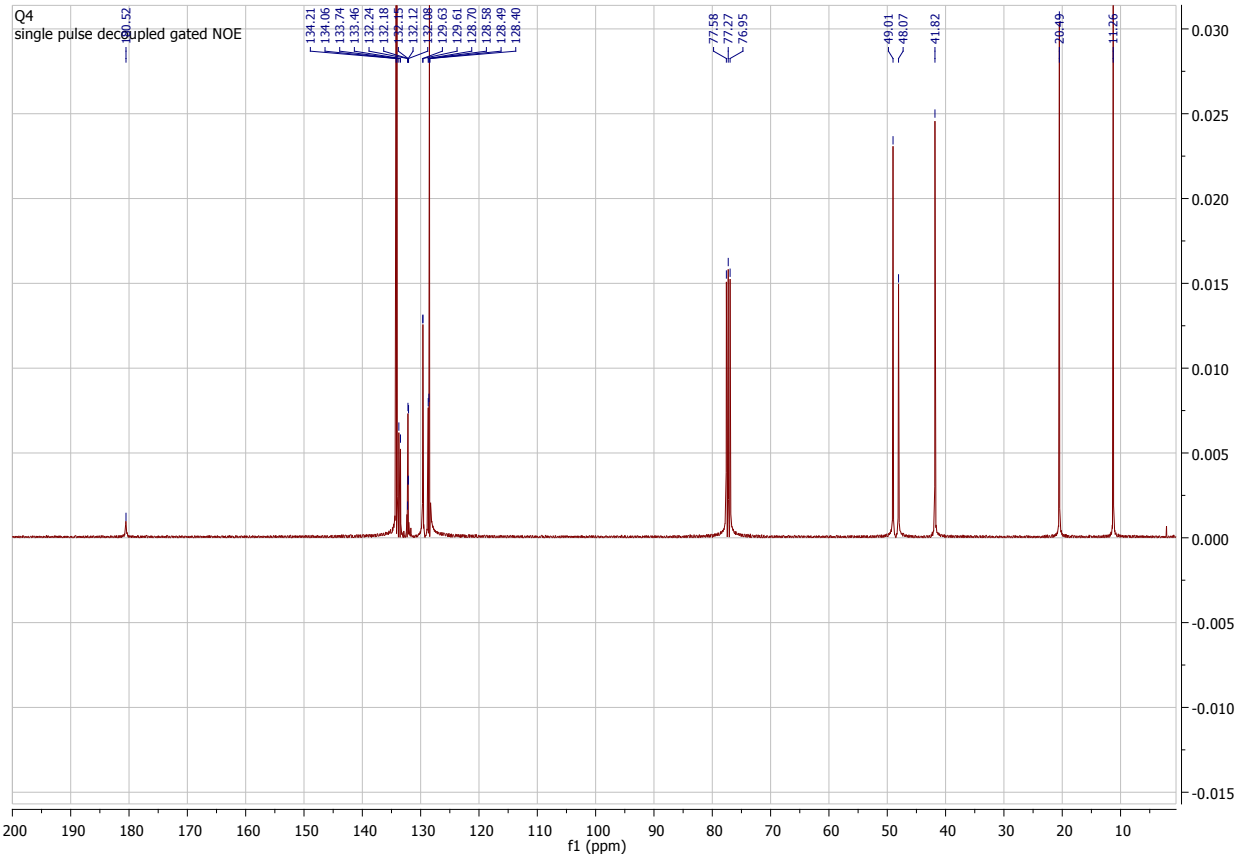

Fig. S77. ^{13}C-NMR spectrum of complex (**10**).

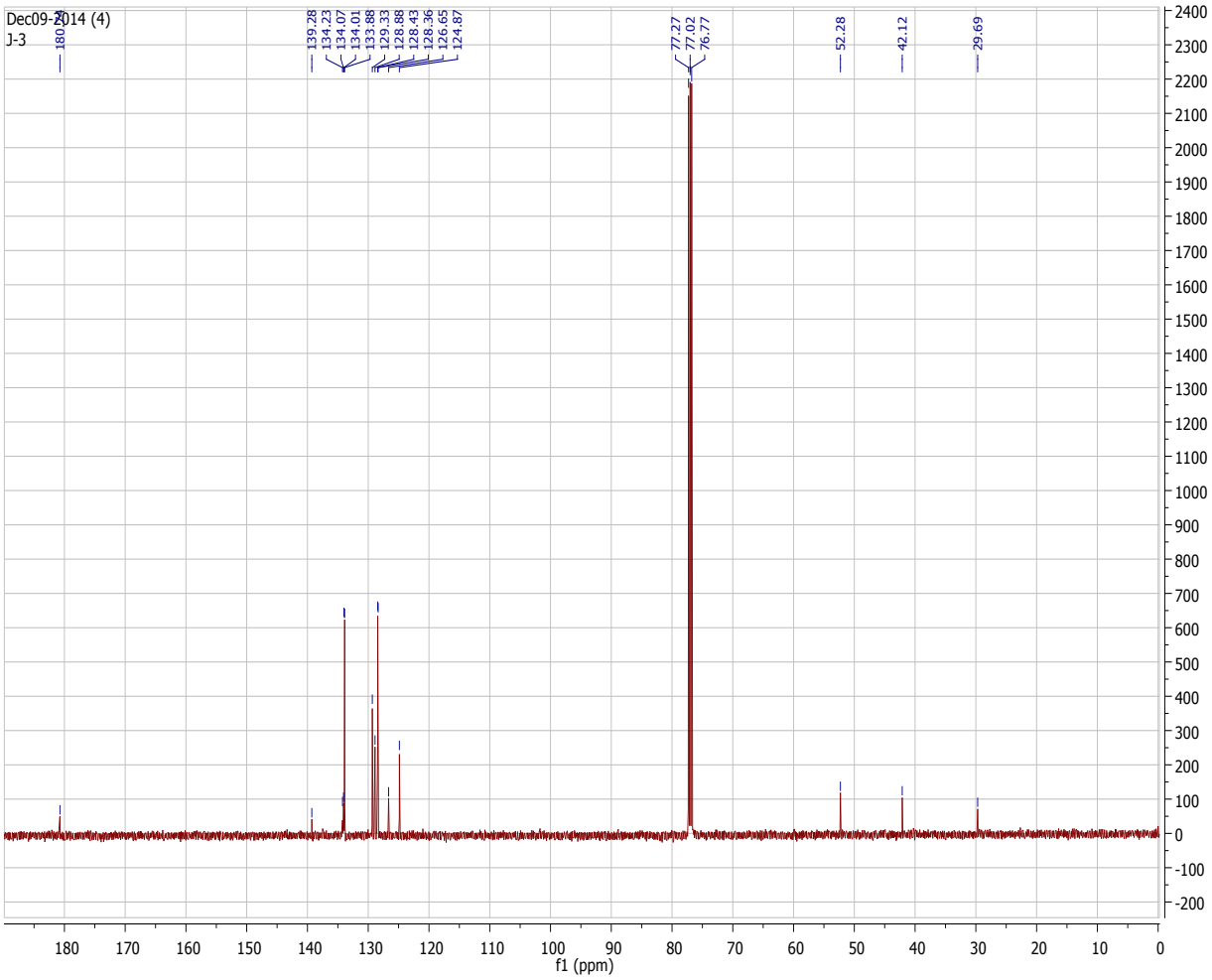

Fig. S78. ^{13}C-NMR spectrum of complex (**11**).

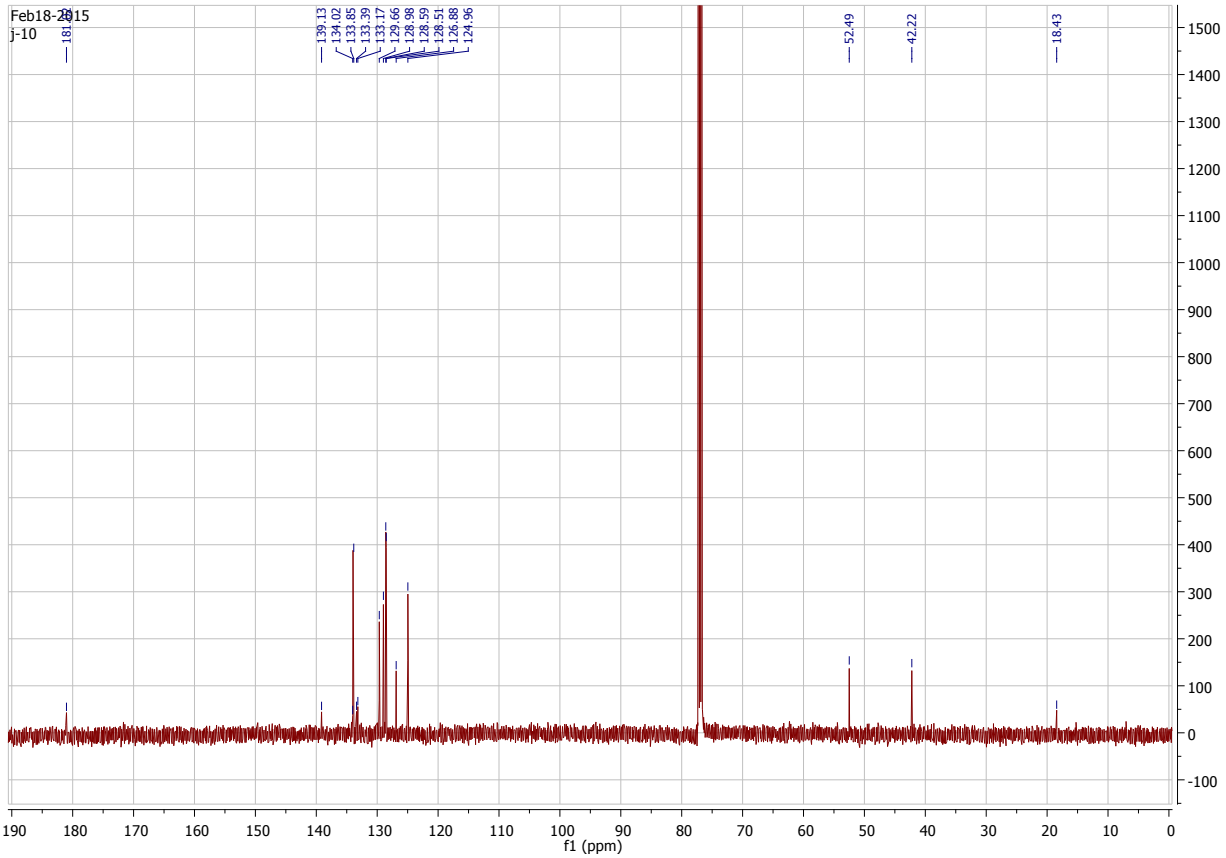

Fig. S79. ^{13}C-NMR spectrum of complex (**12**).

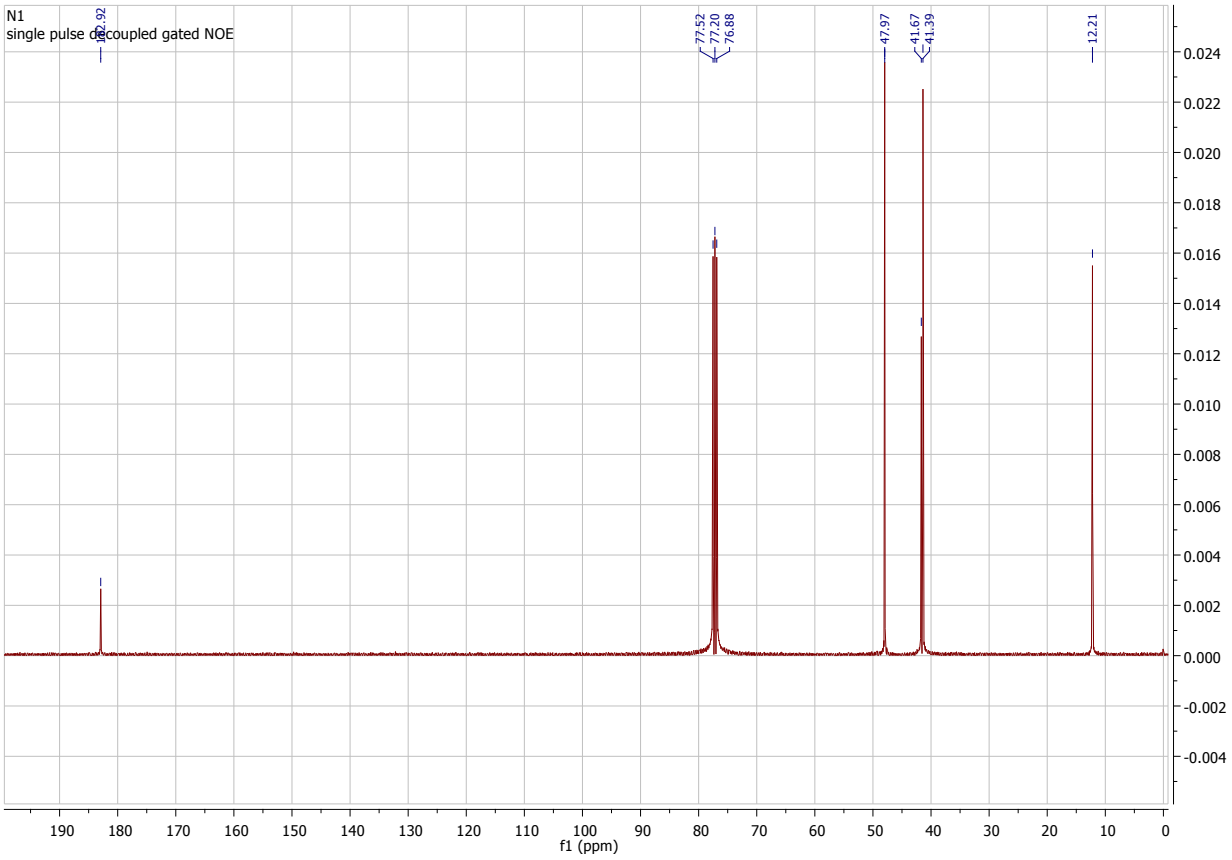

Fig. S80. ^{13}C-NMR spectrum of L-NEt.

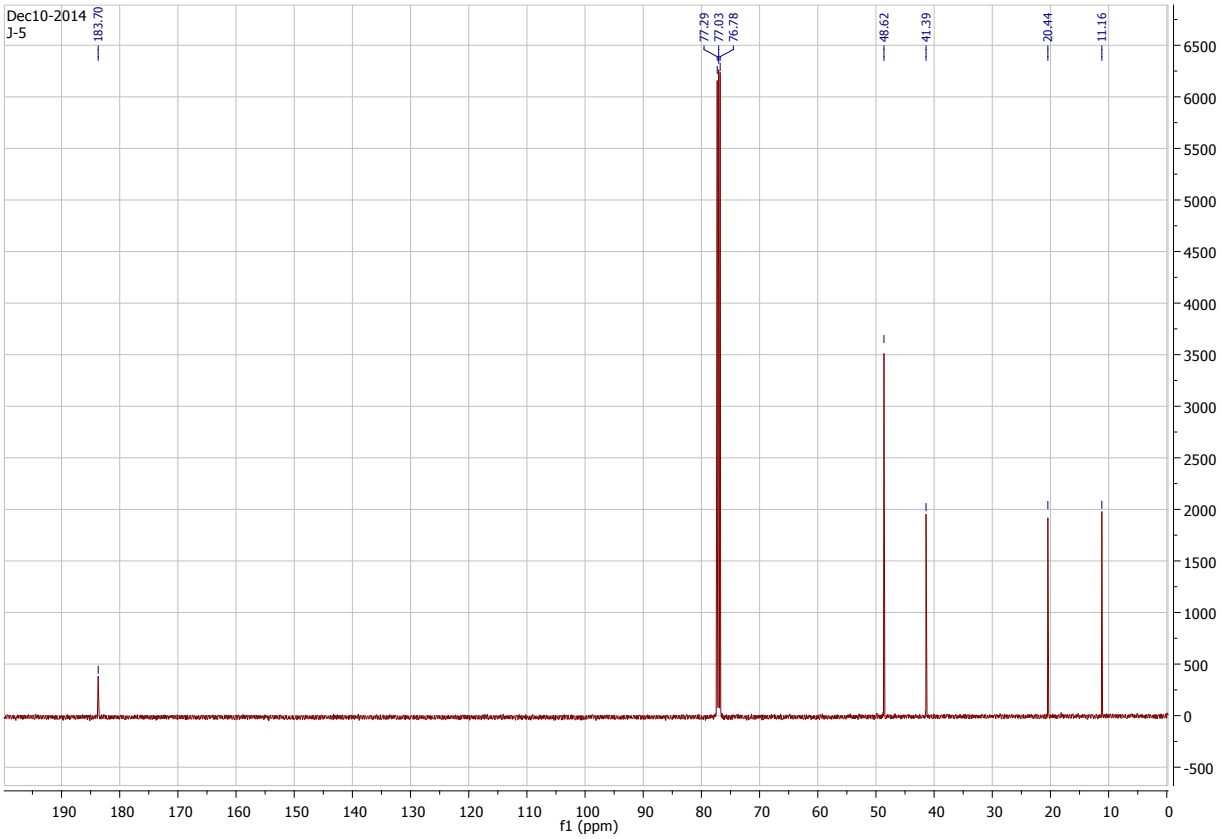

Fig. S81. ^{13}C-NMR spectrum of L-NPr^{n}.

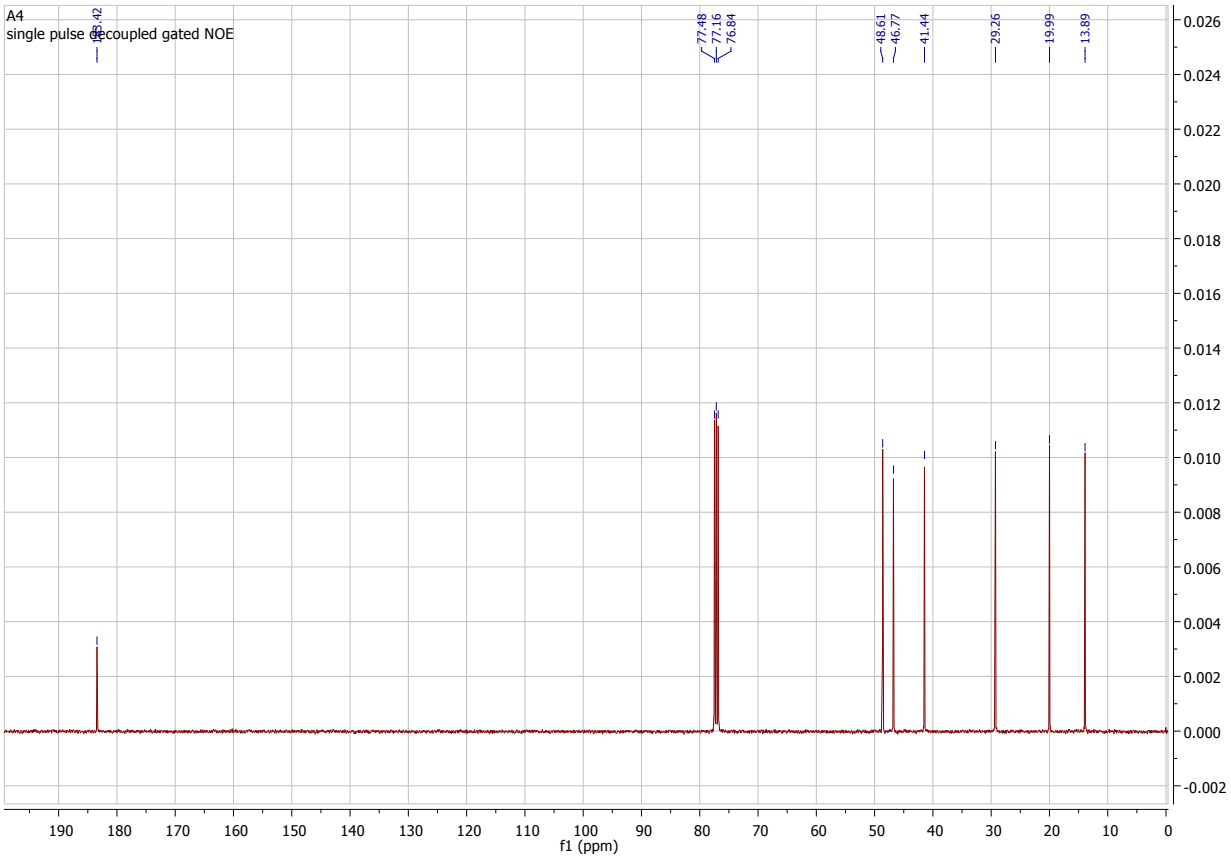

Fig. S82. ^{13}C-NMR spectrum of L-NBu^{n}.

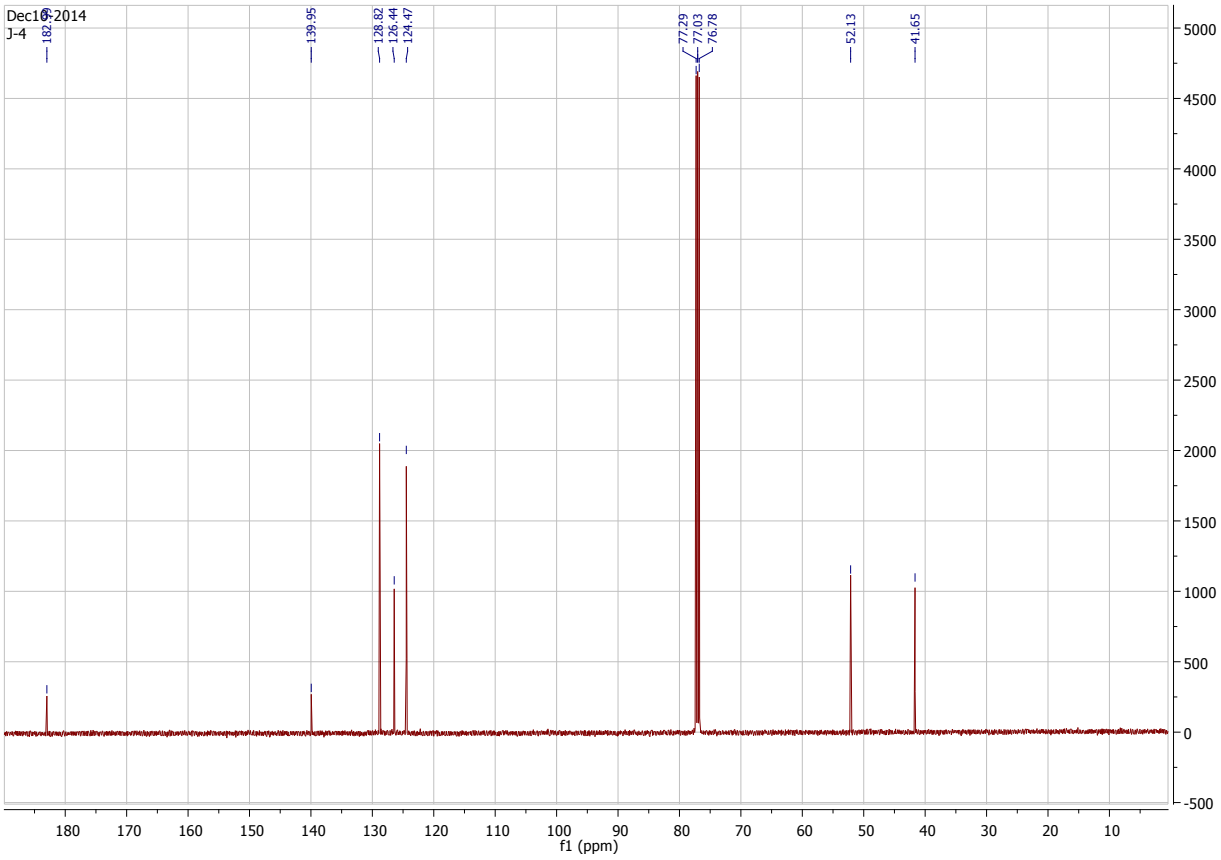

Fig. S83. ^{13}C-NMR spectrum of L-NPh.

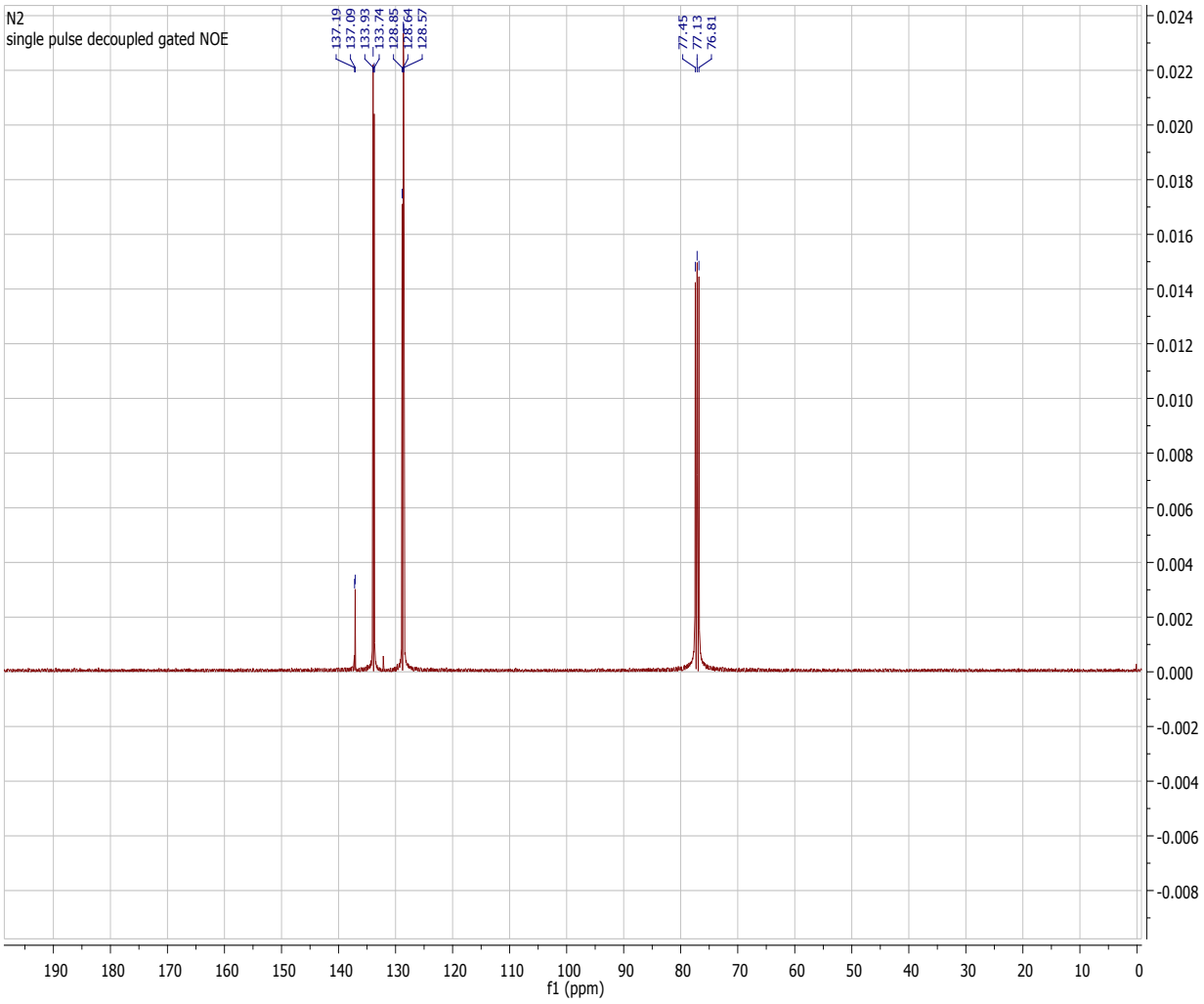

Fig. S84. ^{13}C-NMR spectrum of PPh_3.